

FOAMING CHARACTERISTICS OF REFRIGERANT / LUBRICANT MIXTURES

Final Technical Report

**D. Yogi Goswami
Dinesh O. Shah
Chand K. Jotshi
Sunil S. Bhagwat
Michael Leung
Aaron S. Gregory
Shaoguang Lu**

**SOLAR ENERGY & ENERGY CONVERSION LABORATORY
and
THE CENTER FOR SURFACE SCIENCE & ENGINEERING
Departments of Mechanical and Chemical Engineering
University of Florida
Gainesville, FL 32611**

March 1998

**Prepared for
The Air-Conditioning and Refrigeration Technology Institute
Under
ARTI MCLR Project Number 665-53200**

Mr. David S. Godwin - Project Manager

This program is supported, in part by U.S Department of Energy (Office of Building Technology) grant number DE-FG02-91 CE23810: Materials Compatibility and Lubrication Research (MCLR) on CFC-Refrigerant Substitutes. Federal funding supporting this program constitutes 93.57% of allowable costs. Funding from non-government sources supporting this program consists of direct cost sharing of 6.43% of allowable costs, and significant in-kind contributions from the air-conditioning and refrigeration industry.

DISCLAIMER

The U.S Department of Energy's and the air-conditioning industry's support for the Materials Compatibility and Lubricants Research (MCLR) program does not constitute an endorsement by the U.S. Department of Energy, nor by the air-conditioning and refrigeration industry, of the views expressed herein.

NOTICE

This report was prepared on account of work sponsored by the United States Government. Neither the United States Government, nor the Department of Energy, nor the Air-Conditioning and Refrigeration Technology Institute, nor any of their employees, nor of any of their contractors, subcontractors, or their employees, makes any warranty, expressed or implied, or assumes any legal liability or responsibility for the accuracy, completeness, or usefulness of any information, apparatus, product or process disclosed or represents that its use would infringe privately-owned rights.

COPYRIGHT NOTICE

(for journal publications submissions)

By acceptance of this article, the publisher and/or recipient acknowledges the right of the U.S. Government and the Air-Conditioning and Refrigeration Technology Institutes, Inc. (ARTI) to retain a non-exclusive, royalty-free license in and to any copyrights covering this paper.

TABLE OF CONTENTS

LIST OF TABLES & FIGURES	iii
ABSTRACT & ACKNOWLEDGEMENTS	vii
1. INTRODUCTION	1
2. LITERATURE REVIEW	3
3. REFRIGERANT AND LUBRICANT PROPERTIES	
3.1 Experimental Refrigerant/Lubricant Pairs	6
3.2 Measurement of Lubricant Properties at 25°C	
3.2.1 Density	7
3.2.2 Viscosity	
Background	7
Experimental Procedure	8
Results and Discussion	8
3.2.3 Static Surface Tension	
Background	10
Experimental Procedure	11
Results and Discussion	13
4. SURFACE PROPERTIES OF REFRIGERANT/LUBRICANT MIXTURES	
4.1 Baseline Static Surface Tension	
4.1.1 Background	14
4.1.2 Results and Discussion	14
4.2 Dynamic Surface Tension	
4.2.1 Background	16
4.2.2 Experimental Apparatus	18
4.2.3 Experimental Procedure	18
4.2.4 Results and Discussion:	
Dynamic <i>Surface</i> Tension (Baseline)	20
4.2.5 Results and Discussion:	
Dynamic <i>Interfacial</i> Tension (Baseline)	22
4.2.6 Results and Discussion:	
Dynamic <i>Interfacial</i> Tension (Single-component HFCs)	25
4.2.7 Results and Discussion:	
Dynamic <i>Interfacial</i> Tension (Blended HFCs)	36

5. FOAMING CHARACTERISTICS OF REFRIGERANT/LUBRICANT MIXTURES

5.1 Introduction.....	46
5.2 Baseline Aeration	
5.2.1 Background.....	46
5.2.2 Experimental Procedure.....	47
5.2.3 Flowmeter Calibration.....	49
5.2.4 Results and Discussion.....	49
5.3 Pressure-Drop Induced Foaming of HFC/POE Mixtures	
5.3.1 Background.....	61
5.3.2 Experimental Apparatus.....	61
5.3.3 Experimental Procedure.....	64
5.3.4 Results and Discussion.....	67
5.4 Desorption Rates	
5.4.1 Background.....	73
5.4.2 Experimental Procedure.....	73
5.4.3 Results and Discussion.....	74
5.5 ASTM Standard Test Method for Foaming Characteristics	
5.5.1 Introduction.....	78
5.5.2 Experimental Design.....	78
5.5.3 Experimental Procedure.....	80
5.5.4 Results and Discussion.....	81

6. ABSORPTION RATES

6.1 Introduction.....	82
6.2 Apparatus.....	82
6.3 Calibration.....	84
6.4 Procedure and Measurements.....	84
6.5 Results and Discussion.....	85

7. SUMMARY & CONCLUSIONS

7.1 The Correlation and Significance of the Properties Measured.....	117
7.2 Significance of the Baseline Tests.....	119
7.3 Alternative Refrigerant/Lubricant Mixtures.....	119
7.4 Comparison of (H)CFC Pairs with HFC Pairs.....	120

REFERENCES.....	122
------------------------	------------

APPENDIX.....	124
----------------------	------------

LIST OF TABLES & FIGURES

3. REFRIGERANT AND LUBRICANT PROPERTIES

Table 3.1	Experimental refrigerant/lubricant pairs	6
Table 3.2	Measured lubricant viscosity at ambient temperature.....	10
Table 3.3	Static surface tension of pure lubricants at 25°C	13
Figure 3.1	Configuration of the cone and the plate in the viscometer	9
Figure 3.2	Apparatus of the cone-and-plate viscometer.....	9
Figure 3.3	Wilhelmy plate method theory.....	12
Figure 3.4	Wilhelmy plate method apparatus.....	12

4. SURFACE PROPERTIES OF REFRIGERANT/LUBRICANT MIXTURES

Figure 4.1	Static surface tension of R-12/mineral oil mixtures	15
Figure 4.2	Evolution of a single bubble from the capillary using the maximum bubble pressure method	17
Figure 4.3	Maximum bubble pressure apparatus	19
Figure 4.4	Dynamic surface tension plot for pure lubricants at 25°C	21
Figure 4.5	Dynamic surface tension of 4GS mineral oil with 10% (by weight) baseline refrigerant.....	23
Figure 4.6	Dynamic surface tension of 3GS mineral oil with 10% (by weight) baseline refrigerant.....	24
Figure 4.7	Dynamic interfacial tension of baseline oils with R-22.....	26
Figure 4.8	Dynamic interfacial tension vs. bubble frequency progression using R-125 & Witco SL68 polyolester system.....	28
Figure 4.9	Dynamic interfacial tension vs. POE type using R-125.....	29
Figure 4.10	Dynamic interfacial tension vs. POE type using R-32.....	30
Figure 4.11	Dynamic interfacial tension vs. POE type using R-134a.....	31
Figure 4.12	Dynamic interfacial tension vs. POE type using R-143a.....	32
Figure 4.13	Dynamic interfacial tension vs. HFC injection type using Witco SL68 polyolester.....	34
Figure 4.14	Dynamic interfacial tension vs. HFC injection type using ICI RL68H polyolester	35
Figure 4.15	Dynamic interfacial tension vs. bubble frequency progression using R-404A & ICI RL68H polyolester system	37
Figure 4.16	Dynamic interfacial tension vs. bubble frequency progression using R-407C & Witco SL68 polyolester system.....	38
Figure 4.17	Dynamic interfacial tension vs. bubble frequency progression using R-410A & Witco SL68 polyolester system.....	39

Figure 4.18	Dynamic interfacial tension vs. POE type using R-404A.....	40
Figure 4.19	Dynamic interfacial tension vs. POE type using R-407C.....	41
Figure 4.20	Dynamic interfacial tension vs. POE type using R-410A.....	42
Figure 4.21	Dynamic interfacial tension vs. HFC blend type using Witco SL68 polyolester.....	44
Figure 4.22	Dynamic interfacial tension vs. HFC blend type using ICI RL68H polyolester.....	45

5. FOAMING CHARACTERISTICS OF REFRIGERANT/LUBRICANT MIXTURES

Figure 5.1	Aeration column apparatus used for foamability and foam stability.....	48
Figure 5.2	Baseline aeration: flowrate comparison using 30 ml 3GS and R-22.....	50
Figure 5.3	Baseline aeration: flowrate comparison using 30 ml 3GS and R-12.....	50
Figure 5.4	Baseline aeration: flowrate comparison using 30 ml 4GS and R-22.....	51
Figure 5.5	Baseline aeration: flowrate comparison using 50 ml 4GS and R-22.....	51
Figure 5.6	Baseline aeration: flowrate comparison using 30 ml 4GS and R-12.....	52
Figure 5.7	Baseline aeration: mineral oil comparison using 30 ml lubricant and R-22 at 350 ml/min.....	52
Figure 5.8	Baseline aeration: mineral oil comparison using 30 ml lubricant and R-22 at 700 ml/min.....	53
Figure 5.9	Baseline aeration: mineral oil comparison using 30 ml lubricant and R-12 at 350 ml/min.....	53
Figure 5.10	Baseline aeration: mineral oil comparison using 30 ml lubricant and R-12 at 700 ml/min.....	54
Figure 5.11	Baseline aeration: mineral oil comparison using 30 ml lubricant and R-12 at 1000 ml/min.....	54
Figure 5.12	Baseline aeration: refrigerant comparison using 30 ml 4GS and refrigerant at 700 ml/min.....	55
Figure 5.13	Baseline aeration: refrigerant comparison using 30 ml 3GS and refrigerant at 700 ml/min.....	55
Figure 5.14	Baseline foamability and foam stability (30 ml 3GS and R-22).....	58
Figure 5.15	Baseline foamability and foam stability (30 ml 3GS and R-12).....	58
Figure 5.16	Baseline foamability and foam stability (30 ml 4GS and R-22).....	59
Figure 5.17	Baseline foamability and foam stability (50 ml 4GS and R-22).....	59
Figure 5.18	Baseline foamability and foam stability (30 ml 4GS and R-12).....	60
Figure 5.19	HFC pressure-release foaming apparatus.....	62

Figure 5.20	HFC pressure-release foaming for 1:1 ratio, 20 psi pressure drop	68
Figure 5.21	HFC pressure-release foaming for various HFC:POE ratios (R-134a and 20 psi pressure drop)	70
Figure 5.22	HFC pressure-release foaming for a 50 psi pressure drop (3:1 HFC : POE ratio)	72
Figure 5.23	HFC pressure-release foaming for a 50 psi pressure drop (1:1 HFC : POE ratio)	72
Figure 5.24	Initial desorption rates for 134a varying HFC : POE ratio and pressure drop time	75
Figure 5.25	Initial desorption rates for HFCs subjected to a 50 psi pressure drop	77
Figure 5.26	ASTM Standard Test Method for Foaming Characteristics	79

6. ABSORPTION RATES

Table 6.1	Experimental results for the absorption of HFC refrigerants and their blends at room temperature (24°C)	87
Table 6.2	Experimental results for the absorption of HFC refrigerants and their blends at 34°C	88
Table 6.3	Experimental results for the absorption of HFC refrigerants and their blends at 44°C	89
Table 6.4	Experimental results for the absorption of HFC refrigerants and their blends at -12°C	90
Figure 6.1	Absorption rate test facility	83
Figure 6.2	Absorption of R-32 in POE at room temperature (24°C)	91
Figure 6.3	Absorption of R-125 in POE at room temperature (24°C)	92
Figure 6.4	Absorption of R-134a in POE at room temperature (24°C)	93
Figure 6.5	Absorption of R-143a in POE at room temperature (24°C)	94
Figure 6.6	Absorption of R-404A in POE at room temperature (24°C)	95
Figure 6.7	Absorption of R-407C in POE at room temperature (24°C)	96
Figure 6.8	Absorption of R-410A in POE at room temperature (24°C)	97
Figure 6.9	Comparison of experimental data with published values	98
Figure 6.10	Absorption of R-32 in POE at 34°C	99
Figure 6.11	Absorption of R-125 in POE at 34°C	100
Figure 6.12	Absorption of R-134a in POE at 34°C	101
Figure 6.13	Absorption of R-143a in POE at 34°C	102
Figure 6.14	Absorption of R-404A in POE at 34°C	103
Figure 6.15	Absorption of R-407C in POE at 34°C	104
Figure 6.16	Absorption of R-410A in POE at 34°C	105
Figure 6.17	Absorption of R-32 in POE at 44°C	106
Figure 6.18	Absorption of R-134a in POE at 44°C	107
Figure 6.19	Absorption of R-143a in POE at 44°C	108

Figure 6.20	Absorption of R-404A in POE at 44°C.....	109
Figure 6.21	Absorption of R-407C in POE at 44°C.....	110
Figure 6.22	Absorption of R-410A in POE at 44°C.....	111
Figure 6.23	Absorption of R-32 in POE at -12°C.....	112
Figure 6.24	Absorption of R-143a in POE at -12°C.....	113
Figure 6.25	Absorption of R-404A in POE at -12°C.....	114
Figure 6.26	Absorption of R-407C in POE at -12°C.....	115
Figure 6.27	Absorption of R-410A in POE at -12°C.....	116

7. SUMMARY & CONCLUSIONS

Table 7.1	Comparisons of interest. (H)CFCs with mineral oils and HFCs with POEs.....	121
Figure 7.1	Schematic representation of the correlation between relevant surface properties of the refrigerant/lubricant mixtures.....	118

APPENDIX

Table A3.1	Lubricant Densities.....	125
Table A3.2	Lubricant Viscosities.....	126
Table A3.3	Lubricant Static Surface Tension.....	128
Table A4.1	Static Surface Tension vs. Refrigerant/Lubricant Composition.....	130
Table A4.2	Dynamic Surface Tension: Pure Lubricants.....	132
Table A4.3	Dynamic Surface Tension: Lubricants with 10% Refrigerant.....	136
Table A4.4	Dynamic Interfacial Tension: Baseline Pairs.....	140
Table A4.5	Dynamic Interfacial Tension: Single-component HFCs.....	143
Table A4.6	Dynamic Interfacial Tension: HFC Blends.....	155
Table A5.1	Baseline Aeration Tests: APPROACH 1.....	164
Table A5.2	Baseline Aeration Tests: APPROACH 2.....	167
Table A5.3	HFC Pressure-Release Foaming Tests.....	168
Table A5.4	HFC Pressure-Release Desorption Data Summary.....	177

ABSTRACT

This report presents the results of experimental measurements on refrigerant/lubricant mixtures of chlorofluorocarbon (CFC) 12 and hydrochlorofluorocarbon (HCFC) 22 with mineral oil, as well as hydrofluorocarbons (HFC) 32, 125, 134a, 143a, 404A, 407C and 410A with synthetic polyolester (POE) lubricants. Viscosity, static and dynamic surface tension, foamability, foam stability, absorption rate and desorption rate data are reported for the nine refrigerant/lubricant pairs: 2 (H)CFC/mineral oil pairs and 7 HFC/POE pairs.

Numerous experimental apparatuses have been constructed for the purpose of performing the experiments described in this report, including Wilhelmy plate and maximum bubble pressure devices for measuring static and dynamic surface tension, respectively. In addition, multiple foaming devices were conceived to perform foamability, foam stability and desorption rate tests on the refrigerant/lubricant pairs under various temperature and pressure conditions. Furthermore, a uniquely designed pressure vessel was fabricated to carry out the absorption rate study.

All of the experimental data have been tabulated and are presented graphically. Relevant comparisons are made regarding the performance of the baseline pairs versus the HFC/POE pairs.

ACKNOWLEDGEMENTS

The investigators would like to thank the many people for making this project possible. Our gratitude is extended to Allied Signal and Sid Harvey for the donation of the refrigerants, and to Witco Chemical Corporation and ICI Chemicals and Polymers for the donation of the lubricants. Bill Walter, Howard Sibley, David Kneeskern, Michael Dormer and Xiaomei Yu of the Carrier Corporation are all deserving of our appreciation for inviting some of the investigative team to their labs during the summer of 1996. Thanks to them, the information gathered proved to be essential in making our experiments safe and efficient. In addition, our appreciation is extended to Robert Yost, of ICI Fluorochemicals Applications Laboratory, for his help and information. Many of the experimental apparatuses could not have been conceived without the invaluable effort put forth by Tracy Lambert and Charles Garretson of the University of Florida Chemical and Mechanical Engineering Departments, respectively. Thanks are also due to the project manager, David Godwin, and to the Air-Conditioning and Refrigeration Technology Institute for their guidance and support throughout the project.

1. INTRODUCTION

The air-conditioning and refrigeration industry has moved to HFC refrigerants which have zero ozone depletion and low global warming potential due to regulations on CFC and HCFC refrigerants and concerns for the environment. The change in refrigerants has prompted the switch from mineral oil and alkylbenzene lubricants to polyolester-based lubricants.

Properties of CFC/mineral oil and HCFC/mineral oil mixtures were well understood through both the laboratory evaluation and actual experience in the field. Equipment designs took into account the properties of the refrigerant/lubricant mixtures which lubricate the moving parts in the compressor and travel throughout the system. Previous studies, sponsored by the ARTI/DOE, have measured equilibrium properties of new refrigerants and lubricants, such as solubility, viscosity and density. At this time, very little work has been done to evaluate the properties under transient conditions. Design engineers would benefit from a better understanding of, 1) the rate of absorption of refrigerants into lubricants, 2) the rate at which the lubricant gives up the refrigerant when exposed to a pressure drop, and 3) the foaming characteristics of the mixture as the refrigerant leaves the solution.

The objectives of this investigation are to experimentally determine the absorption and desorption rates of HFC and blended refrigerants in polyolester lubricant and the characteristics of the foam formed when the refrigerant leaves the refrigerant/lubricant mixture after being exposed to a pressure drop. The relevant foaming properties being measured are viscosity, static and dynamic surface tension, foamability, and foam stability. The refrigerants being examined include baseline refrigerants: CFC-12 (R-12) and HCFC-22 (R-22); alternative refrigerants:

HFC-32 (R-32), HFC-125, HFC-134a, and HFC-143a; and blended refrigerants: HFC-404A, HFC-407C, and HFC-410A. The baseline refrigerants are tested with ISO 32 (Witco 3GS) and ISO 68 (Witco 4GS) mineral oils while the alternative and blended refrigerants are tested with two ISO 68 polyolesters (Witco SL68 and ICI RL68H).

This report summarizes the progress of this investigation in the past twelve months. Experimental procedures employed to measure the properties mentioned above are presented along with their results. All experimental data are tabulated in the [Appendix](#).

2. LITERATURE REVIEW

From the literature search it was observed that previous studies on the absorption/desorption characteristics of refrigerant and lubricant mixtures are scarce. Most of the available literature is for solubility and oil concentration tests. The objective in a solubility test is to determine the maximum quantity of a refrigerant absorbed in a lubricant at various temperatures and pressures under the state of equilibrium. Similarly, oil concentration refers to the amount of oil present in a refrigerant/lubricant mixture at various conditions. A number of methodologies have been employed in these tests and they are discussed below.

A standardized method for withdrawing samples from the test system has been described in the 1995 Revision of ANSI/ASHRAE Standard 41.4-1984. Van Gaalen et al. (1991a, 1991b) used this method to check the liquid refrigerant/lubricant compositions. Principally, in this method, a liquid sample is withdrawn from the system into an evacuated chamber. The sample is then placed in a vacuum environment and heated up to 150°C to evaporate all the refrigerant content. The difference in weight before and after the process reflects the amount of refrigerant in the liquid sample.

Some methods were designed to conveniently measure the refrigerant/oil compositions online in a vapor compressor system. Bayani et al. (1995) measured the oil concentration of R-134a/oil mixture with a vibrating tube type density flowmeter. Based upon the known density, composition of the mixture can be calculated.

Oil concentration can also be estimated from its optical properties. When a monochromatic light source is propagated through a refrigerant/oil solution, the light is increasingly absorbed with increasing concentration of oil in the solution. Thus, the difference between the incident and the transmitted beam intensities yields an estimation of the concentration. Suzuki et al. (1993) demonstrated that absorption of infrared light in R-12/oil and R-134a/oil solutions strongly depends on the oil concentration. After a calibration curve relating the light transmittance of a solution to the oil concentration is established, it can be used for online measurements.

All of the above methodologies have been considered for the absorption/desorption tests. However, these approaches have some drawbacks. The method utilizing the 1995 Revision of ANSI/ASHRAE Standard 41.4-1984 is convenient to measure the solubility of refrigerants in lubricants. However, this method is inconvenient to measure the absorption and desorption rates since samples must be taken frequently or even continuously for higher accuracy. The test procedures become difficult to execute and a large amount of lubricant and refrigerant are required for the test. For the method that uses a density flowmeter, a circulation of the liquid has to be maintained. This additional effort is indeed not necessary for a static test. In the optical method, a calibration curve must be obtained and the optical setup appears complicated.

The proposed weight gain method, compared to the ones discussed above, is believed to be simple and accurate. The absorption and desorption of oil can be monitored continuously. To measure the foaming characteristics (stability, density, bubble size and viscosity), straightforward procedures are used. Sharma and Shah (1984) and Blute et al. (1994) have reported these procedures.

ASHRAE (1993) gives the information on various properties of refrigerant/lubricant combinations including the alternative refrigerants of interest. However, the property data presented in the ASHRAE publication pertains only to the CFC refrigerants and mineral oil lubricants. Yanagisawa et al. (1986, 1991) have provided data for thermophysical properties of the CFC refrigerant/mineral oil combinations as well as their absorption/desorption/foaming characteristics. There are very few publications on the thermophysical properties of the alternative HFC refrigerants and synthetic lubricants mixtures. These include Chang and Nagashima (1993), Komatsuzaki et al. (1991, 1994), and Short (1989). However, these studies do not address the foaming characteristics as a result of a sudden pressure drop. Only recently, Sibley (1993) emphasized the importance of foaming characteristics of the new refrigerant/lubricant mixtures in the design of equipment. Sibley also presented some new preliminary data for a R-134a/polyolester mixture.

This preliminary review of the literature shows the importance of a thorough study of the absorption/desorption/foaming characteristics of the alternative HFC refrigerants and synthetic lubricating oil mixtures, which will provide data for better equipment design as well as ways (e.g., foaming agents) to improve the characteristics themselves.

3. REFRIGERANT AND LUBRICANT PROPERTIES

3.1 Experimental Refrigerant/Lubricant Pairs

Measurements were conducted on a total of nine refrigerant/lubricant pairs which are listed below in [Table 1](#). The baseline pairs used in this study are CFC-12/mineral oil and HCFC-22/mineral oil. These were each tested with both a 32-grade mineral oil as well as a 68-grade mineral oil. In addition, four HFCs (R-32, R-125, R-134a and R-143a) were tested with two different 68-grade polyolesters (POEs). Three HFC blends (R-404A, R-407C, R-410A) were also used in this project. It should be noted that a majority of the absorption and desorption rate experiments, as well as the HFC foaming tests, were conducted using the ICI RL68H polyolester.

Table 3.1 Experimental refrigerant/lubricant pairs

Refrigerant	Lubricant	Lubricant Brand/Type
<i>Baseline (H)CFCs</i>		
(CFC) R-12	ISO 32, 68 mineral oil	Witco 3GS, Witco 4GS
(HCFC) R-22	ISO 32, 68 mineral oil	Witco 3GS, Witco 4GS
<i>Single-component HFCs</i>		
R-32	ISO 68 polyolester	ICI RL68H, Witco SL68
R-125	ISO 68 polyolester	ICI RL68H, Witco SL68
R-134a	ISO 68 polyolester	ICI RL68H, Witco SL68
R-143a	ISO 68 polyolester	ICI RL68H, Witco SL68
<i>Blended HFCs</i>		
R-404A	ISO 68 polyolester	ICI RL68H, Witco SL68
R-407C	ISO 68 polyolester	ICI RL68H, Witco SL68
R-410A	ISO 68 polyolester	ICI RL68H, Witco SL68

3.2 Measurement of Lubricant Properties

While there are tabulated properties which are known for the aforementioned lubricants, a series of tests were performed to evaluate some baseline properties, namely density and viscosity, at standard temperature (25°C) and pressure (1 atm), which are not included in the manufacturer's data. The purpose of these tests is to establish data for the pure lubricants at ambient conditions, the same conditions which exist for much of the foaming characteristics and surface property tests, as well as some of the absorption and desorption tests.

3.2.1 Lubricant Density

Densities of the pure lubricants were simply calculated from a simple volume and weight study. In essence, a standard amount of lubricant (15.0 ± 0.1 ml) was poured into a graduated container and weighed. The weight divided by the volume yielded the lubricant densities. Both of the mineral oils yielded densities close to 0.8 g/ml while the polyolesters yielded slightly greater densities of 0.9 g/ml. Experimental data from these trials are listed in the [Appendix \(Table A3.1\)](#).

3.2.2 Lubricant Viscosity

Background

Although the viscosity grades of the lubricants are known at 40°C, all four lubricants were tested at 25°C with a cone-and-plate viscometer to ensure that the lubricants do not have any irregular behavior at ambient conditions. The viscometer is

comprised of a flat plate and a cone whose apex touches the plate as shown in [Figure 3.1](#). The cone rotates with respect to the plate and a constant shear rate is applied throughout the sample.

Experimental Procedure

A schematic of the experimental apparatus is illustrated in [Figure 3.2](#). A temperature bath is initially turned on to equilibrate at the desired temperature of 25°F. Once the bath has equilibrated, viscosity measurements can be made with the digital viscometer. According to the specifics of the cone and plate (i.e. angle of cone edge with respect to the plate), shear rates are determined from the spindle speed which is adjustable. Approximately 2 ml of a lubricant sample is placed in the cup which contains the plate whose temperature is controlled by the bath. The cup is then locked into position, which is calibrated to where the apex of the cone just touches the plate. The spindle is turned at one of the four speeds. Each speed corresponds to a shear rate, each of which is independent of liquid viscosity. Viscosity measurements are read at varying shear rates for each trial.

Results and Discussion

The measured viscosities (in cp) are shown in [Table 3.2](#). Within each trial, roughly constant viscosities were observed. However, within each sample, there was some degree of variance among the trials. This can be attributed to the experimental error associated with cleaning the cone and plate after each trial with distilled water and

Figure 3.1 Configuration of the cone and the plate in the viscometer

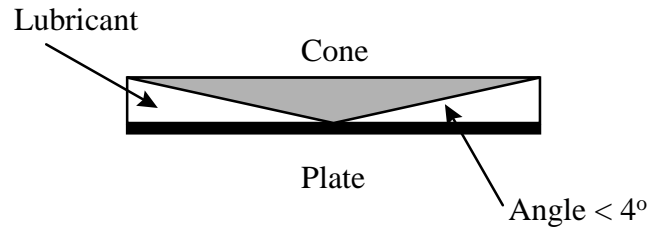
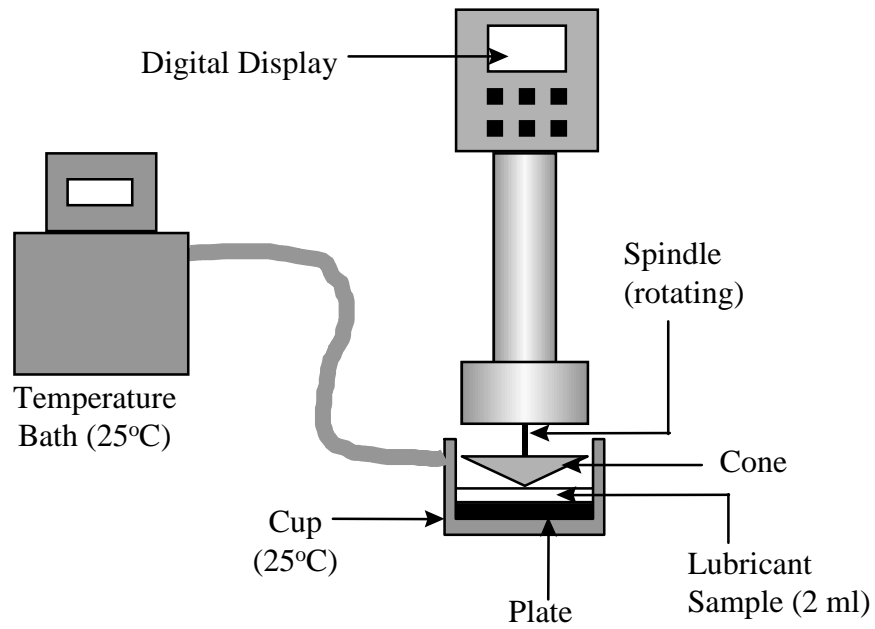


Figure 3.2 Apparatus of the cone-and-plate viscometer



acetone. If there is even a trace of water or acetone on either the plate or the cone, there will be some degree of error. Nevertheless standard deviations of all trials are less than 2.5 cp. Final values of the lubricant viscosities were determined from taking an average of all values of each shear rate for each lubricant. In most cases, two full trials (3 shear rates per trial) are averaged. Overall, the ICI, SL68 and 4GS samples tested around 100 cp. The 3GS sample tested around 50 cp.

Table 3.2 Measured lubricant viscosity at ambient temperature
(Refer to [Table 3.2](#) in the Appendix)

Lubricant Type	Nominal Viscosity Grade (cp) at 40°C	Viscosity (cp) at 25°C	Standard Deviation
ICI RL68H	68	90.3	±2.3
Witco 4GS	68	90.8	±2.5
Witco 3GS	32	47.5	±2.1
Witco SL68	68	111.2	±2.2

3.2.3 Static Surface Tension

Background

Equilibrium surface tension is one characteristic of a liquid which is related to the liquid's foaming properties. In essence, the lower the equilibrium surface tension, the less work that is needed to expand that surface (i.e. from aeration) and thus, form bubbles from that liquid. As these bubbles aggregate, a foam is produced. The Wilhelmy plate method was used to perform all static surface tension measurements of the lubricants under ambient conditions. The method is traditionally used to help analyze a surfactant's foaming ability and foam stability. A thin platinum plate is placed on the surface of the

lubricant where some of the lubricant adheres to the walls of the plate as pictured in [Figure 3.3](#). The surface tension is taken as the ratio of the force (dynes) that is used to lift the plate off the surface of the liquid to the wetted length (cm) which is twice the length of the plate's edge when perfectly horizontal to the liquid's surface. The apparatus is calibrated with distilled water, acetone and methanol as testing materials of known surface tension at room temperature.

Experimental Procedure

A surface tensiometer, picture in [Figure 3.4](#), is used to conduct the static surface tension tests. A thin platinum plate (1 cm wide, 2.5 cm long, approximately 0.1 mm thick), once it has been sterilized under a burner flame for a few seconds, is hung on the tensiometer with a thin platinum rod and locked into position. A laboratory jack with rotary adjustment is used to elevate the lubricant sample to the platinum plate. Approximately 15 ml of a lubricant sample is poured into a shallow glass dish (2 inches in diameter) and elevated until the plate adheres to the lubricant's surface. Then, the plate-side of the tensiometer is unlocked. A beam on the tensiometer is adjusted on the scale until the plate is lifted from the lubricant surface. The surface tension is then read from the tensiometer. After each reading, the plate is removed, rinsed with distilled water, and fired with the burner. The platinum piece is handled with tweezers so as not to transfer any perspiration from the hands which can affect surface tension measurements.

Figure 3.3 Wilhelmy plate method theory

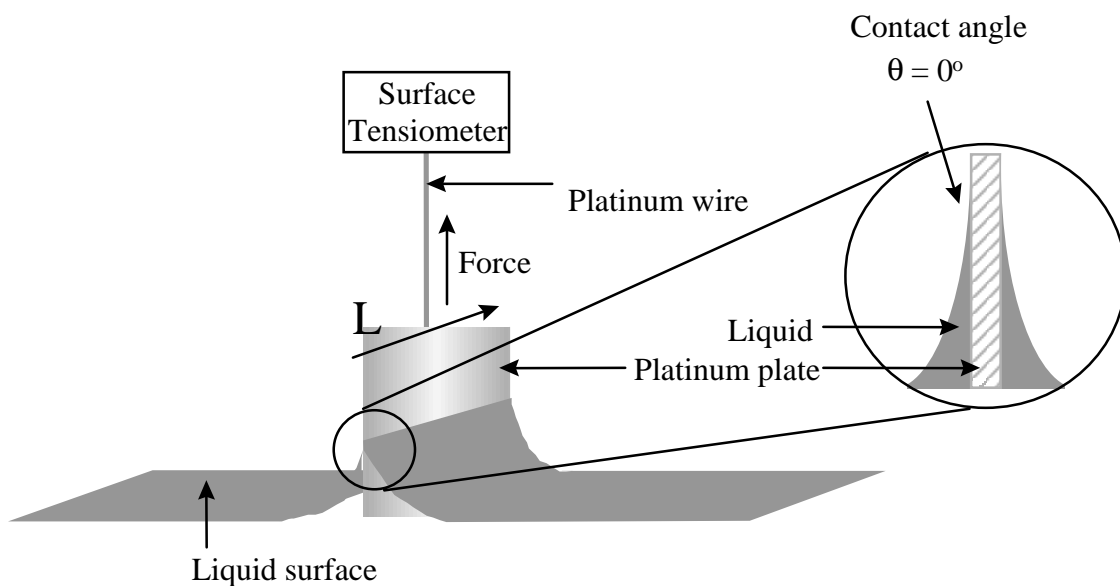
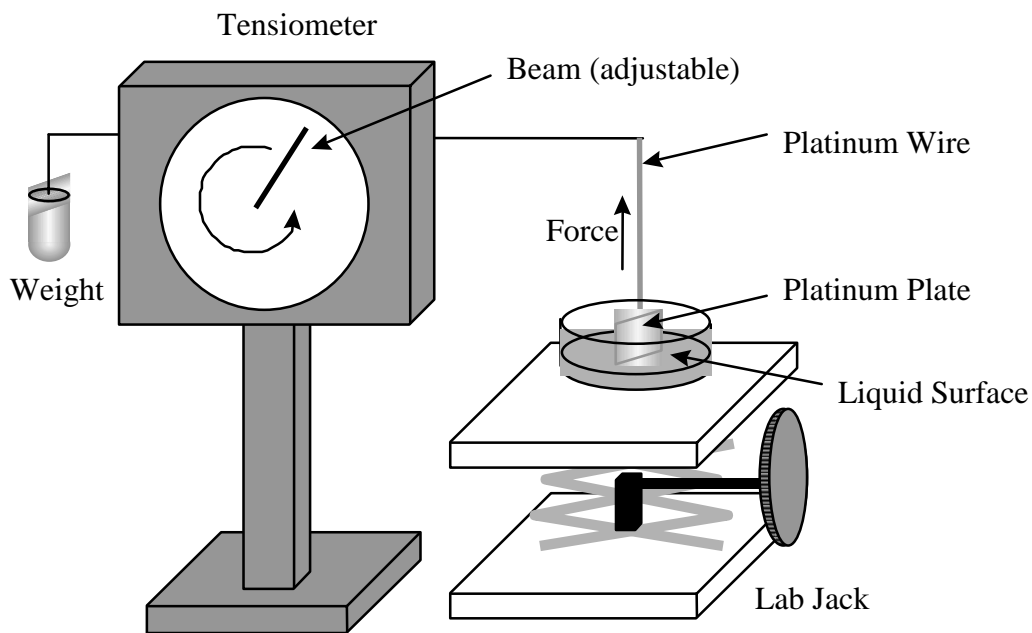


Figure 3.4 Wilhelmy plate method apparatus



The first test was performed with pure lubricant to help establish a benchmark to which the surface tension of refrigerant/lubricant mixtures and dynamic surface tension curves can be compared in the future. Then, the method was used to measure static surface tension of the baseline refrigerant/lubricant pairs. For the baseline tests, liquid refrigerant samples (R-12 and R-22) were added to each mineral oil in incremental amounts until a refrigerant composition of 10% (within approximately 1%) by weight was achieved. Precise compositional data was not known because of the high volatility rate of the refrigerants.

Results and Discussion

The average static surface tension results, from numerous trials, are shown in Table 3.3. The polyolesters, as well as both the mineral oils have similar surface tensions, however the polyolesters have a lower surface tension than the mineral oils by about 3 dynes/cm.

The static surface tension data of refrigerant/lubricant mixtures at various compositions are presented in the following chapter.

Table 3.3 Static surface tension of pure lubricants at 25°C
(Refer to [Table A3.3](#) in the Appendix)

Lubricant Type	Surface Tension (dyn/cm)	Standard Deviation
Witco 4GS	31.6	±0.17
Witco 3GS	31.5	±0.13
Witco SL68	28.9	±0.14
ICI RL68H	28.6	±0.06

4. SURFACE PROPERTIES OF REFRIGERANT/LUBRICANT MIXTURES

4.1 Baseline Static Surface Tension

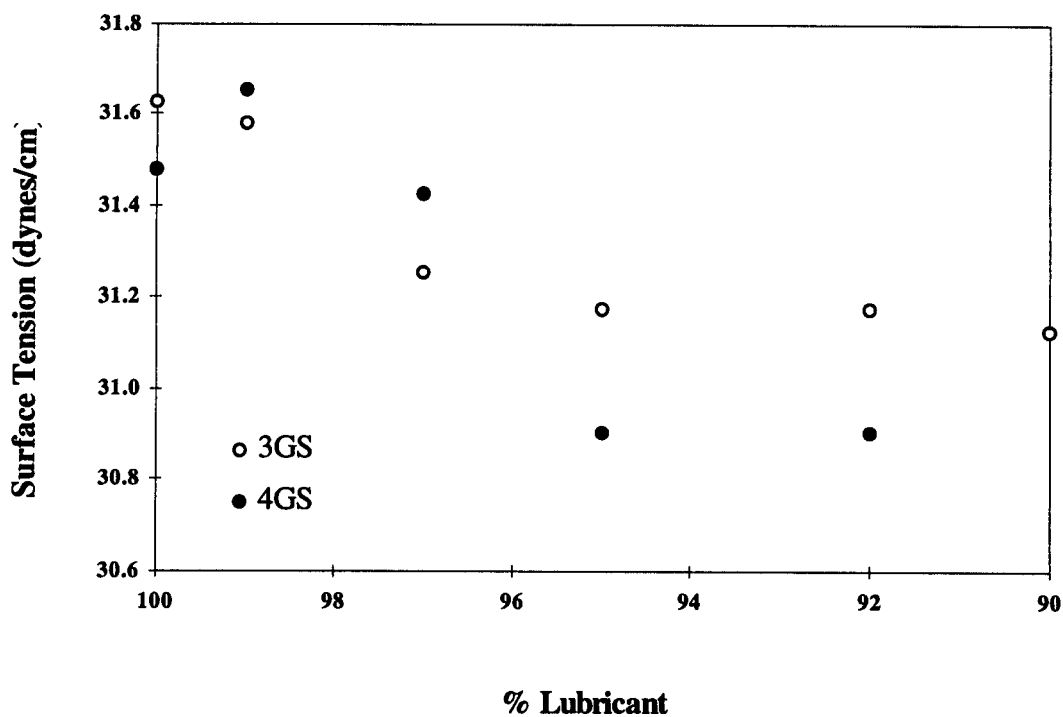
4.1.1 Background

The Wilhelmy plate method ([Section 3.2.3](#)) was used to measure static surface tension of the refrigerant/lubricant baseline pairs. The difference being that instead of a tensiometer, a force transducer was used to measure the force required to lift the Wilhelmy plate from the refrigerant/lubricant mixture surface. For the baseline test, liquid refrigerant samples (R-12 and R-22) were added to each mineral oil in incremental amounts until a refrigerant composition of 10% (within approximately 1%) by weight was achieved. Precise compositional data was not known because of the high volatility rate of the refrigerants.

4.1.2 Results and Discussion

For the tests performed on the refrigerant/lubricant mixtures, the static surface tension at various compositions is presented in [Figure 4.1](#). The figure reveals a greater decrease in surface tension with composition for the R-12/4GS sample than the R-12/3GS sample. Based upon this phenomenon, one would conclude that the 4GS lubricant should produce foam more easily than the 3GS lubricant in a foam column aerated with R-12. The lowering of surface tension correlates to a higher surface activity of the refrigerant/lubricant molecular interaction. Stable surface tension concentration corresponds to a system whose surface activity is not significantly enhanced by the interaction of refrigerant and lubricant. Thus, for the R-12/4GS sample, the refrigerant

Figure 4.1 Static surface tension of R-12/mineral oil mixtures
(Refer to [Table 4.1](#) in the Appendix)



seems to behave as a surfactant, adhering to the surface rather than in the bulk of the lubricant. For the 3GS system, the R-12 appears to be contained in the bulk. These facts correlate rather well when size of the molecules is considered. Refrigerants R-12 and R-22 are small, one-carbon-chain molecules. The mineral oils, however, are long-chain hydrocarbons but the size distribution in the 3GS oil is significantly lower than that of the 4GS oil. Hence, the interaction is greater for the R-12/4GS sample. These lubricants were also tested with R-22. However, upon examination of [Tables 4.1.4](#) and [4.1.5](#) in the Appendix, the R-22 mixtures behaved contrary to the R-12 mixtures. In short, the data reveals a greater lowering in static surface tension for the 3GS oil than for the 4GS oil.

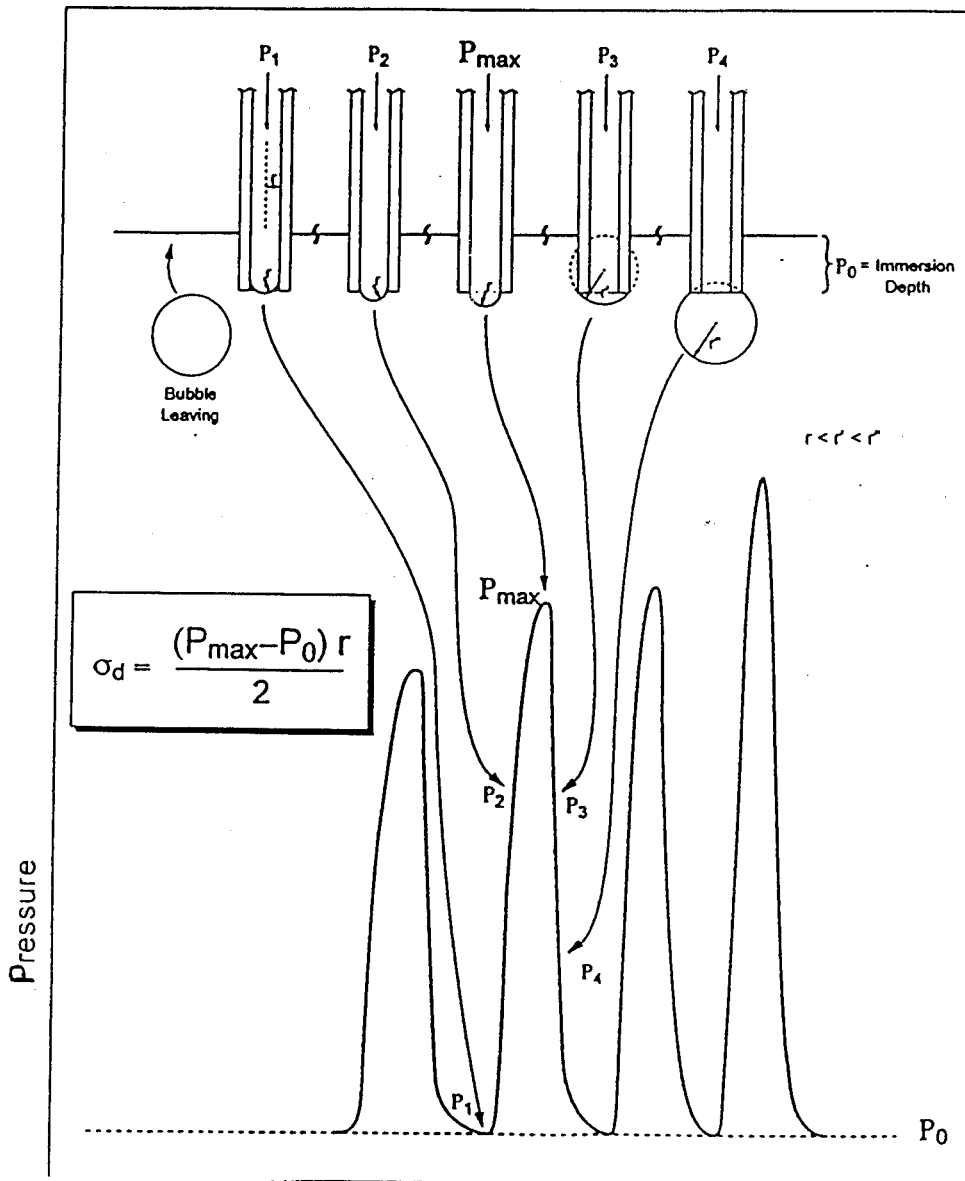
4.2 Dynamic Surface Tension

4.2.1 Background

The influence of refrigerants in refrigerant/lubricant mixtures can have a profound effect on the dynamic surface tension of the system and, thus, have an effect on the foaming characteristics of the refrigerant/lubricant system. These measurements are important for examining the change, or lack of change, in surface tension.

The maximum bubble pressure method (MBPM) is used to measure the dynamic bubble pressure. In essence, a tube is immersed below the surface of a liquid. A gas is then allowed to flow through the tube while monitoring its pressure. Initially, a curved, liquid gas interface forms inside the tube. Following this stage, the pressure rises to force the curved interface down to the end of the tube. When the bubble achieves a perfectly hemispherical shape at the end of the tube, maximum bubble pressure exists which can be related to surface tension. [Figure 4.2](#) illustrates the lifetime bubble pressure of each

Figure 4.2 Evolution of a single bubble from the capillary using the MBP method (Gilman, 1993)



bubble. The equation shown in the figure relates this maximum bubble pressure to surface tension.

4.2.2 Experimental Apparatus

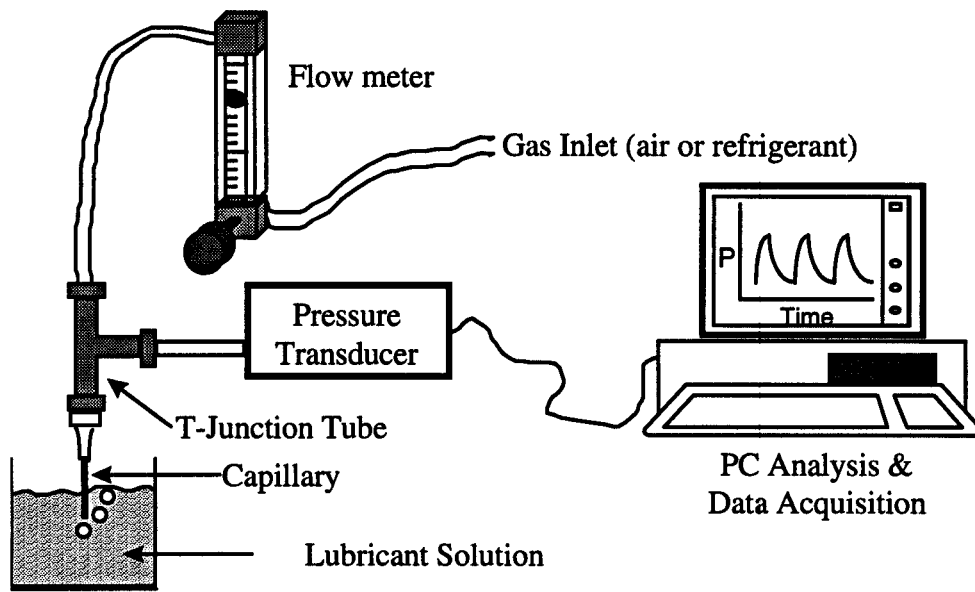
The experimental setup is illustrated in [Figure 4.3](#). A fine, stainless steel capillary (diameter on the order of 0.01 inches), is immersed 1 cm below the surface of the liquid for each trial. Bubbles are produced continuously by blowing gas through the tube and the bubble rates are controlled by a rotameter. The pressure of each bubble was monitored by a differential pressure transducer, which is connected to an oscilloscope and a data acquisition system. Thus, both bubble lifetime (frequency) and maximum bubble pressure are calculated for each flow rate.

4.2.3 Experimental Procedure

The apparatus is calibrated with two standards, twice distilled water and High Performance Liquid Chromatography (HPLC) grade methanol (99%). These substances are almost pure and definitely non-surface active, hence, their surface tension does not change with bubble frequency. They were used to establish high and low extremes used to relate transducer voltage output to surface tension.

Usually, each trial consists of varying the flow rate of vapor in order to obtain a series of bubble rate/surface tension pairs. The pairs can be obtained by randomly selecting flow rates, but the method is usually performed starting at high flow rates and progressively decreasing to virtually static conditions, or starting at low flow rates and

Figure 4.3 Maximum bubble pressure apparatus



progressively increasing the bubble frequency till individual bubbles cannot be resolved. This allows for more efficient sampling.

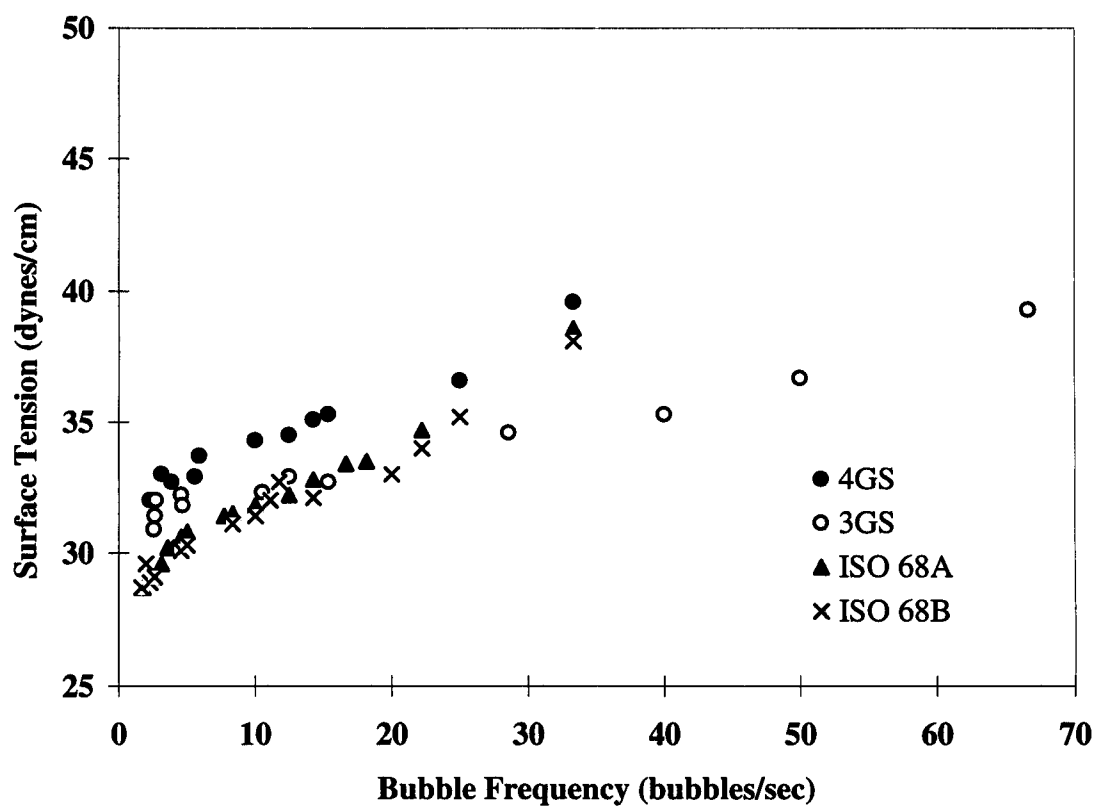
The lubricants, in the presence of refrigerants, were tested at various bubble frequencies to establish dynamic surface tension plots which can be compared to similar plots for refrigerant/lubricant mixtures. The tests were repeated with lubricant samples containing 10% refrigerant by weight and these results were then compared to the original curves for the pure lubricants to analyze changes and overall effect of the refrigerants. As with the static surface tension measurements of the refrigerant/lubricant mixtures, the composition of the mixture was not known exactly (within 1%).

Since the foaming system most relevant to the refrigeration compressor involves only refrigerant and lubricants mixtures, the majority of the experiments using the maximum bubble pressure apparatus involved injecting refrigerant vapor through the capillary as opposed to air (which yields dynamic *surface* tension results), thus yielding dynamic *interfacial* tension (IFT) results.

4.2.4 Results & Discussion: Dynamic Surface Tension (Baseline Tests)

Figure 4.4 reveals that the mineral oils have distinct dynamic surface tension behavior and their relevance increases with increasing bubble frequency. In addition, the 4GS data have a steeper increase in surface tension with bubble rate while the 3GS data have a flatter increase which, in theory, indicates that the 3GS oil is comprised of smaller molecules than the 4GS oil. Indeed, this is the case. The figure also shows that the synthetic polyolesters have similar dynamic behavior when compared to each other. In terms of bubble frequency resolution, the 3GS sample allows a bubble rate in the

Figure 4.4 Dynamic surface tension plot for pure lubricants at 25°C
(Refer to [Table A4.2](#) in Appendix)



neighborhood of 70 bubbles per second, a value which is much higher than any other bubble rate attainable with the other sample. This is most likely due to the fact that the 3GS sample has a considerably lower viscosity than the other three lubricants.

The dynamic surface tension test results of the refrigerant/lubricant mixtures injected with air are presented in [Figures 4.5](#) and [4.6](#), which show the influence of both R-12 and R-22 on the 3GS and 4GS mineral oil samples. There is little difference among the refrigerants on a given sample. As the R-12 and R-22 data points seem to fall on top of each other. The main discrepancy among the mineral oil samples is that the 4GS sample ([Figure 4.5](#)) seems to have a greater lowering of the surface tension, by about 1-2 dynes/cm at low bubble rates and by 2-5 dynes/cm at high bubble rates, than the 3GS sample ([Figure 4.6](#)), whose surface tension is lowered by less than 1 dyne/cm at all bubble frequencies. The synthetic polyolesters were also tested and there seems to be very little difference, regardless of bubble frequency, between the polyolesters themselves. They show smaller differences (1 dyne/cm or less) at low bubble rates and a greater difference (4 dynes/cm) at higher bubble rates.

4.2.5 Results & Discussion: Dynamic *Interfacial* Tension (Baseline Tests)

Results for the baseline lubricants, with 10% R-22, are shown in [Figure 4.7](#). It appears that there is one major difference between injecting refrigerant, as opposed to air, through the capillary and it is that, at low bubble frequencies, the interfacial tension of the lubricants begins to increase from a point where the surface tension is already lowered approximately 2 dynes/cm for both 4GS and 3GS mineral oils. Both curves have a similar, characteristic steep rise which does not say much about the size of the molecules

Figure 4.5 Dynamic surface tension of 4GS mineral oil with 10% (by weight) baseline refrigerant (Refer to [Table A4.3.2](#) in Appendix)

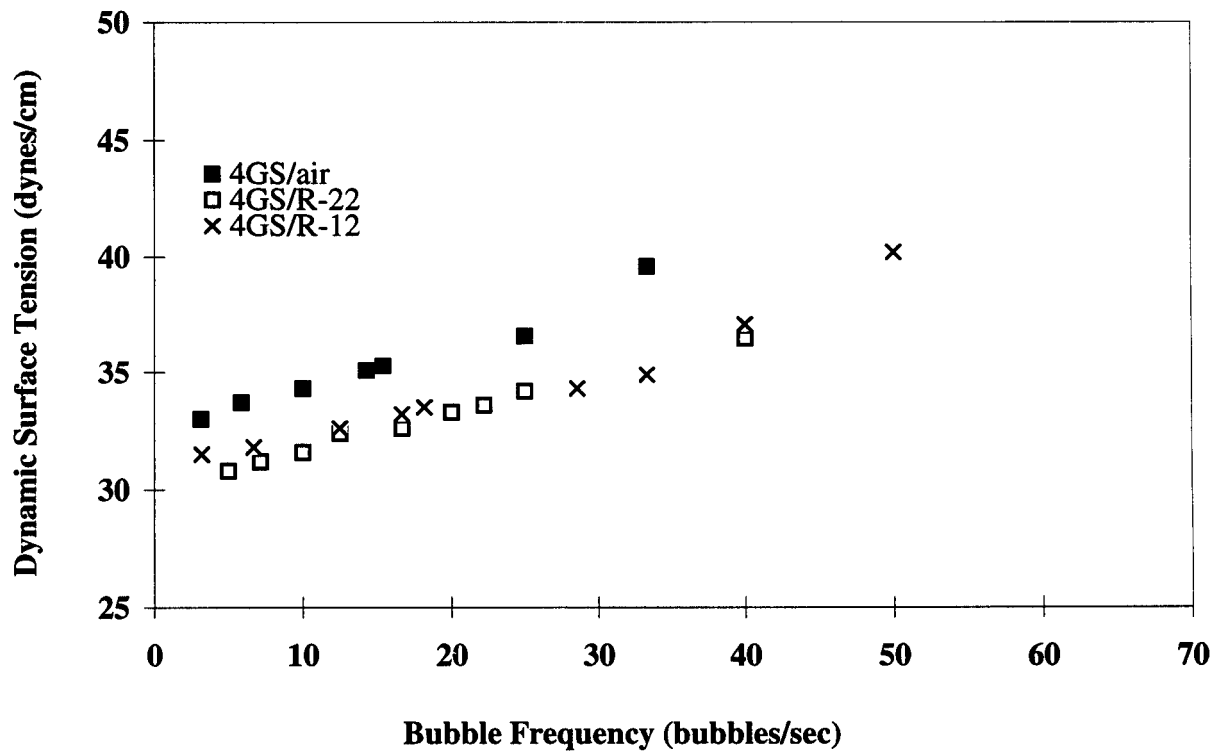
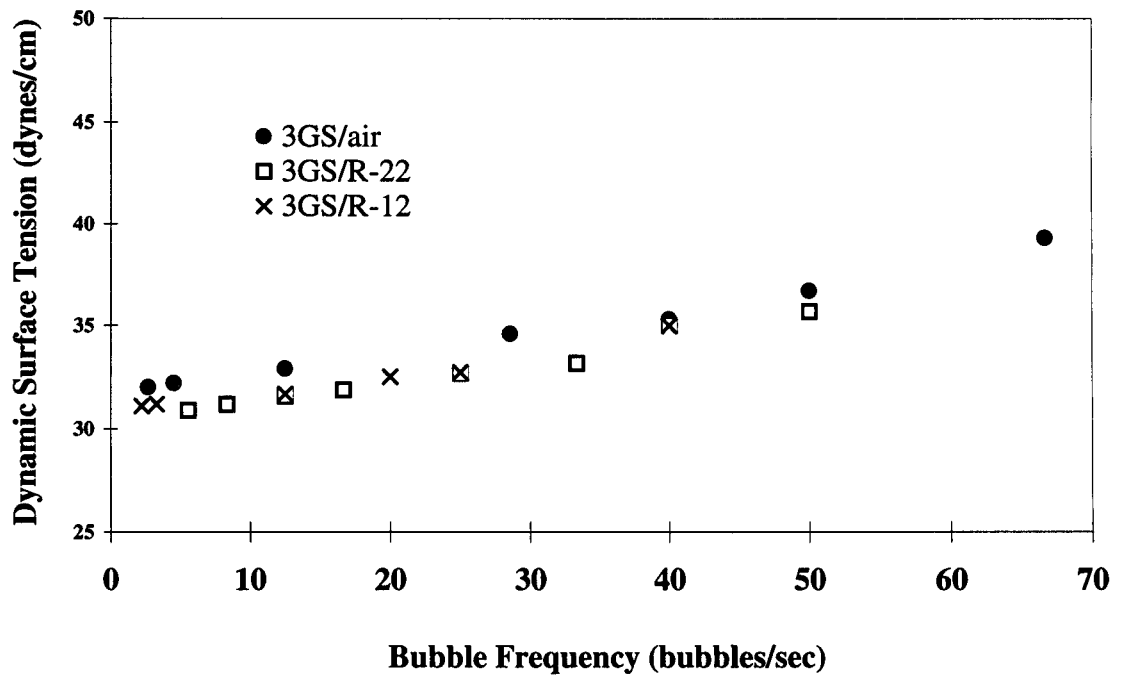


Figure 4.6 Dynamic surface tension of 3GS mineral oil with 10% (by weight) baseline refrigerant (Refer to [Table A4.3.2](#) in Appendix)



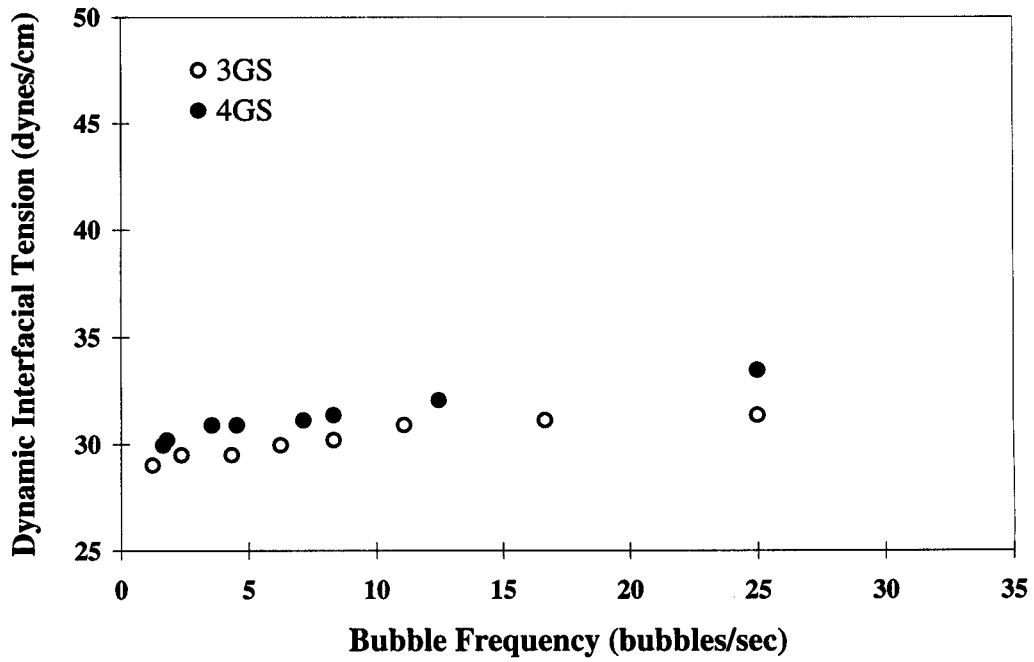
which are adhering to the interface. Recall that the larger 4GS molecules result in a much steeper increase than the smaller 3GS molecules (see [Figure 4.4](#)), whose data displayed a more gradual increase in dynamic surface tension with increasing bubble frequency.

4.2.6 Results & Discussion: Dynamic Interfacial Tension (Single-component HFCs)

The effect of HFCs on POE lubricants is measured by how much dynamic interfacial tension deviates from the original air/POE surface tension curve determined in [Figure 4.4](#). Recall that the greater the lowering of the dynamic surface tension, the greater the foamability and foam stability.

Although the MBPM using HFC/POE systems (without air injection) is a more accurate method for studying dynamic interfacial tension of the refrigerant/lubricant mixtures, there is some degree of error that must be accounted for when running each trial. It has been documented in previous studies that HFC refrigerants such as R-32, R-125, R-134a and R-143a have some degree of miscibility with polyolester lubricants (Zoz et al., 1994). While there is only a small amount of refrigerant that is passed through the capillary during each MBP trial, it is assumed that the lubricant concentration at the end of each trial is not 100%. Since the R-32/POE system was found to be only partially miscible in previous research (Zoz et al., 1994), the R-125 and R-124a refrigerants are more likely to affect the MBP measurements than R-32. Thus, the R-125/Witco SL68 POE pair was chosen to test the significance of the experimental error involved. This was done by performing the MBP test twice: first, steadily increasing the bubble frequency from near static conditions to high bubble frequencies, and second, starting at a high

Figure 4.7 Dynamic interfacial tension of baseline oils with R-22
(Refer to [Table A4.4.1](#) in [Appendix](#))



bubble rate and progressively decreasing the bubble rate till near static conditions are achieved (less than 1 bubble/sec bubble frequency). A third trial was performed to ensure the validity of the correlation.

Direction of Bubble Frequency Progression

The R-125/Witco SL68 POE trials ([Figure 4.8](#)) revealed that there is relatively little difference between beginning the trials from low (trials 1 and 3) or high (trial 2) bubble rates. Even though there is some degree of compositional change in the liquid lubricant, it appears that the amount of refrigerant is small enough to neglect this difference.

Comparison of POE Lubricants using single-component HFCs

Each POE lubricant, ICI RL68H and Witco SL68, was tested with aforementioned, non-chlorinated HFCs. It was observed that the ICI lubricant yielded slightly higher dynamic interfacial tension curves than the Witco lubricant ([Figures 4.9 through 4.11](#)) for R-32, R-125 and R-134a. However, this was not the case with R-143a ([Figure 4.12](#)). The greatest discrepancy between the two lubricants was exhibited in the R-125 system ([Figure 4.9](#)) where the difference in the two curves ranged from 1 to 4 dynes/cm from bubble frequencies between 0 and 20 bubbles/second. Although the ICI sample produced a greater dynamic interfacial tension curve than the Witco sample at all bubble rates, [Figures 4.10 and 4.11](#) show that the difference is rather insignificant.

Figure 4.8 Dynamic interfacial tension vs. direction of bubble frequency progression using R-125 & Witco SL68 POE system
(Refer to [Tables A4.5.3, A4.5.4 and A4.5.7](#) in the Appendix)

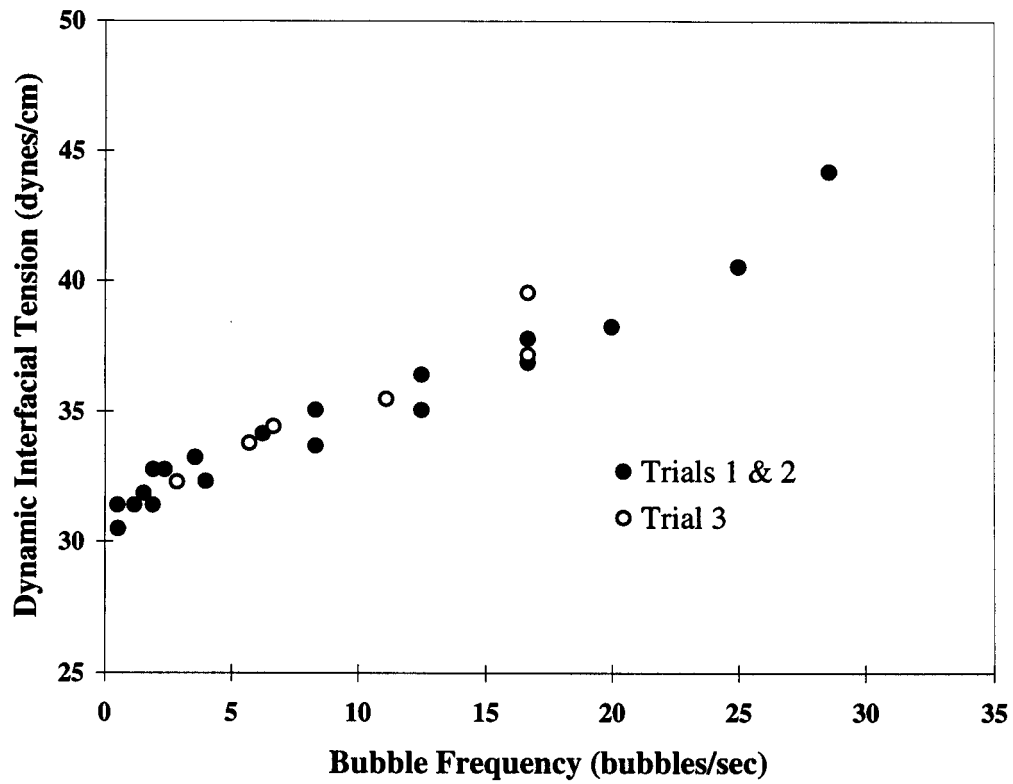


Figure 4.9 Dynamic interfacial tension vs. POE type using R-125
(Refer to [Tables A4.5.3](#), [A4.5.4](#) and [A4.5.7](#) in the Appendix)

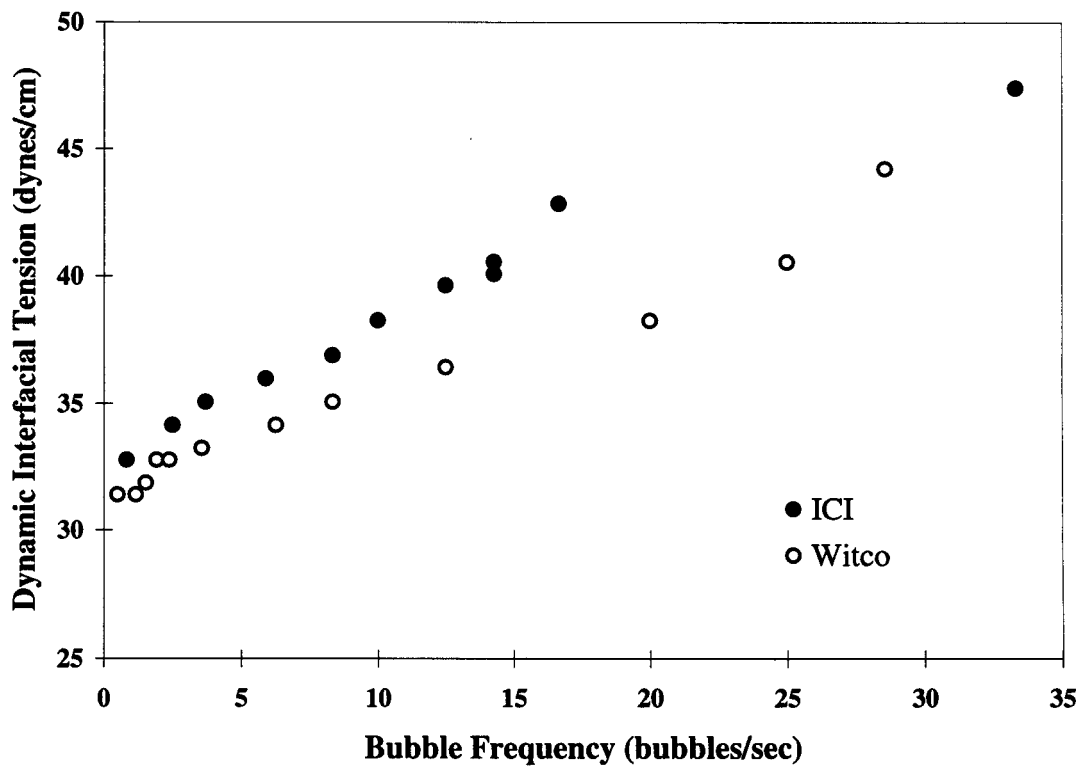


Figure 4.10 Dynamic interfacial tension vs. POE type using R-32
(Refer to [Table A4.5.5](#) in the [Appendix](#))

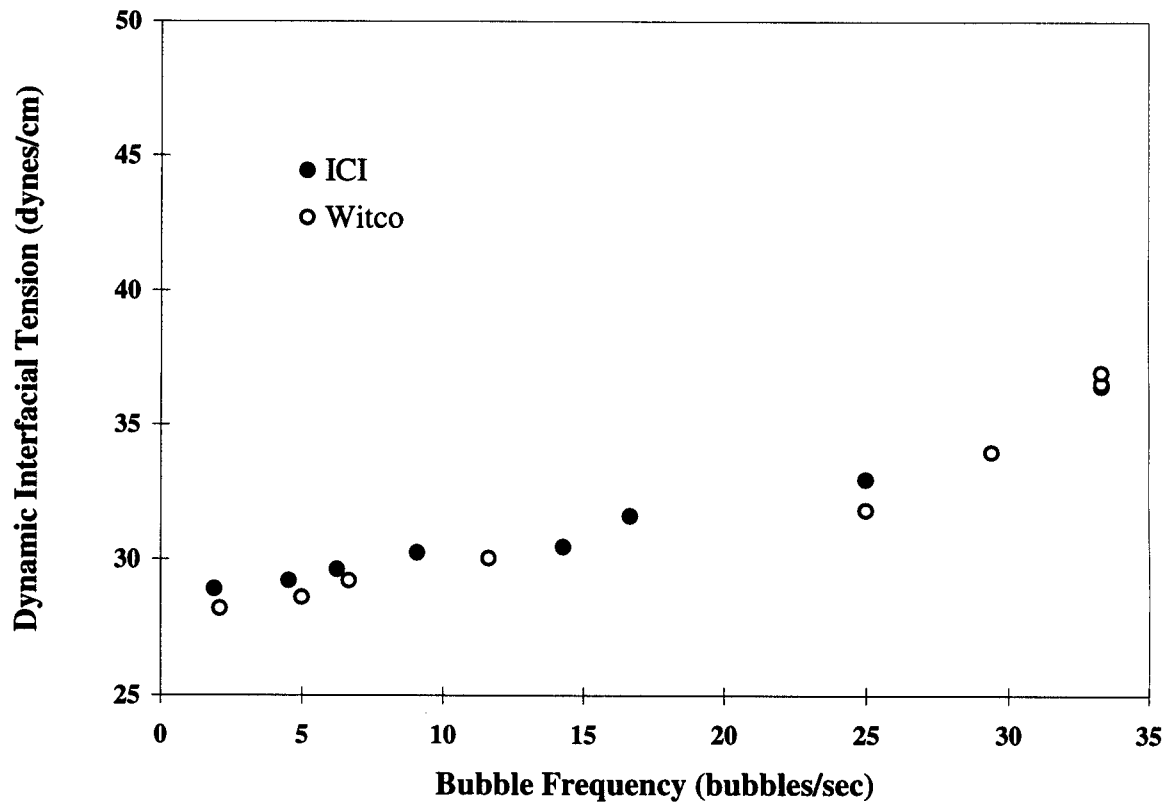


Figure 4.11 Dynamic interfacial tension vs. POE type using R-134a
(Refer to [Table A4.5.1](#) and [A4.5.2](#) in the [Appendix](#))

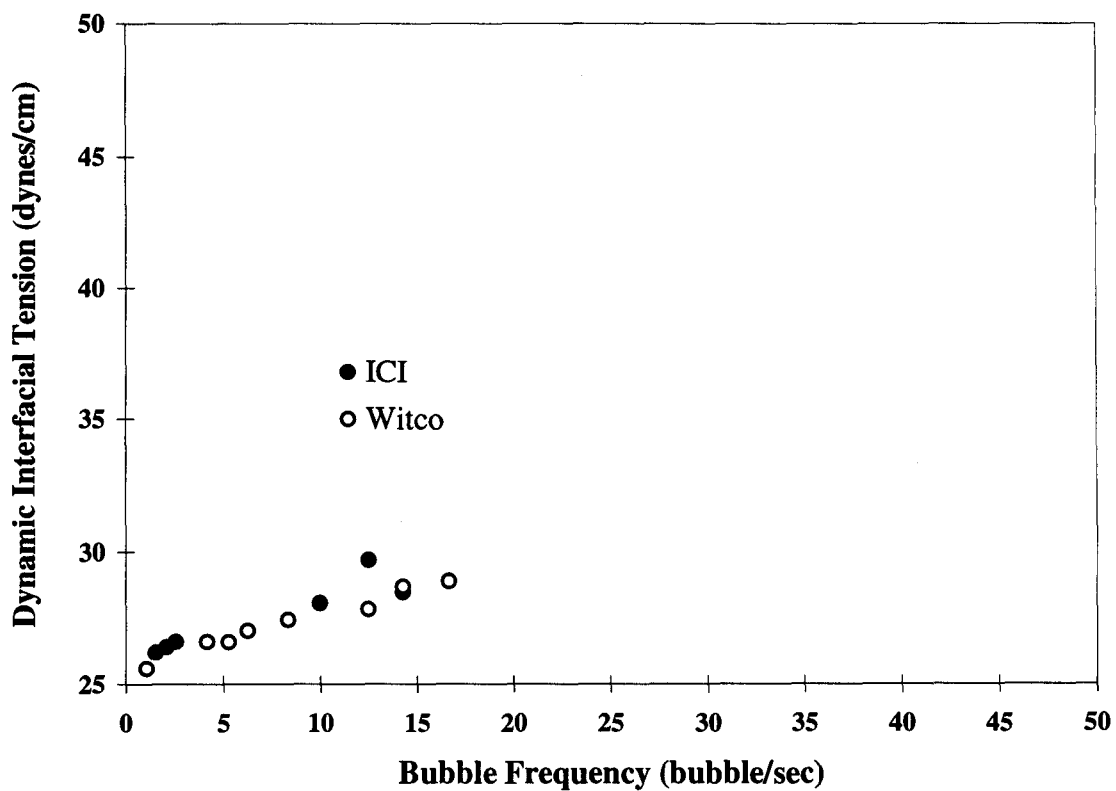
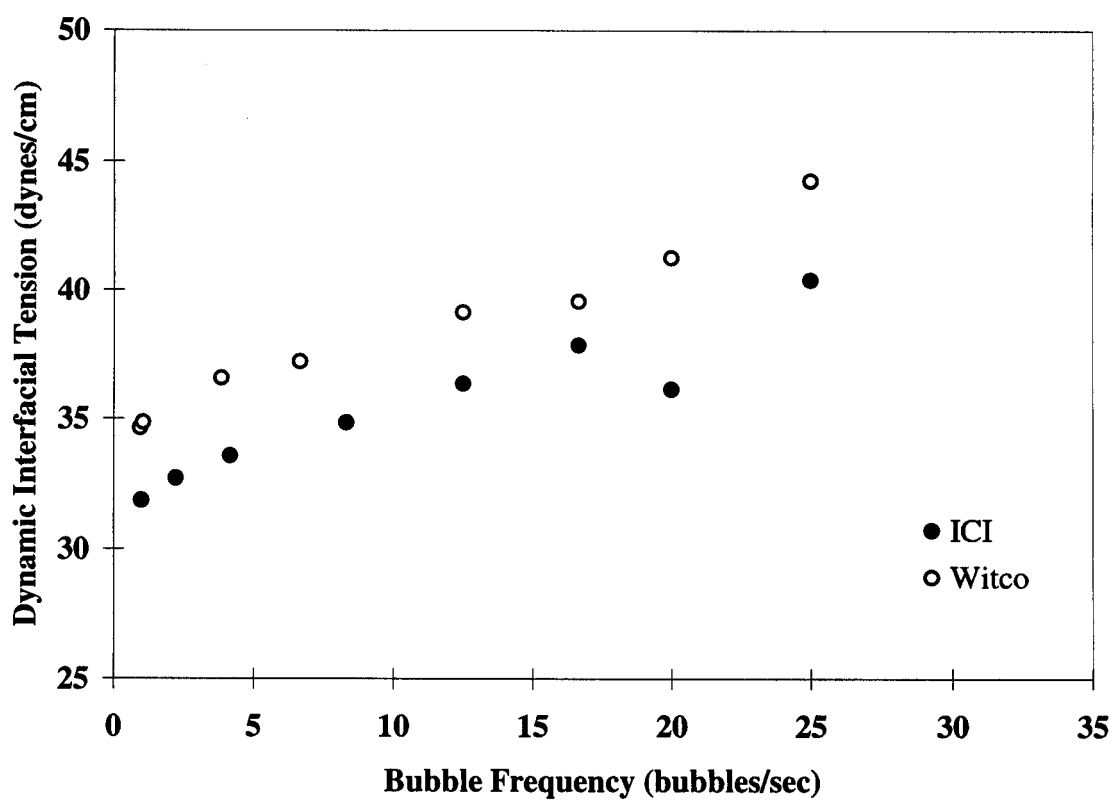


Figure 4.12 Dynamic interfacial tension vs. POE type using R-143a
(Refer to [Table A4.5.6](#) in the [Appendix](#))



Original paper did not include a page 33.

Figure 4.13 Dynamic interfacial tension vs. HFC injection type using Witco SL68 POE
 (Refer to Tables A4.5.1 through A4.5.7 in the Appendix)

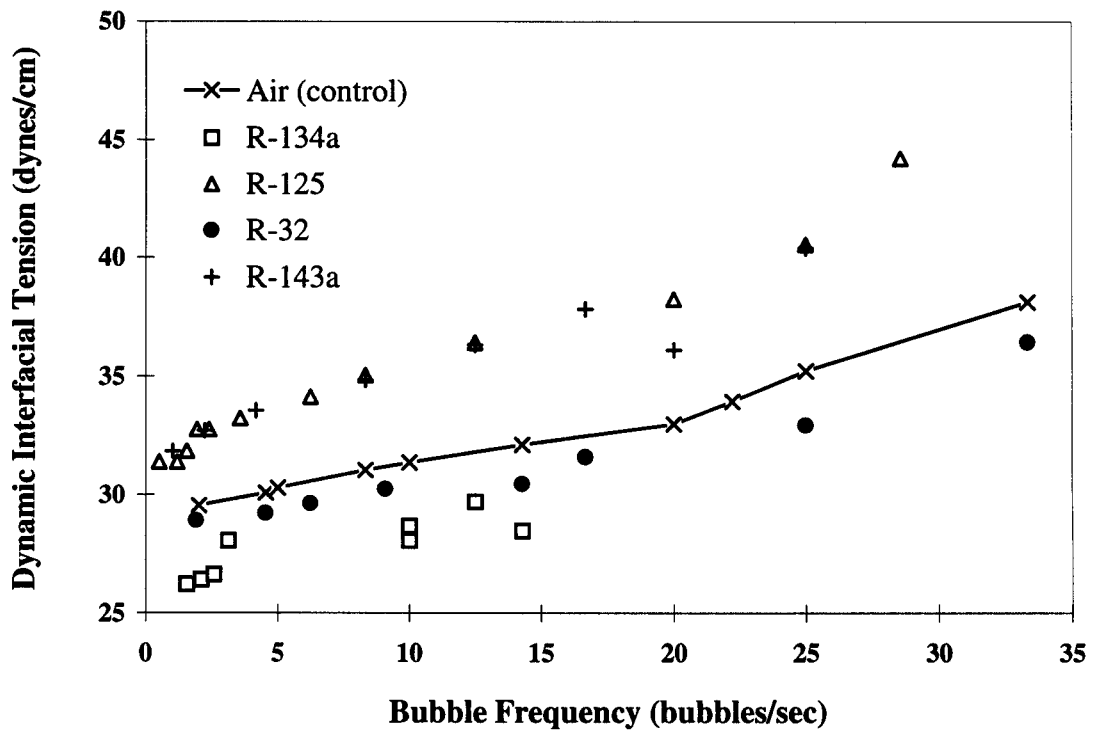
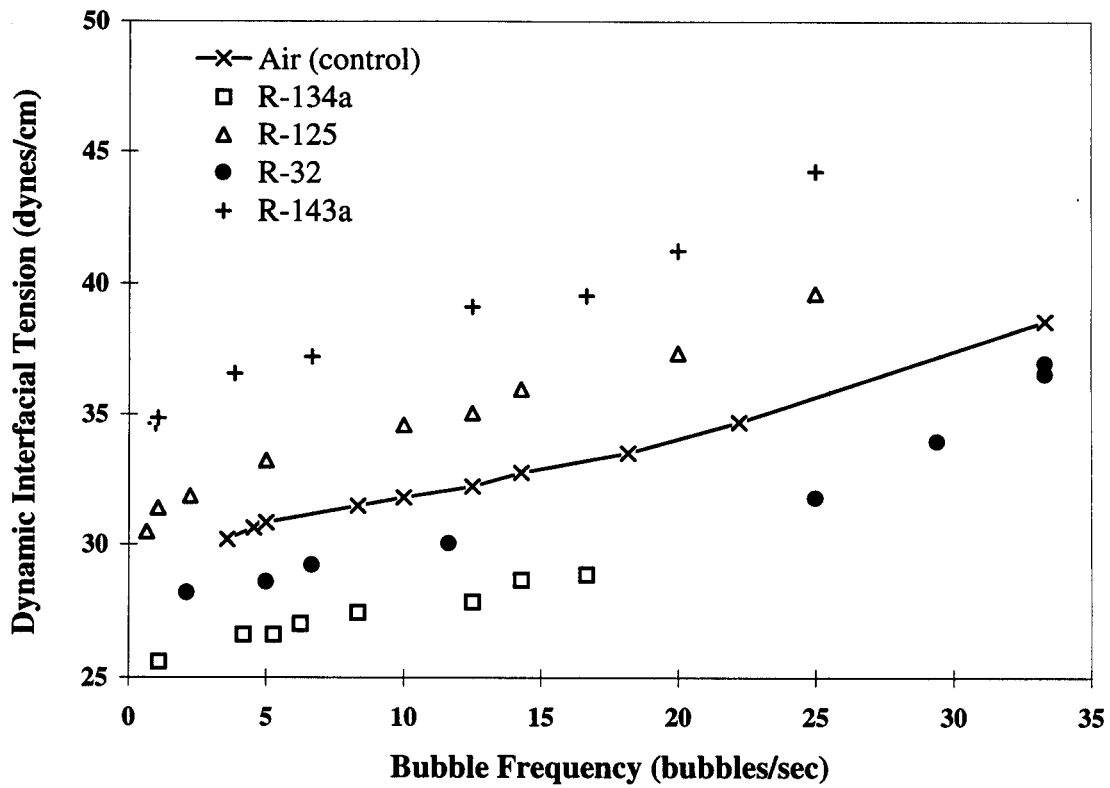


Figure 4.14 Dynamic interfacial tension vs. HFC injection type using ICI RL68H POE
 (Refer to [Tables A4.5.1](#) through [A4.5.7](#) in the [Appendix](#))



4.2.7 Results & Discussion: Dynamic *Interfacial* Tension (Blended HFCs)

The only change in the experimental methodology from previous maximum bubble pressure experiments is that the blended refrigerants must be drawn off initially in liquid form to ensure that the composition of each blend remains constant from the time they are in the storage container to the time they are injected through the fine capillary. Once the blends are vaporized as they pass through the pressure regulator, they can be regulated with the same rotameter that has been used for the previous MBP trials.

Direction of Bubble Frequency Progression

Although previous results (Figure 4.8) revealed that there is little difference between the direction bubble frequency progresses, the blends were tested twice in this same manner. Figures 4.15 to 4.17 support the previous findings.

Comparison of POE Lubricants using HFC Blends

Both trials (low-to-high and high-to-low) were combined for each blended HFC/POE pair and used to quantify any possible discrepancies between lubricants for a given blended refrigerant. Figure 4.18 shows that there is practically no difference between the lubricants on R-404A. For R-407C (Figure 4.19), the ICI and Witco plots begin to deviate at approximately 15 bubbles per second. Below 15 bubbles/sec, the two plots are identical. Although Figure 4.20 displays somewhat of an unimpressive scatter, it can be inferred that the R-410A/Witco POE system possesses higher interfacial tension values than the R-412A/ICI POE system at all bubble frequencies between 0 and 35 bubbles per second.

Figure 4.15 Dynamic interfacial tension vs. direction of bubble frequency progression using R-404A & ICI RL68H POE
(Refer to [Tables A4.6.1](#) and [A4.6.5](#) in the [Appendix](#))

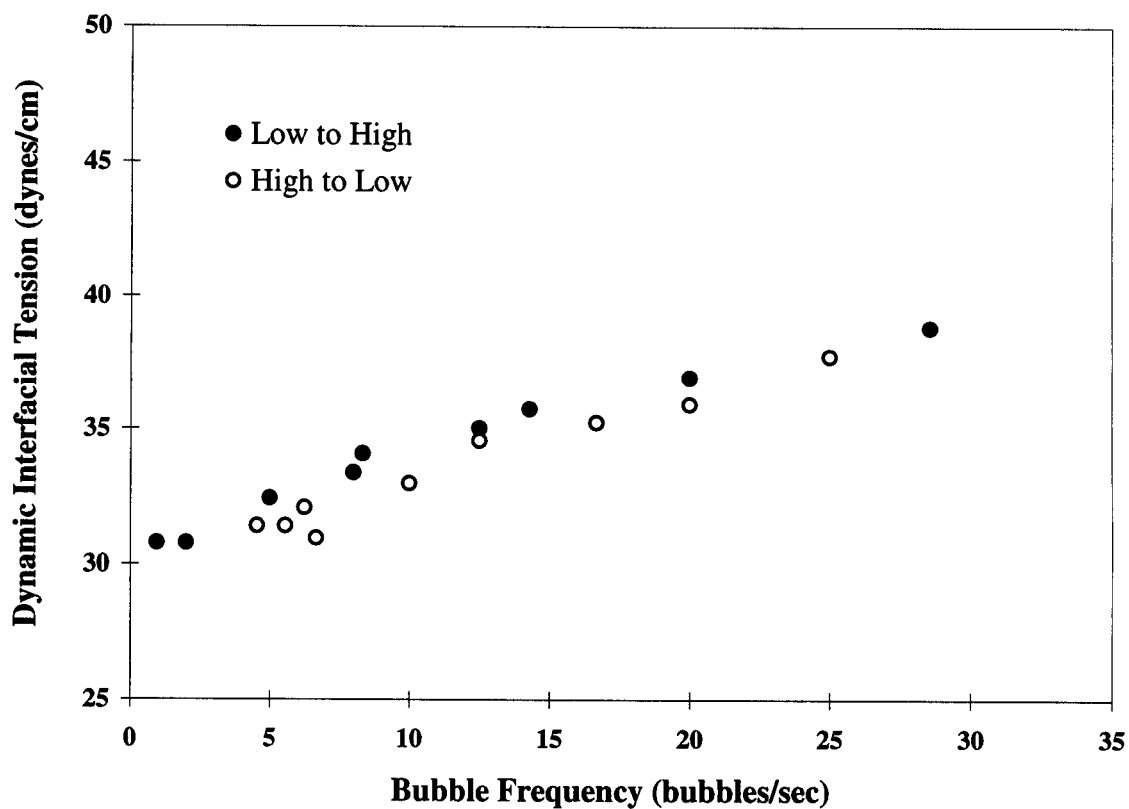


Figure 4.16 Dynamic interfacial tension vs. direction of bubble frequency progression using R-407C & Witco SL68 POE (Refer to Tables A4.6.2 and A4.6.6 in the Appendix)

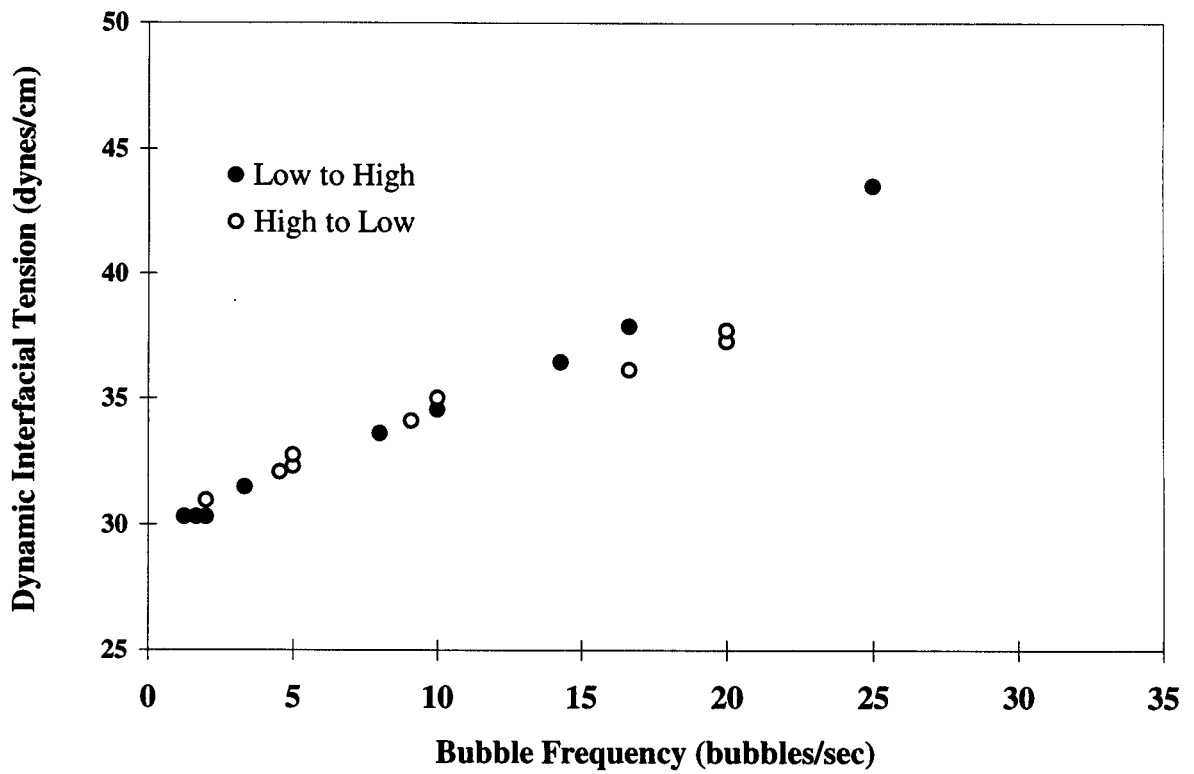


Figure 4.17 Dynamic interfacial tension vs. direction of bubble frequency progression using R-410A & Witco SL68 POE (Refer to [Tables A4.6.3](#) and [A4.6.5](#) in the [Appendix](#))

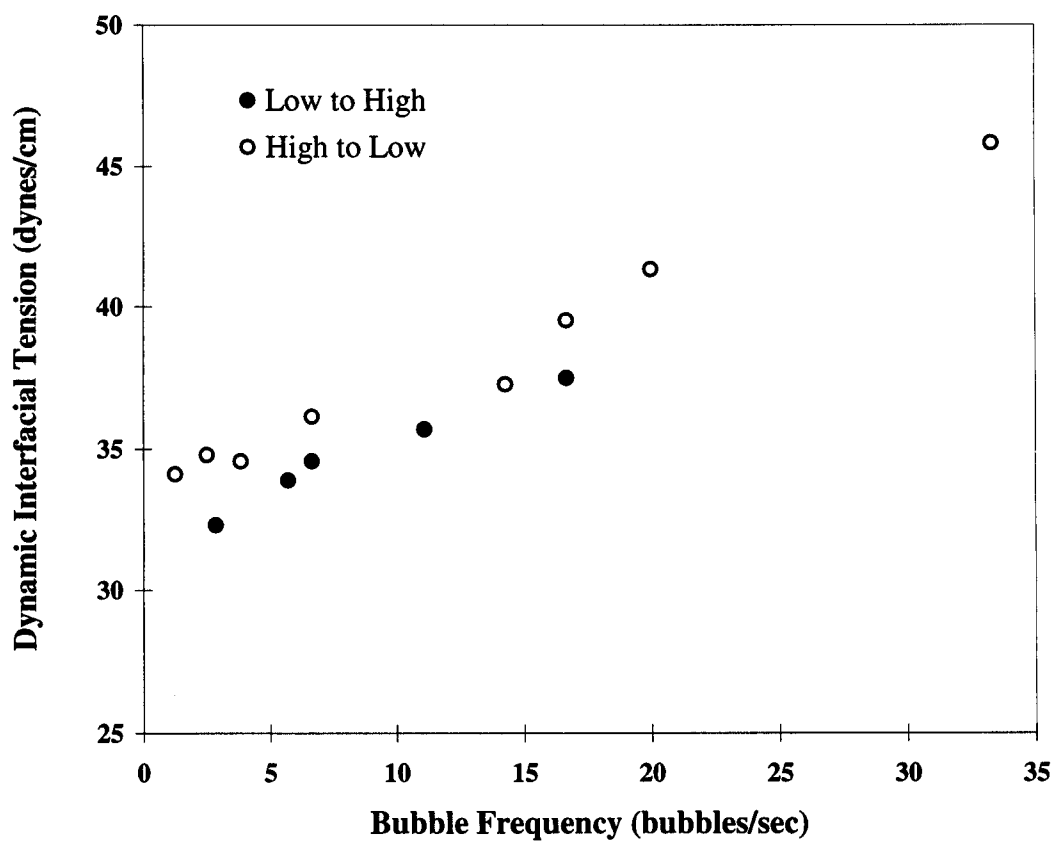


Figure 4.18 Dynamic interfacial tension vs. POE type using R-404A
(Refer to [Tables A4.6.1](#) and [A4.6.4](#) in the [Appendix](#))

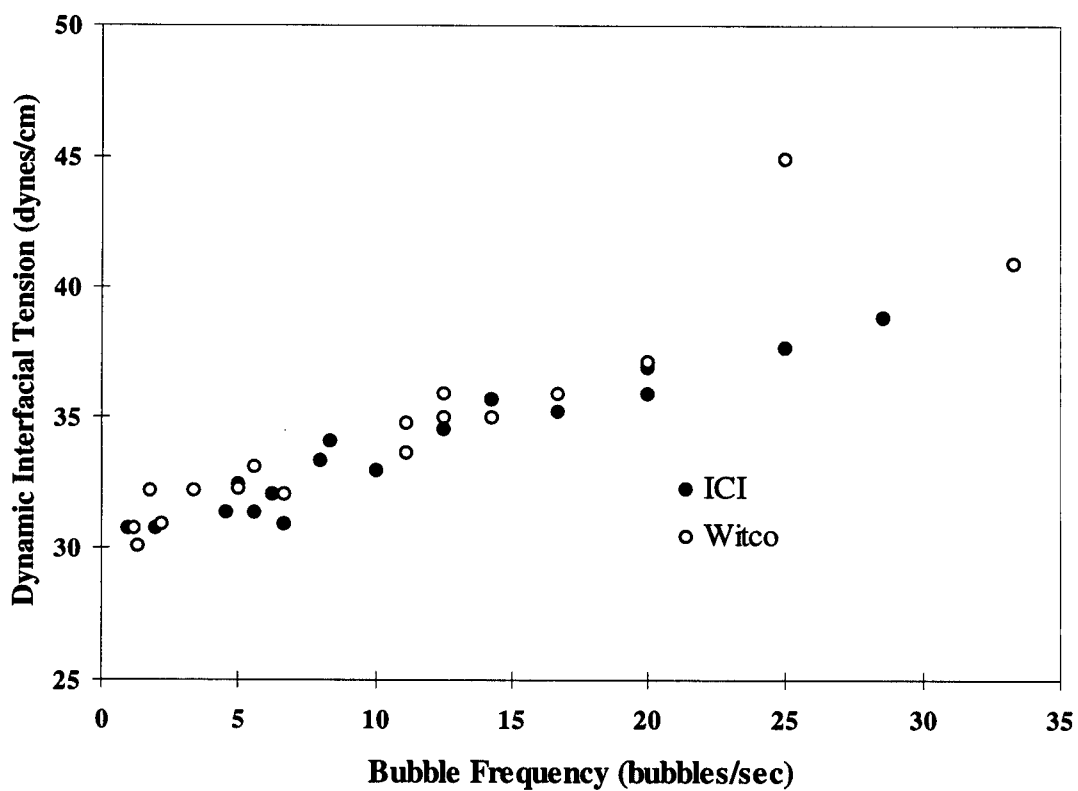


Figure 4.19 Dynamic interfacial tension vs. POE type using R-407C
 (Refer to [Tables A4.6.2](#) and [A4.6.6](#) in the [Appendix](#))

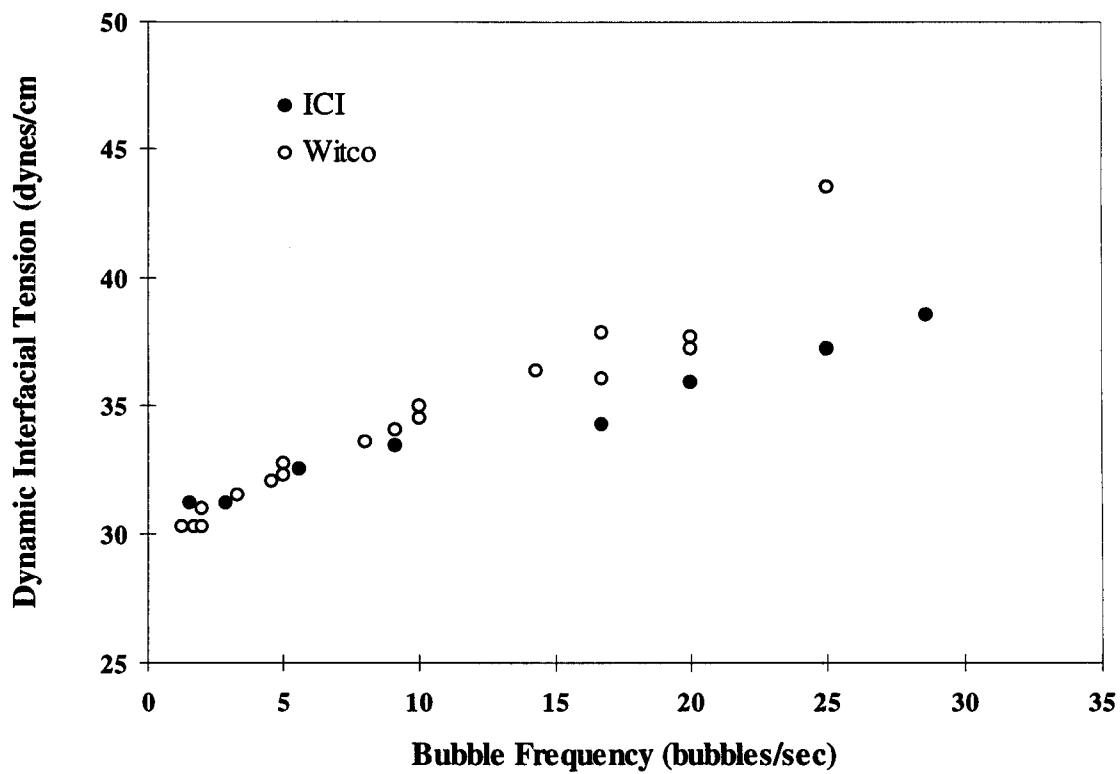
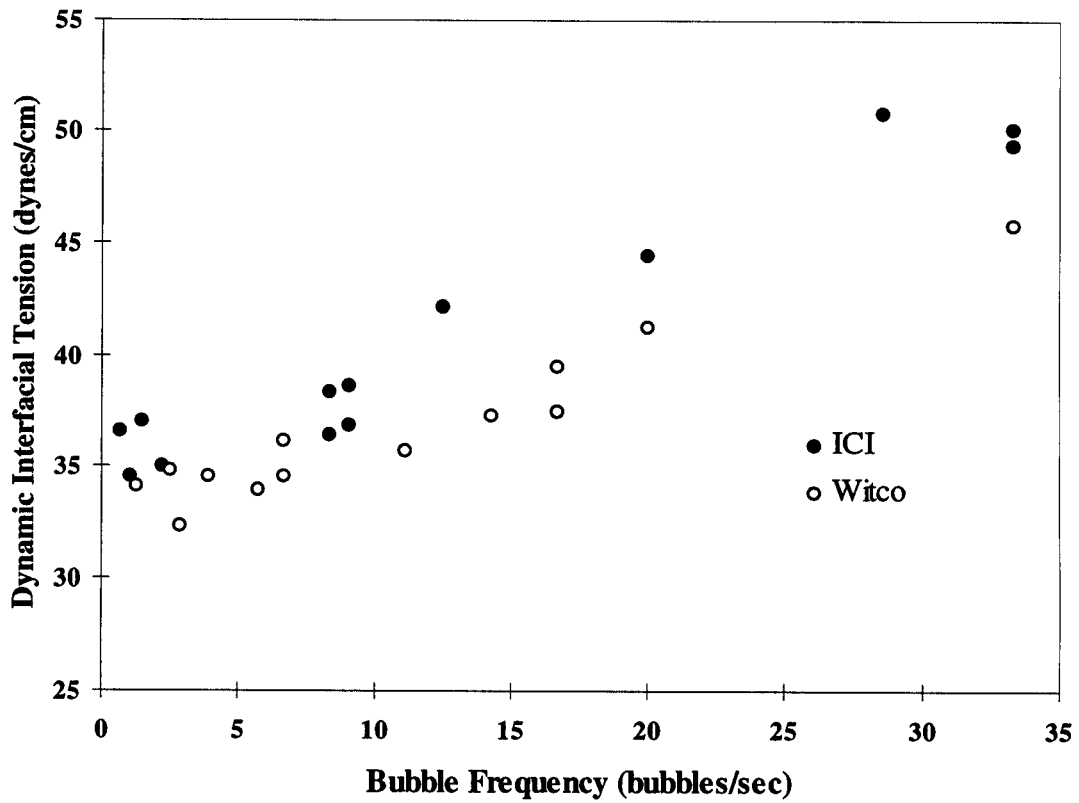


Figure 4.20 Dynamic interfacial tension vs. POE type using R-410A
(Refer to [Tables A4.6.3](#) and [A4.6.5](#) in the [Appendix](#))



Comparison of Blended HFC/POE Interfacial Tension with Air/POE Surface Tension

All curves for both Witco (Figure 4.21) and ICI (Figure 4.22) polyolester systems were situated above the air/POE surface tension curve. Although this fact cannot be directly attributed to the HFC quantities within each blend, it should be noted that R-404A is 44% R-125 and 52% R-143a, the two HFCs which exhibit higher dynamic IFT than the baseline air/POE surface tension curve. In addition, R-410A is 50% R-125 with the other 50% being R-32, and HFC whose dynamic interfacial tension curve is close to, albeit lower than, the air/POE curve.

Figure 4.21 Dynamic interfacial tension vs. HFC blend type using Witco SL68 POE
 (Refer to [Tables A4.6.1](#) through [A4.6.6](#) in the [Appendix](#))

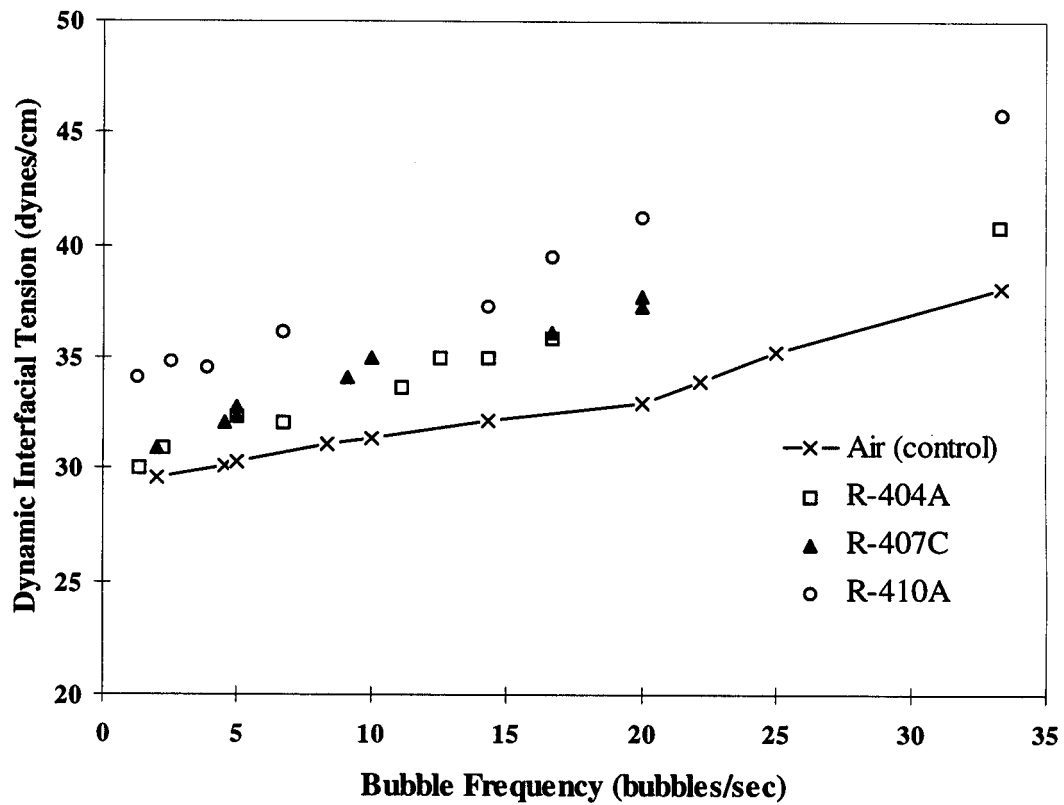
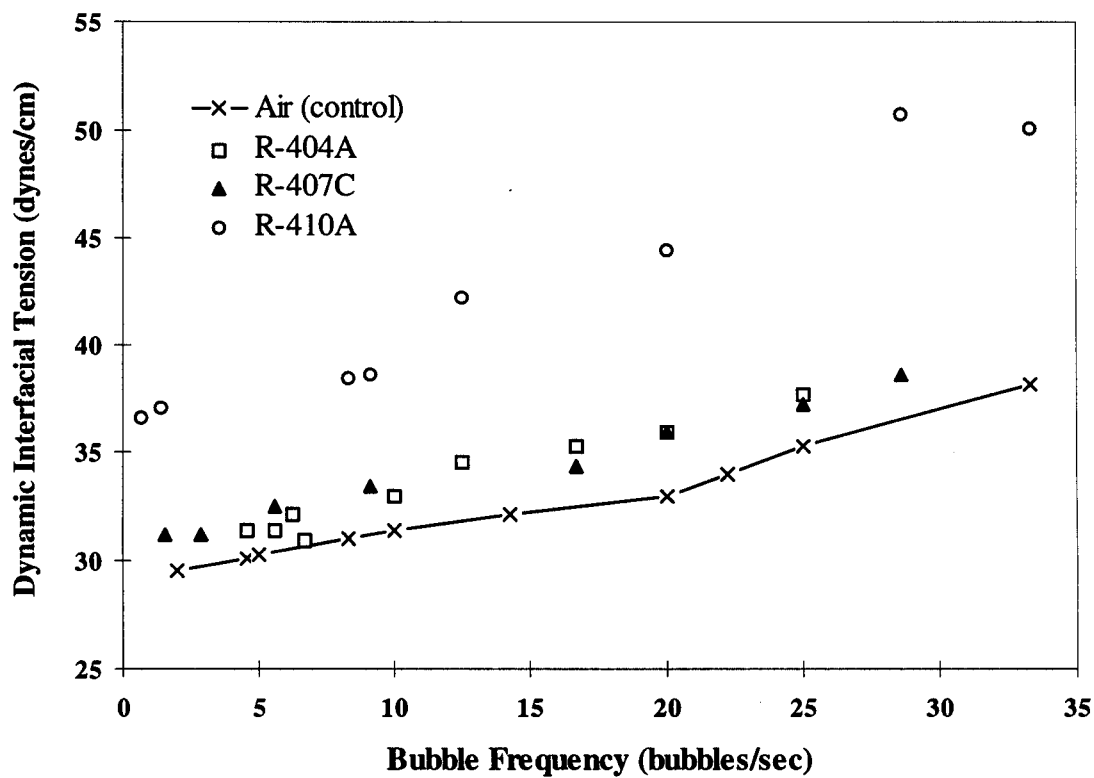


Figure 4.22 Dynamic interfacial tension vs. HFC blend type using ICI RL68H POE
 (Refer to [Tables A4.6.1](#) through [A4.6.6](#) in the [Appendix](#))



5. FOAMING CHARACTERISTICS OF REFRIGERANT/LUBRICANT

5.1 Introduction

Two different methods were used to generate foam columns from gaseous refrigerants and liquid phase lubricants. The first method, namely aeration, was used to perform tests on the baseline CFC and HCFC refrigerants with the corresponding mineral oils. In addition, the HFCs were tested with the polyolesters. However, since the HFC/polyolester pairs did not produce any froths of significant height or duration, another method was used. The HFC/polyolester pairs required a different approach to producing foam, in that a pressure drop was required to form the foams that could be measured and compared. These methods were performed to study foaming ability and foam stability of the various refrigerant/lubricant pairs. Other foaming characteristics such as bubble size and drainage rate were also observed.

5.2 Baseline Aeration

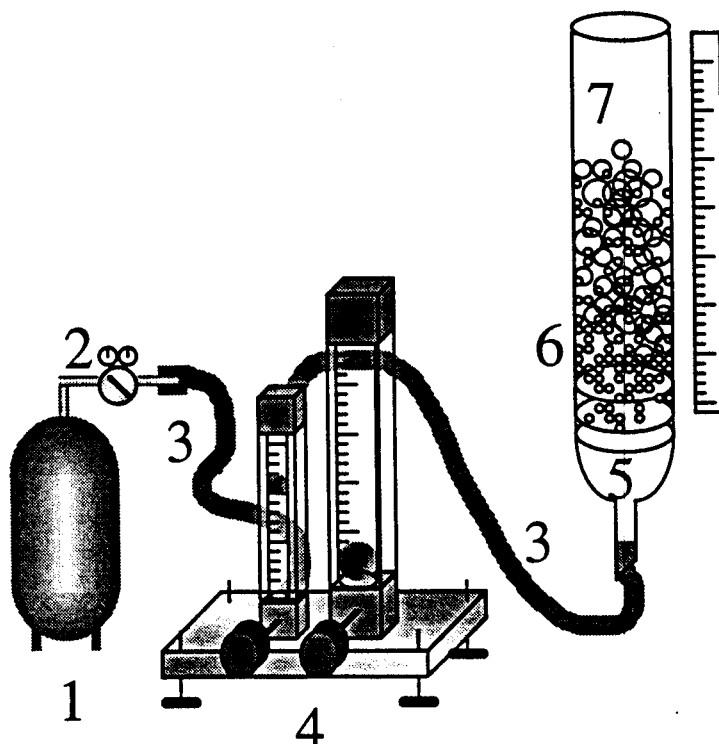
5.2.1 Background

In this method, foam is produced by injecting gaseous refrigerant through a fritted disk filter which is located at the entry of a long glass foam column tube. This experimental procedure is widely used and effective for measuring foaming characteristics of chlorinated refrigerants with mineral oil as the refrigerant is introduced to the lubricant in a more regulated fashion than simple agitation with pressure release.

5.2.2 Experimental Procedure

The apparatus used for conducting the aeration tests is pictured in [Figure 5.1](#). For each trial, either 30 ml or 50 ml of one of the lubricants is poured into the tube and is allowed to settle on top of the disk filter. Special care is taken to avoid lubricant contact with the inside walls of the glass column, so as not to irregularly affect the foaming data. Foam is then produced as refrigerant vapor is passed through the fritted disk filter into the lubricant. The smaller of the two rotameters is designed to accurately regulate the refrigerant *flow* rate up to 1 liter per minute, while the larger rotameter is to be utilized for higher *flow* rates. At least three different *flow* rates (350, 700, 1000 ml/min) are tested for every trial run. The height of the lubricant sample is recorded. The foam height at any given time is measured to be the distance from the top of the foam column to the initial height of the liquid which is subject to foaming. The *flow* of refrigerant is continued until the foam column reaches its maximum height. This takes approximately 30 seconds to 2 minutes, depending on the flow rate and the foamability of the refrigerant/lubricant pair. At this point, the maximum foam height is recorded every 30 seconds until the foam column collapses to considerably less than 1 cm. The tube is then drained completely, rinsed with acetone to dissolve any remnants of lubricant. The connecting vinyl tubing is then attached to a deionized water faucet and allowed to rinse for approximately 10 to 15 minutes. After draining the water out, the tube is then air-blown for 5 minutes to remove any remaining water. Once fully dry, the tube is ready for another trial.

Figure 5.1 Aeration column apparatus used for foamability and foam stability



1. PRESSURIZED REFRIGERANT

CFC-12, HCFC-22
HFCs: 32, 125, 134a, 143a
flowrates: 350, 700, 1000 ml/min

2. PRESSURE REGULATOR

Victor Equipment Company

3. CLEAR VINYL TUBING

Fisher Scientific
(similar to Tygon)
 1/4" Inside Diameter
 1/16" Wall Thickness

4. ROTAMETER FLOW METERS

Gilmont Instruments
Model GF-4540 Accucal
 Small Tube Size 220 (0 - 1 liter/min)
 Large Tube Size 250 (for >1 liter/min)
 Equipped with Glass Bobs

5. FRITTED DISK FUNNEL

(Attached to Tube)
Pyrex Brand
 Medium frit
 60 ml Capacity
 40 mm Inside Diameter

6. LUBRICANT SAMPLE

Witco SUNISO 3GS (Mineral Oil)
Witco, SUNISO 4GS (Mineral Oil)
Witco SUNISO SL68 (Polyolester)
ICI Emkarate RL68H (Polyolester)
 30 ml or 50 ml per trial

7. GLASS FOAM COLUMN TUBE

(Attached to Funnel)
 40" Height
 38 mm Inside Diameter

5.2.3 Flowmeter Calibration

The rotameters used for this experiment are calibrated for air and water by the manufacturer, Gilmont Instruments, Inc. In order to accurately measure the amount of refrigerant that passes through the rotameter, the calibration numbers given for air must be converted to values for gaseous refrigerant. This is easily performed by knowing the flow rate of air (q_A), the density of air (ρ_A) and the density of refrigerant (ρ_R) in the gas phase at 25°C. These values are inserted into the following equation to give a calibrated flow rate of refrigerant.

$$q_R = q_A \sqrt{\frac{\rho_A}{\rho_R}}$$

5.2.4 Results and Discussion

It was found that the polyolester samples do not produce significant foam with HFC refrigerants. Thus, the experimental data reflects only those trials, which involve the baseline pairs (chlorinated refrigerant/mineral oil), that produced stable froths of significant (i.e. measurable) height and persistence. In terms of repeatability, the initial (maximum) foam height and foam lifetime data are consistent. The variance lies with foam heights taken between time zero and time of foam collapse.

The tabulated and graphical results are presented using two different approaches. Approach 1 (Figures 5.2 through 5.13) lists a detailed account of the foam column lifetime with respect to time for each trial run, while Approach 2 (Figures 5.14 through 5.18) considers foamability verses foam stability for the refrigerant/lubricant pairs. In

Figure 5.2 Baseline aeration: flowrate comparison using 30 ml 3GS and R-22
(Refer to [Table A5.1.1](#) in the [Appendix](#))

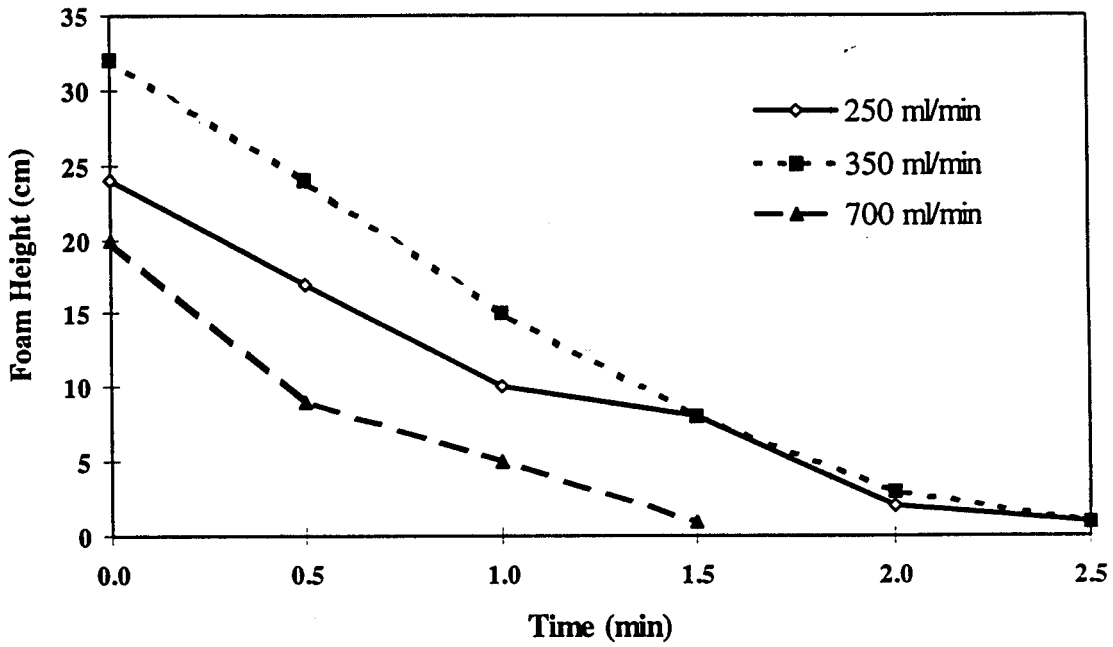


Figure 5.3 Baseline aeration: flowrate comparison using 30 ml 3GS and R-12
(Refer to [Table A5.1.2](#) in the [Appendix](#))

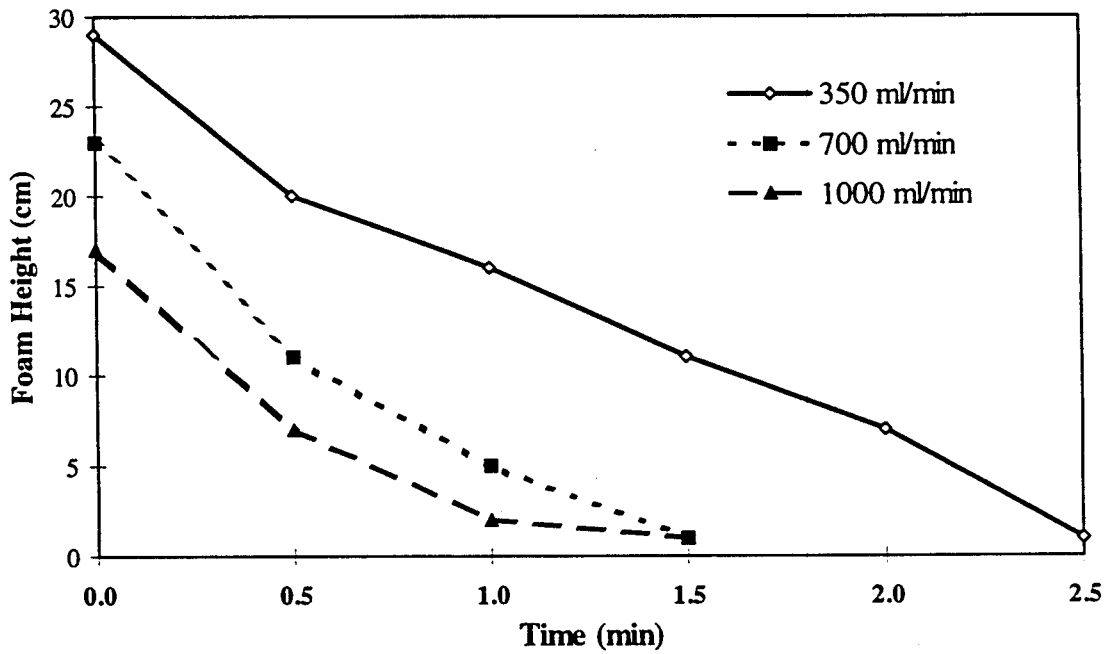


Figure 5.4 Baseline aeration: flowrate comparison using 30 ml 4GS and R-22
(Refer to [Table A5.1.3](#) in the [Appendix](#))

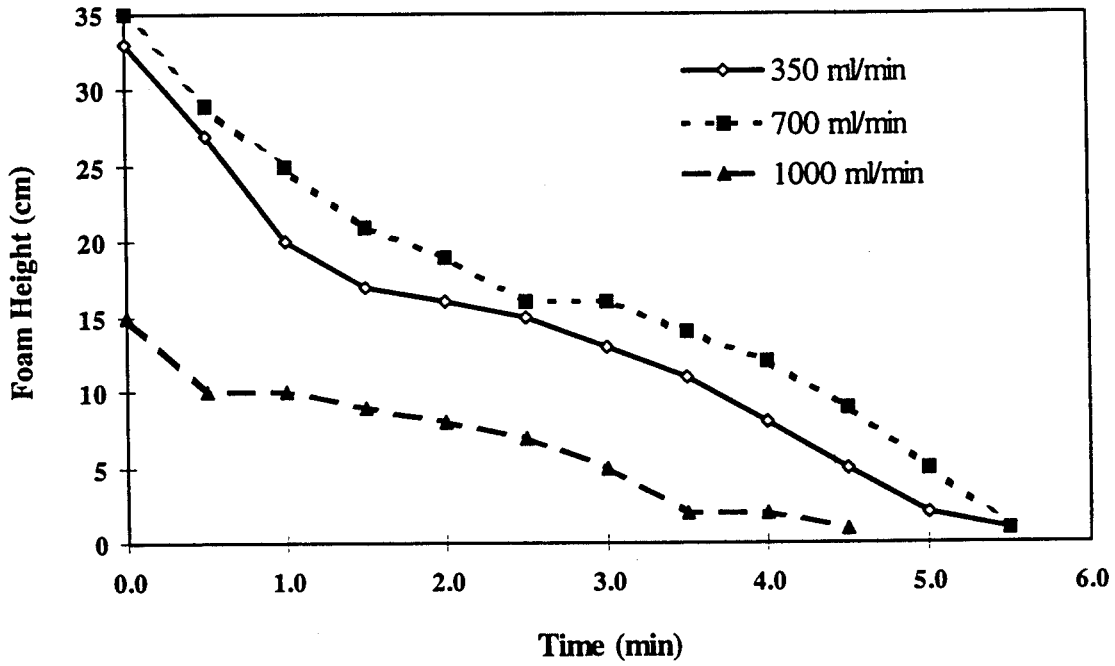


Figure 5.5 Baseline aeration: flowrate comparison using 50 ml 4GS and R-22
(Refer to [Table A5.1.4](#) in the [Appendix](#))

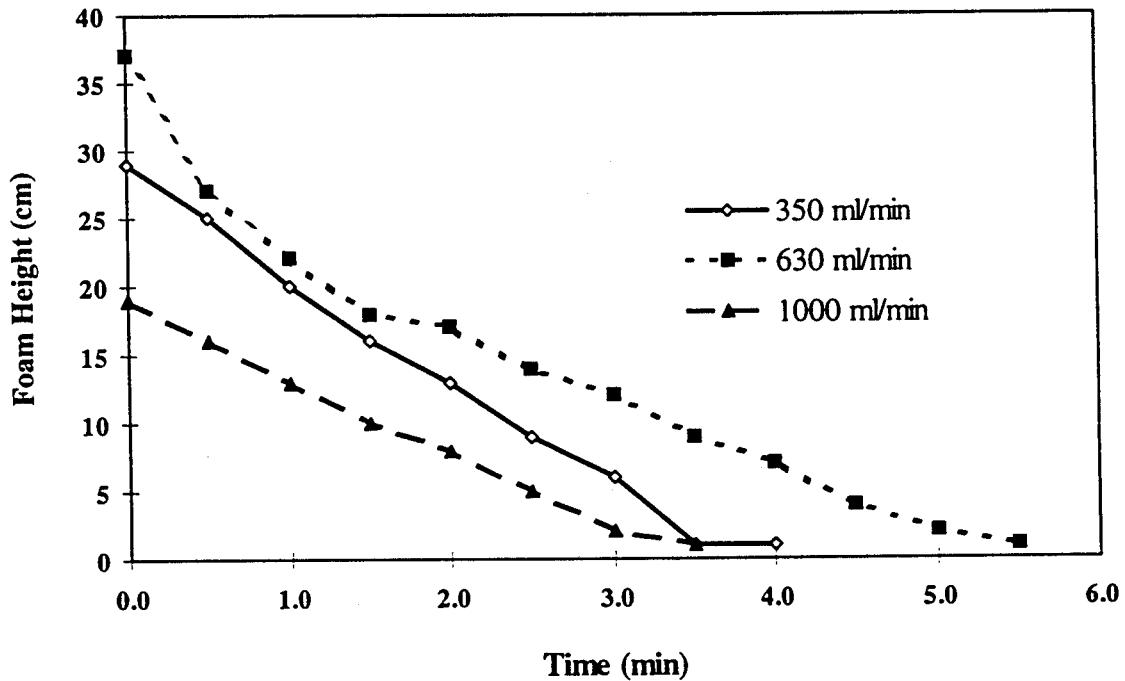


Figure 5.6 Baseline aeration: flowrate comparison using 30 ml 4GS and R-12
(Refer to [Table A5.1.5](#) in the [Appendix](#))

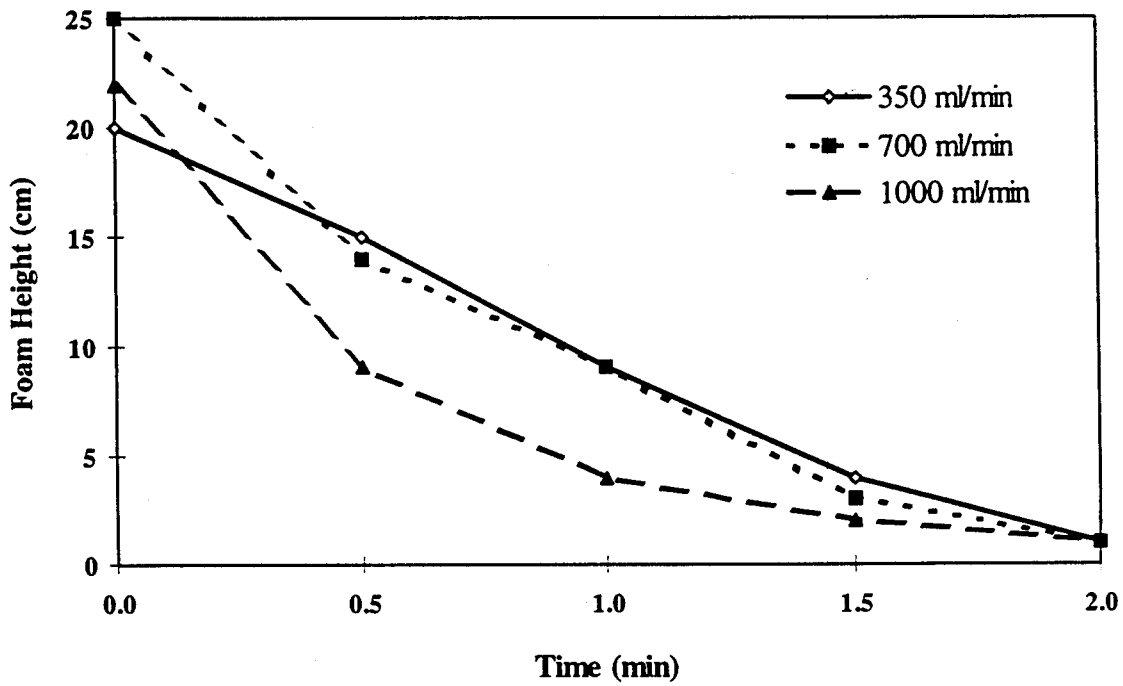


Figure 5.7 Baseline aeration: mineral oil comparison (4GS vs. 3GS)
using 30 ml lubricant and R-22 at 350 ml/min
(Refer to [Tables A5.1.1](#) and [A5.1.3](#) in the [Appendix](#))

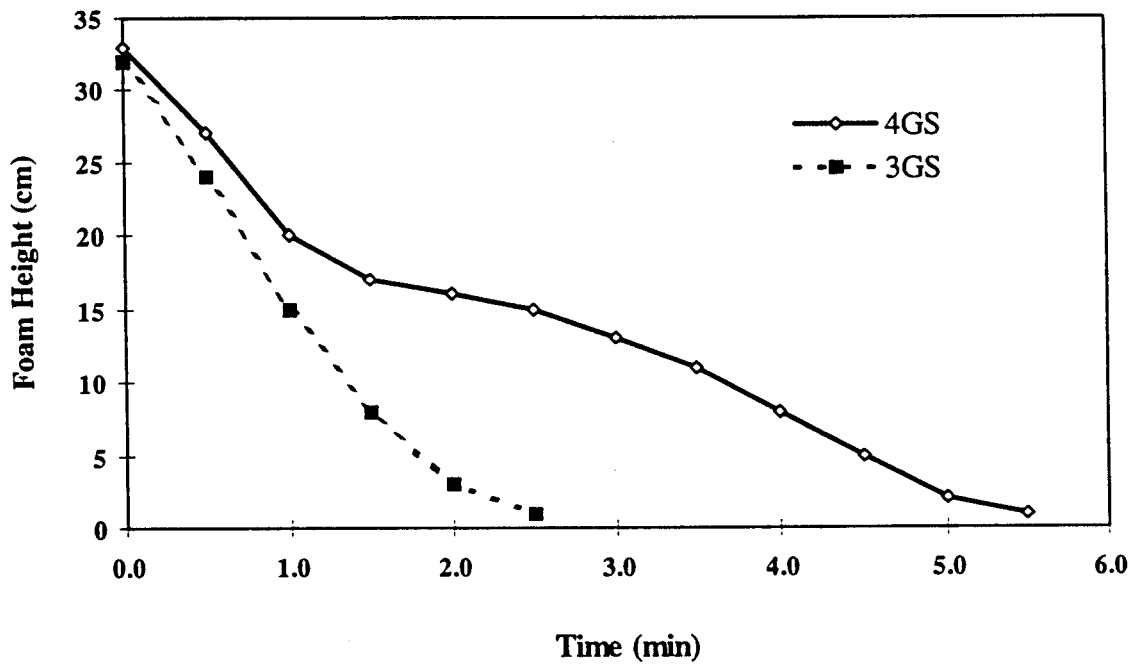


Figure 5.8 Baseline aeration: mineral oil comparison (4GS vs. 3GS) using 30 ml lubricant and R-22 at 700 ml/min (Refer to [Tables A5.1.1](#) and [A5.1.3](#) in the [Appendix](#))

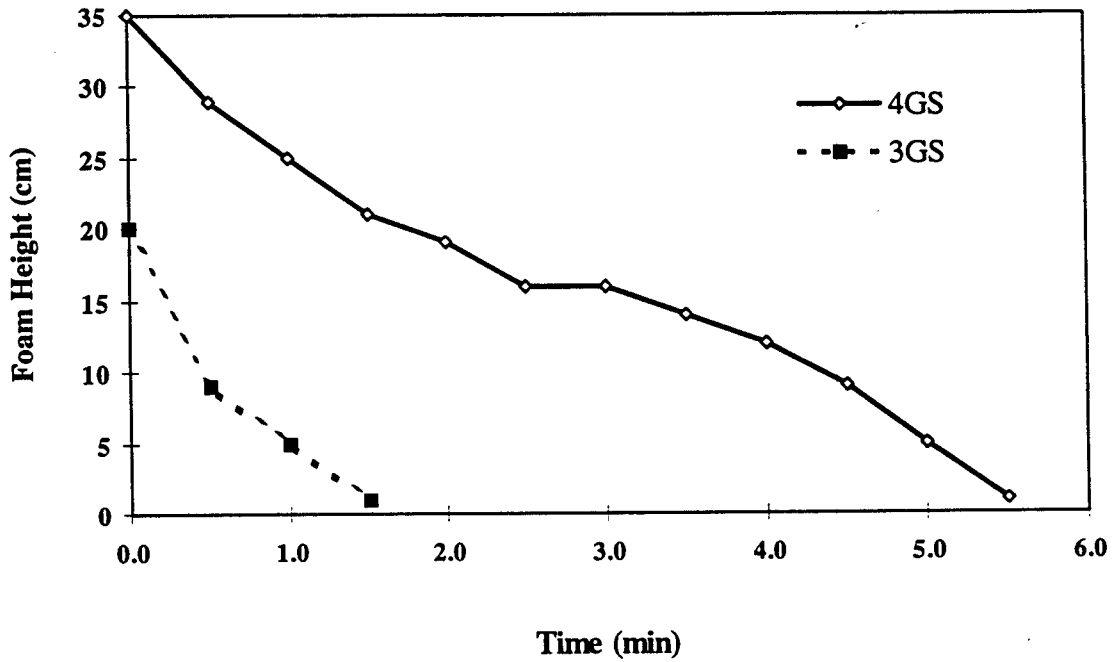


Figure 5.9 Baseline aeration: mineral oil comparison (4GS vs. 3GS) using 30 ml lubricant and R-12 at 350 ml/min (Refer to [Tables A5.1.2](#) and [A5.1.5](#) in the [Appendix](#))

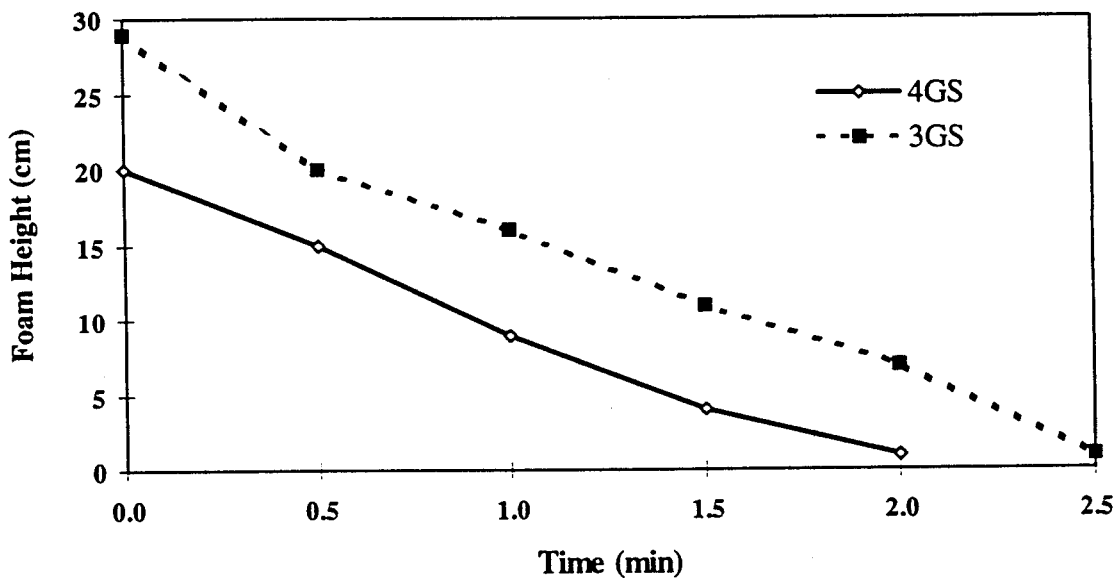


Figure 5.10 Baseline aeration: mineral oil comparison (4GS vs. 3GS)
 using 30 ml lubricant and R-12 at 700 ml/min
 (Refer to [Tables A5.1.2](#) and [A5.1.5](#) in the [Appendix](#))

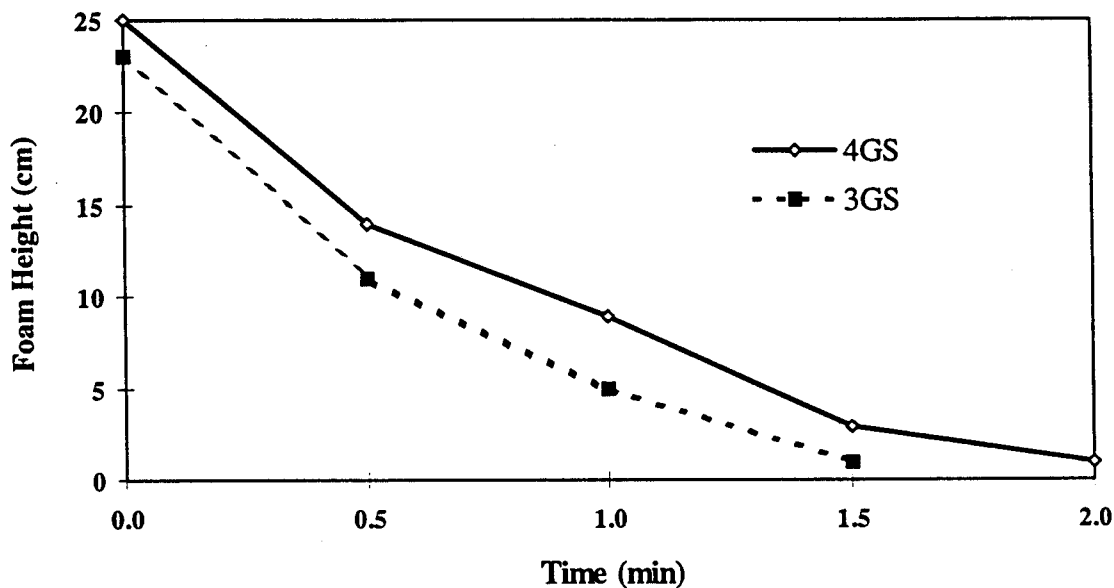


Figure 5.11 Baseline aeration: mineral oil comparison (4GS vs. 3GS)
 using 30 ml lubricant and R-12 at 1000 ml/min
 (Refer to [Tables A5.1.2](#) and [A5.1.5](#) in the [Appendix](#))

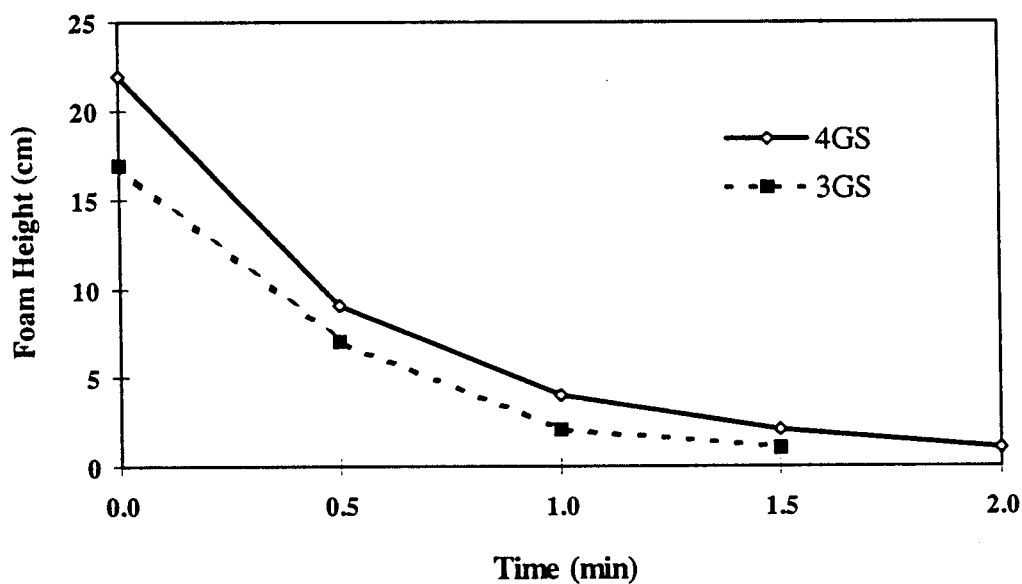


Figure 5.12 Baseline aeration: refrigerant comparison (R-12 vs. R-22)
 using 30 ml 4GS and refrigerant at 700 ml/min
 (Refer to [Tables A5.1.3](#) and [A5.1.5](#) in the [Appendix](#))

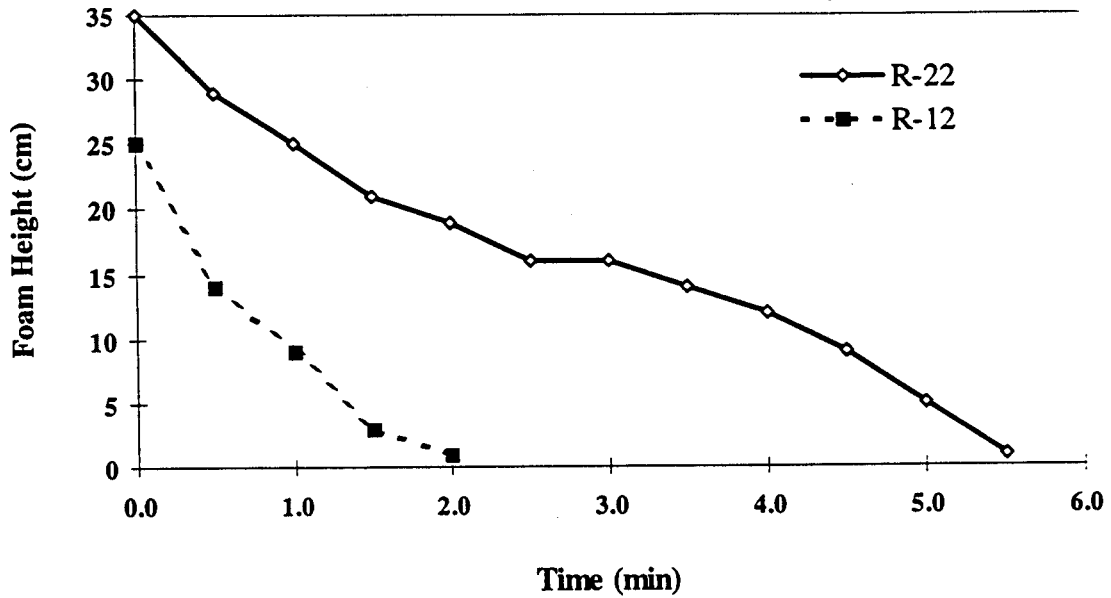
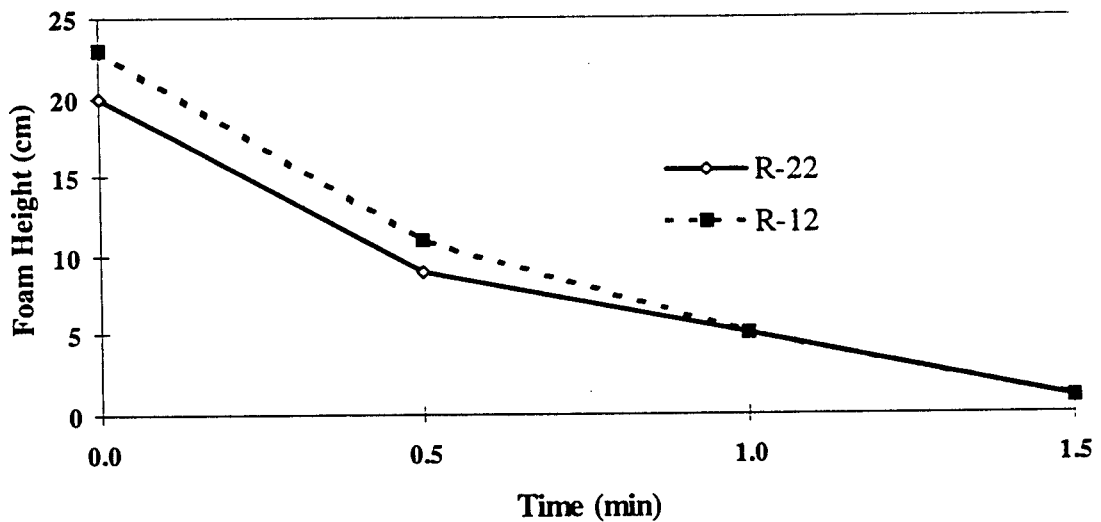


Figure 5.13 Baseline aeration: refrigerant comparison (R-12 vs. R-22)
 using 30 ml 3GS and refrigerant at 700 ml/min
 (Refer to [Tables A5.1.1](#) and [A5.1.2](#) in the [Appendix](#))



essence, Approach 2 is a condensed version of Approach 1, and concentrates on the two variables (Maximum Foam Height and Collapse Time = Foam Lifetime) which provide the foamability/foam stability comparison. The Foam Height verses Time graphs for Approach 1 are divided into 3 sections. The first section (Figures 5.2 through 5.6) simply plots the base trial sets for each flow rate, while the second (Figures 5.7 through 5.11) and third sections (Figures 5.12 and 5.13) compare the lubricant and refrigerant samples, respectively.

For constant lubricant volume R-22 trials (Figures 5.2 and 5.4), the middle flow rate tested produced the greatest initial foam height. This suggests that that there must be some flow rate (amount, in general) that gives a maximum foamability for a given R-22/lubricant pair.

Varying the lubricant volume for the R-22/4GS trials (Figures 5.4 and 5.5), affected foam lifetime. For flow rates less than 1000 ml/min, the larger volume samples (50 ml) produced foam columns that persisted 20% less than the smaller volume samples (30 ml). In terms of the maximum foam height and foam lifetime, the 1000 ml/min trial runs did not change significantly.

The R-12 trials (Figures 5.3 and 5.6) produced foam columns that persisted 50% less than the columns produced with identical, in terms of type and volume, lubricant samples. The 4GS/R-12 set did not reveal any significant variance between flow rates. However, the 3GS/R-12 trial set did reveal that the lowest flow rate (350 ml/min) produced a foam column with the greatest foam height (25% greater than 700 ml/min) and greatest foam lifetime (66% greater than both 350 ml/min and 700 ml/min).

In terms of the Mineral Oil Comparison (Figures 5.7 through 5.11), the largest variance between constant volume (30 ml) 3GS and 4GS samples was achieved with R-22 at 700 ml/min (Figure 5.8), where 4GS foamed considerably higher and for a longer period than 3GS. The least variance between the samples was observed with R-12 at 1000 ml/min (Figure 5.11).

In terms of the Refrigerant Comparison (Figures 5.12 and 5.13), the largest variance between constant flow rate (700 ml/min) R-12 and R-22 samples was achieved with 30 ml of 4GS (Figure 5.12), where R-22 foamed considerably higher and for a longer period than R-12. Figure 5.13 reveals that there is no significant difference between the refrigerants when 30 ml of 3GS is subjected to 700 ml of either refrigerant.

Analyzing Foamability verses Foam Stability from Figures 5.14 through 5.18, each 30 ml 4GS trial set (Figures 5.15 and 5.18) produced foam columns with constant collapse times (6 minutes for R-22, 2.5 minutes for R-12) for all flow rates tested (350, 700, 1000 ml/min for the R-22 sample; 200, 350, 700, 1000 ml/min for the R-12 sample). The 3GS trial sets (Figures 5.14 and 5.17) produced foam columns that were not constant over a range of similar flow rates.

In general, it seems that the foam height is more stable when smaller bubbles are produced as a result of a lower flow rate. When the flow rate is high, larger refrigerant bubbles are produced and thus, there is less film surface area within the foam. This also corresponds to greater amounts of lubricant in the liquid films (lamellae) within the foam. When the large bubbles break, a greater amount of lubricant flows down through the lamellae disrupting the foam and causing faster collapse. Although bubble size for each

Figure 5.14 Baseline foamability and foam stability (30 ml 3GS and R-22)
 (Refer to [Table A5.2](#) in the [Appendix](#))

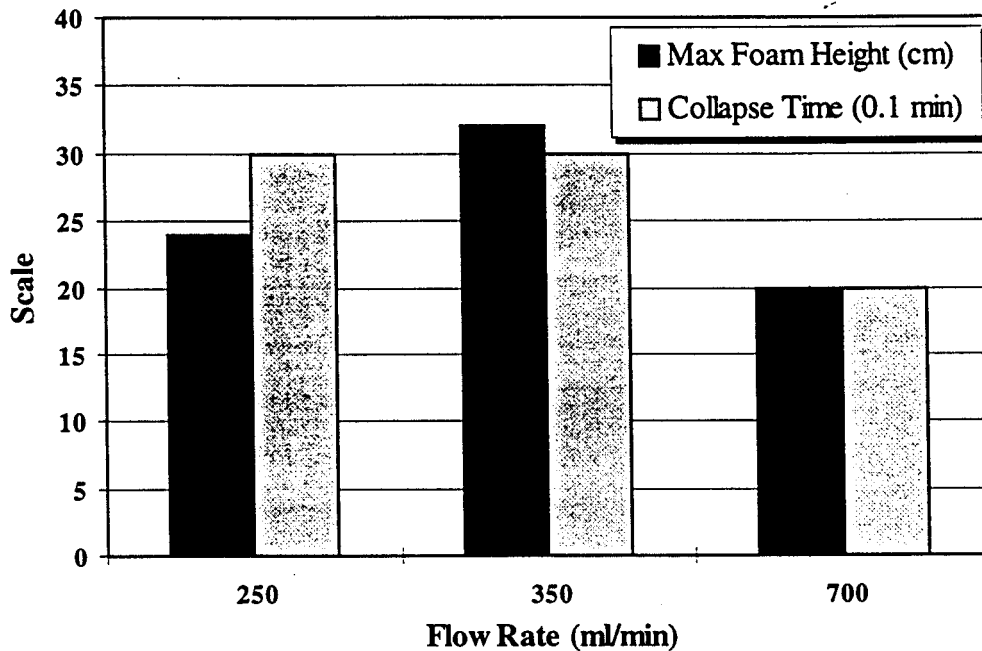


Figure 5.15 Baseline foamability and foam stability (30 ml 3GS and R-12)
 (Refer to [Table A5.2](#) in the [Appendix](#))

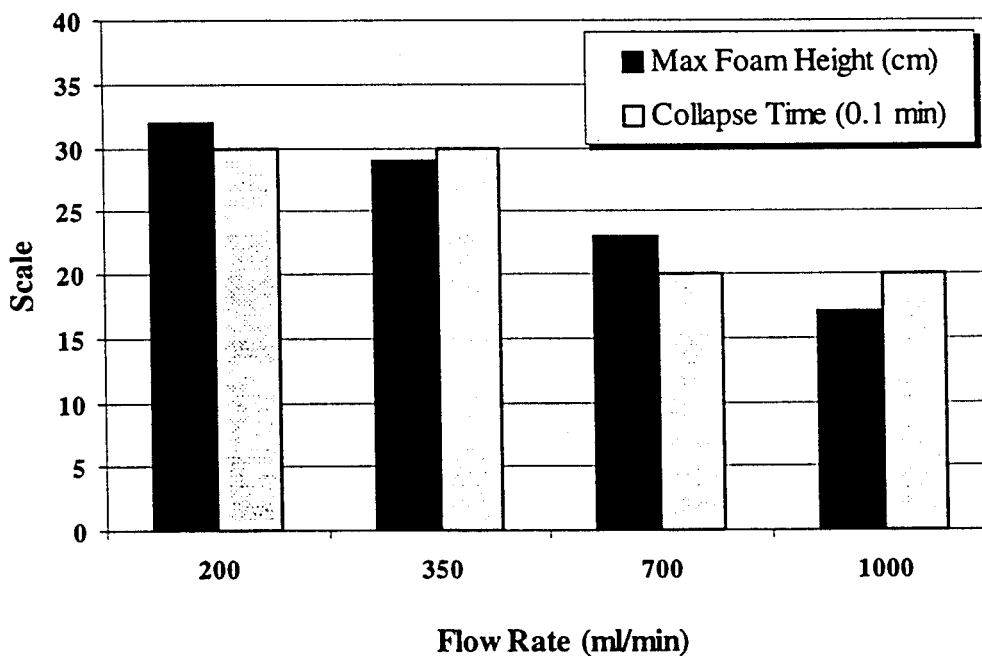


Figure 5.16 Baseline foamability and foam stability (30 ml 4GS and R-22)
 (Refer to [Table A5.2](#) in the [Appendix](#))

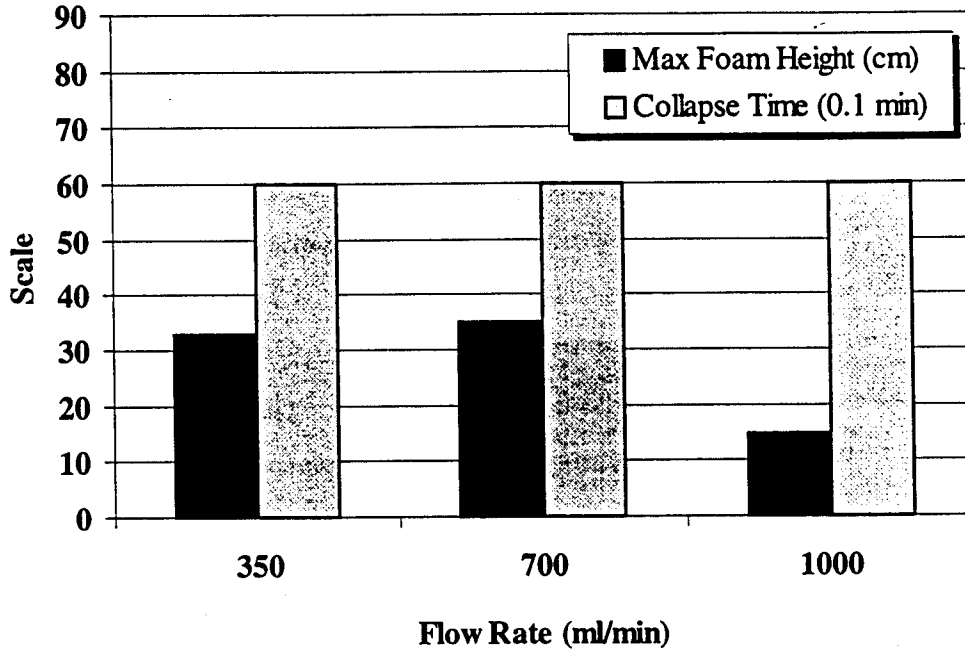


Figure 5.17 Baseline foamability and foam stability (50 ml 4GS and R-22)
 (Refer to [Table A5.2](#) in the [Appendix](#))

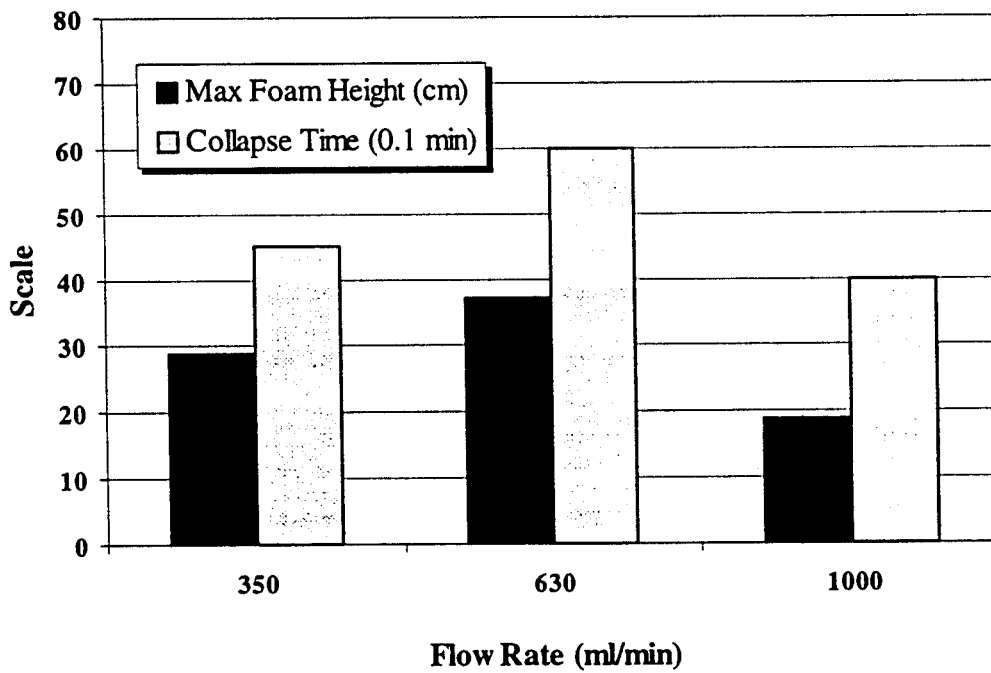
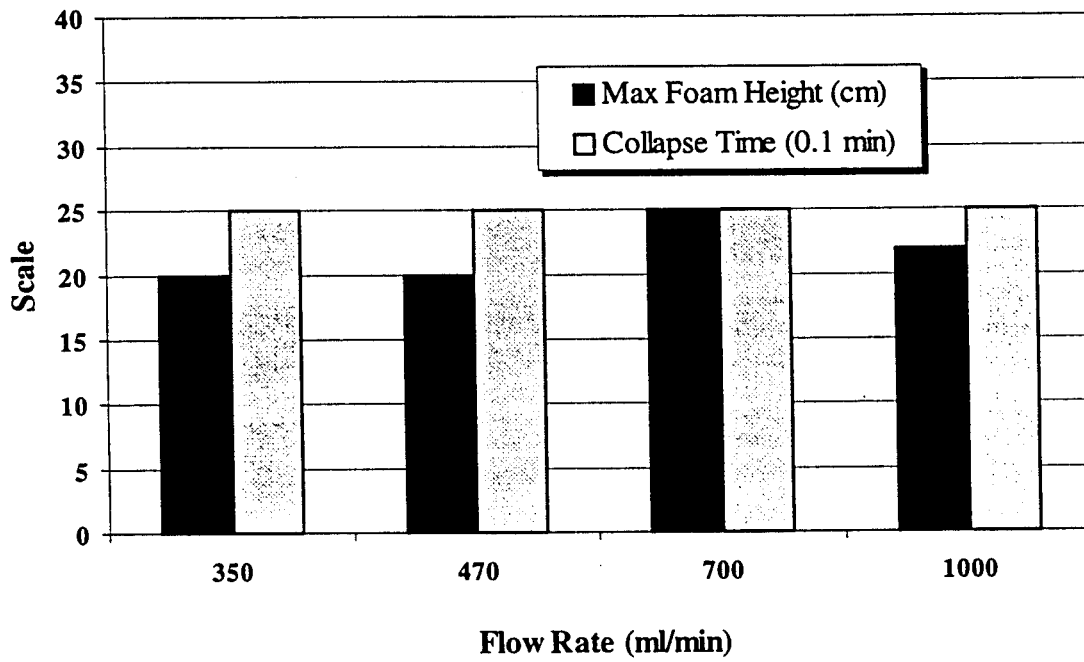


Figure 5.18 Baseline foamability and foam stability (30 ml 4GS and R-12)
(Refer to [Table A5.2](#) in the [Appendix](#))



trial was not measured precisely for the baseline tests, a significant distinction between the trials with high flow rates and low flow rates, has been observed and noted.

5.3 Pressure-Drop Induced Foaming of HFC/POE Mixtures

5.3.1 Background

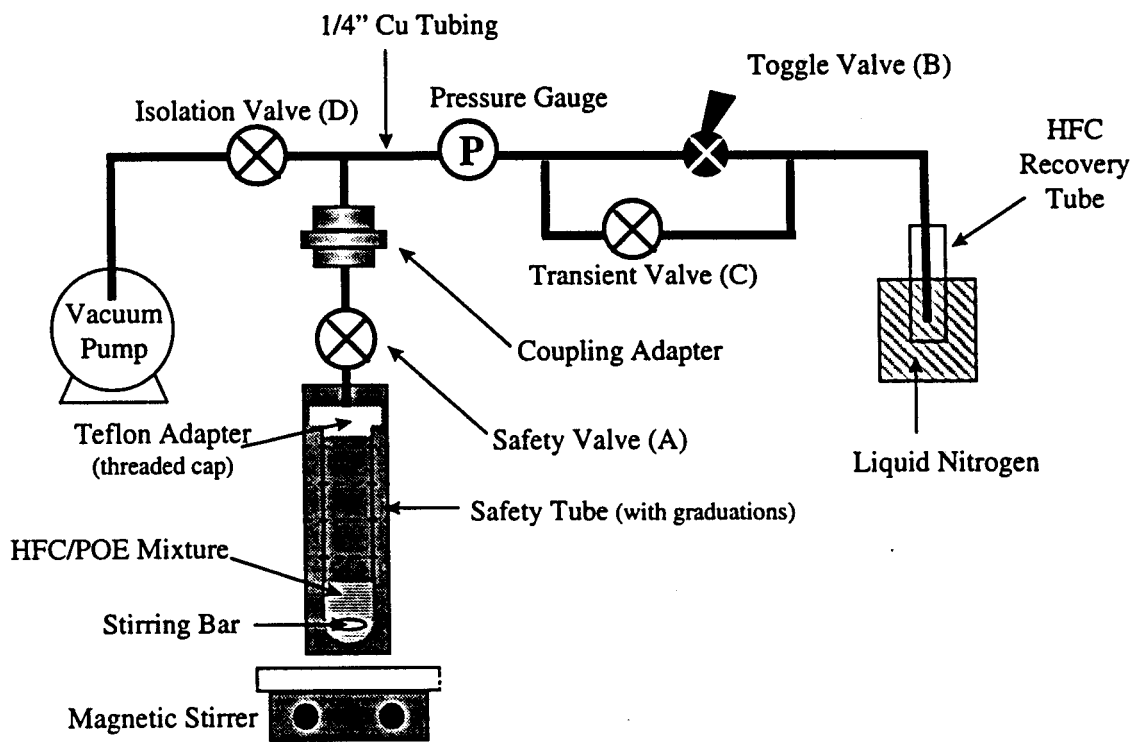
The HFCs tested, both single-component and blended compositions, do not produce stable froths at ambient pressure. In order to conduct foaming experiments under pressure drop situations, a special foaming apparatus is needed to handle high pressure conditions. Although the pressure vessel that is being used to measure absorption and desorption rates was built specifically for pressures up to 100 psi, it is not ideally suited to conduct foamability and foam stability experiments. Hence, a pressure tube was constructed to handle the foaming properties, along with desorption rates, of HFC/POE mixtures.

The principle of the experiment is to build up the pressure of refrigerant/lubricant mixture, release that pressure and observe the foam produced, if any, by this process. This foam arises out of the spontaneous nucleation of refrigerant and lubricant molecules in the mixture, causing the refrigerant to desorb out of the mixture, thus forming bubbles which are predominantly filled with refrigerant gas inside concentrated, lubricant-filled lamellae.

5.3.2 Experimental Apparatus

Figure 5.19 displays the schematic of the apparatus which was specifically designed to induce foaming by refrigerant/lubricant mixtures as a result of a pressure

Figure 5.19 HFC pressure-release foaming apparatus



drop. Pressure of the mixtures is built up inside a heavy-wall, glass tube (Ace Glass, Inc.) that has a polymer coating on its outer surface to ensure safety at higher pressures. The glass tubes purchased for this experiment were designed to handle pressures up to 150 psi. In addition, for further safety, a polypropylene safety tube (with graduations) surrounds the glass pressure tube during the experiment. The pressure tube is 16 inches in length with a 1 inch outside diameter. The bottom is rounded while the top end is threaded to fit a Teflon adapter, which feeds into quarter-inch copper tubing. A stirring bar is used to agitate the refrigerant/lubricant mixture to the desired pressure which is displayed on the pressure gauge. A liquid nitrogen-cooled sink is used to collect the refrigerant once it has been forced out of the refrigerant/lubricant mixture. An HFC recovery tube is submerged in an environment which is cooled by liquid nitrogen. The quarter-inch copper tubing line is led down into this tube to provide a cooler end for the refrigerant to migrate to once the pressure has been released. This allows for liquid refrigerant to form in the tube which provides a relative idea of how much refrigerant is desorbed within each foaming/desorption trial.

One of the more critical additions to the apparatus is the coupling adapter which is connected between the pressure tube and the T-junction located between the (isolation) valve D and the pressure gauge. This adapter serves to remove the pressure tube (with valve A closed), with the refrigerant/lubricant mixture inside, from the apparatus for weighing. Rather than disconnect the line to the vacuum pump and block off the line with some type of plug, valve D was installed to isolate the system during pressure build-up. The safety valve (A), when closed, isolates the mixture from the atmosphere when the refrigerant and lubricant are weighed. The specifics regarding the detachment and

reattachment of the pressure tube with the rest of the apparatus by means of the coupling adapter are described in detail in the following Experimental Procedure section.

5.3.3 Experimental Procedure

Listed below are the 13 steps taken for each foaming trial involving the HFC/POE mixtures.

1. A clean, dry pressure tube is attached to the Teflon adapter and, along with safety valve (A), is detached from the rest of the apparatus by means of the coupling adapter. The coupling adapter is configured such that the ball bearings allow the bottom portion of the adapter to slide into the top of the adapter providing an air-tight connection when attached and a simple yet effective way of weighing the refrigerant/lubricant mixture inside the pressure tube.
2. The tube, valve (A) and the stirring bar are weighed on a balance and this mass is recorded.
3. A specific volume of polyol ester (POE) lubricant is poured into the tube. The tube, valve, stirring bar and POE are weighed on the same balance and the mass is recorded. The mass of the POE lubricant, accurate to 0.1 grams, is then known.
4. The tube/valve system is then reattached to the rest of the apparatus. Valves A and D are opened while valves B and C are closed.

5. The vacuum pump (supplied by Gast), which pulls a vacuum of approximately 27 inches of mercury, is then turned on and the air bubbles are evacuated out of the POE. Tapping the tube or lightly stirring the POE with the magnetic stirring bar is usually beneficial to this process. The vacuum pump is turned on for approximately 5 minutes prior to each foaming/desorption test.

6. After turning the vacuum pump off, valves A and D are closed and the pressure tube/valve A system is then detached and placed in the ice bath, with the tube completely submerged, for 5-10 minutes to chill the surface of the tube. An ice bath is needed to lower the inner surface temperature of the pressure tube itself because a good deal of the refrigerant vaporizes before it reaches the mixture otherwise.

7. Liquid HFC refrigerant is poured into the tube. Valve A is then shut immediately to isolate the refrigerant/lubricant mixture.

8. The tube is wiped dry and the mixture/tube/valve A system is weighed on the balance and this mass is recorded. By subtracting this mass from the mass obtained in [Step 3](#), the mass of the refrigerant, and thus, the refrigerant : lubricant mass ratio, is then known and the mixture is ready for the foaming/desorption trial.

9. The tube/valve A system is reattached to the apparatus again, this time along with the protective, polypropylene safety tube (with gradations for foam height measurement) around the pressure tube. The initial height of the mixture is recorded.

10. Valve A is opened while valves B, C and D are still closed. The mere presence of the refrigerant and lubricant together inside the tube is enough to generate some degree of pressure which can be observed on the pressure gauge. However, in order to generate specific pressures of 20 psi and higher, the magnetic stirring device is used to agitate the mixture.

11. Once the desired pressure is obtained, the magnetic stirring device is turned off. Depending on the desired time of the pressure drop, either valve B or valve C is (gradually) opened over the desired interval. This triggers the desorption of refrigerant out of the lubricant and, in some cases, causes a foam to form.

12. Once the foam reaches its maximum height, valve A is closed and the desorbed mixture is, once again, isolated.

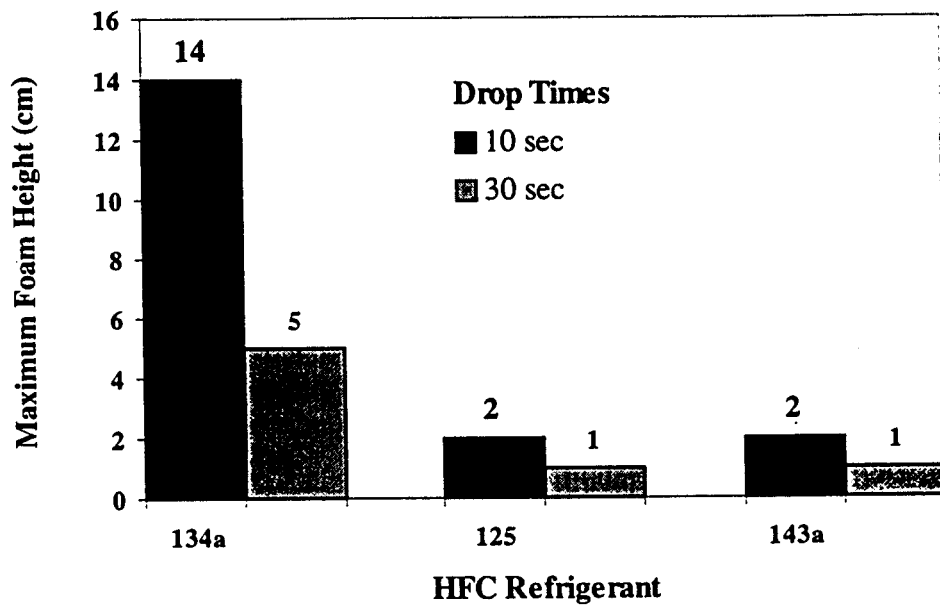
13. The maximum height of the foam formed, if any, is recorded. Subtracting the value obtained in [Step 9](#) reveals the maximum foam height, namely the measure of foamability, for the trial. The lifetime of the foam, should a stable froth be formed, is measured with a stopwatch.

5.3.4 Results and Discussion

Details from the 26 trials are tabulated in the [Appendix \(Table 5.3\)](#) and summarized in [Table 5.3.8](#). R-134a was initially tested, in a 1:1 ratio, with 20 ml of ICI polyol ester at a fast 20 psi pressure drop time of 10 seconds. This mixture was tested twice (trials 1 and 2) to make sure that the two pressure tubes behaved similarly under similar conditions. However, it should be noted that the experiments started with 20 psi pressure drops as opposed to 50 or 70 psi pressure drops. It has been noted that different tubes may behave differently when subjected to more extreme conditions. Nevertheless, trials 1 and 2 yielded similar results as the refrigerant : lubricant ratios were within 0.03 of each other and the foamability values were within one centimeter.

It seems that only the "fast" pressure drop times, namely 10 and 30 seconds, produce any significant foam height. In addition, as one might expect, the fastest pressure drop (i.e. approximately 10 seconds) yielded the greatest amount of foam for all of the 1:1 R-134a/POE and R-125/POE mixtures tested. Although R-125 has not been tested with a pressure drop time of greater than 30 seconds, it can safely be assumed that little or no foam shall be produced as R-134a formed virtually no foam for these pressure drop times and R-134a produced more foam than R-125 for the "fast" pressure drop times. In fact, R-134a mixtures proved to be the most productive foaming HFC when subjected to a 20 psi pressure drop (i.e. without heating, a variable which was not part of the experimental design) with all other variables (pressure drop time, refrigerant : lubricant ratio) held constant. Evidence of this conclusion is shown in [Figure 5.20](#). Recall that R-134a, according to dynamic interfacial tension data, lowered the air/POE

Figure 5.20 HFC pressure-release foaming for 1:1 ratio, 20 psi pressure drop
(Refer to [Table A5.3.8](#) in the [Appendix](#))



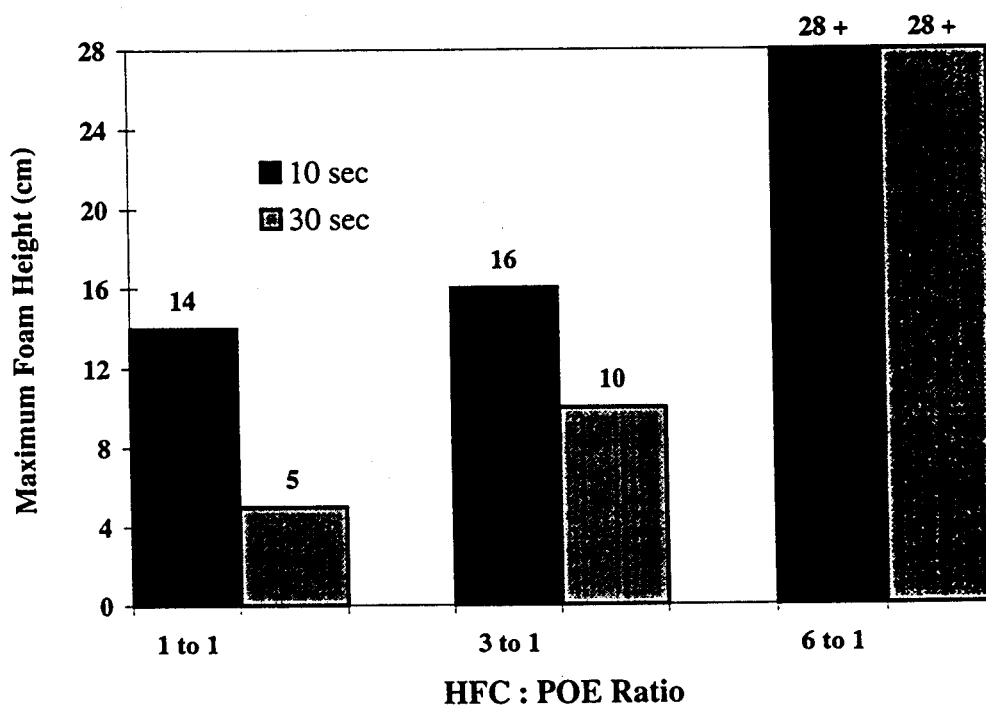
dynamic surface tension plot the most, a characteristic which favors greater foaming (than other single-component HFCs).

R-32, due to its much higher volatility, produced pressures of 50 and 70 psi without difficulty with the existing apparatus. However, it is because of this high pressure within the tube that even 1:1 refrigerant to lubricant ratios could not be tested at 20 psi. Thus, R-32 data does not appear in [Figure 5.20](#). Regardless, the R-32 trials did not produce any significant froth within the column. It should also be noted that R-32 was the *only* HFC to produce pressures up to 70 psi *without* heating. Hence, comparative analyses focus only on the 20 and 50 psi pressure drop trials. It was noted, however, that the 70 psi trials, for both 10 and 30 second drop times at a 1:1 ratio, did not produce any significant foam.

In terms of bubble size and foam stability, the foam bubbles formed are rather large in comparison with the tube and mixture surface diameter. Thus, there is little evidence of any stable "froths" being formed. Usually, for a stable "froth" to be formed, the bubbles are small and cause less drainage when broken. Large bubbles reflect a foam whose lamellae are thicker and thus weigh more. When these large bubbles break, the rate of drainage is high and thus, the stability is minimal. In essence, the mixtures tested at the "fast" pressure drops violently erupt into a foam and then, after a few seconds, subside rapidly with a few small bubbles remaining at the surface.

Specifically looking at HFC:POE ratio ([Figure 5.21](#)), it appears that 1:1 and 3:1 ratios yield similar results for R-134a, the HFC that forms foam the easiest. However, when the ratio was increased to 6:1, the pressure tube became filled with foam (albeit, the

Figure 5.21 HFC pressure-release foaming for various HFC:POE ratios (R-134a and 20 psi pressure drop) (Refer to [Table A5.3.8](#) in the [Appendix](#))



foam was stable for less than 10 seconds). In fact, all four 6:1 ratio trials produced foam columns that reached the maximum recordable height (28 cm). These trials involved both R-134a and R-143a as well as both 10 and 30 second pressure drops times for both refrigerants.

The 60 and 180 second pressure drop times were eventually eliminated from the experimental design as previous trials, under these constraints, did not produce foam columns when subjected to various pressure drops. Although R-134a seems to produce greater foam columns than R-143a for various lubricant/refrigerant systems, R-143a mixtures were readily able to produce pressure build-ups of 50 psi with relatively little stirring as compared to R-134a, which, for lower refrigerant/lubricant mass ratios, required some heating to achieve the 50 psi pressure gradient. A summary of the 50 psi pressure drop data appears in [Figure 5.22](#) (for 1:1 HFC:POE trials) and [5.23](#) (for 3:1 HFC:POE trials). In essence, the 1:1 trials, for a 50 psi pressure drop, did not contain enough refrigerant to produce any significant foam height greater than 2 cm. The 3:1 trials produced greater foam heights, but were significantly less than the 20 psi, 6:1 trials. Thus, it appears that the HFC/POE mixture foamability data presented in this report is a primarily a function of refrigerant : lubricant ratio, as opposed to pressure drop or time of pressure drop.

A relative error of 1 cm for foamability measurements has been reported based on the uncertainty around the circumference of the top of a foam column, for the top of a foam column is rarely flat. It should be noted that only single-component HFC refrigerants have been tested with the pressure-release foaming apparatus.

Figure 5.22 HFC pressure-release foaming for a 50 psi pressure drop (3:1 ratio)
 (Refer to [Table A5.3.8](#) in the [Appendix](#))

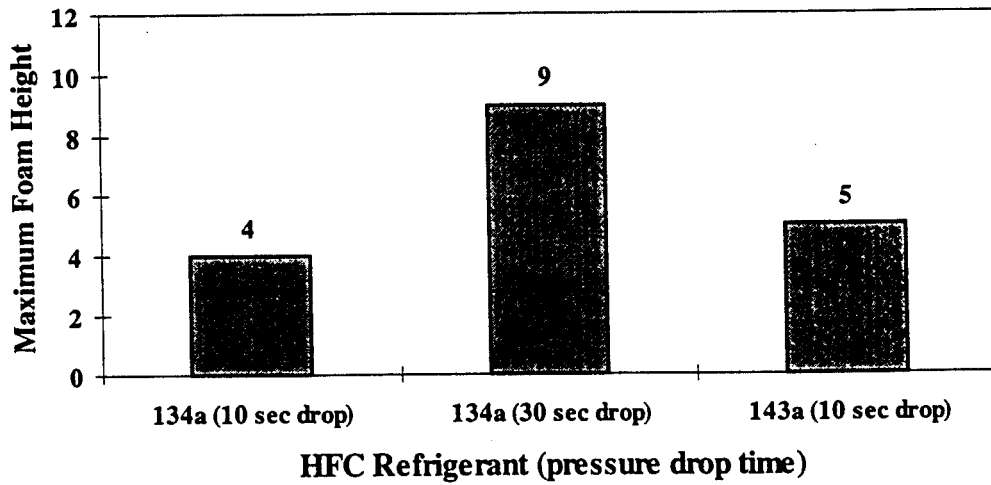
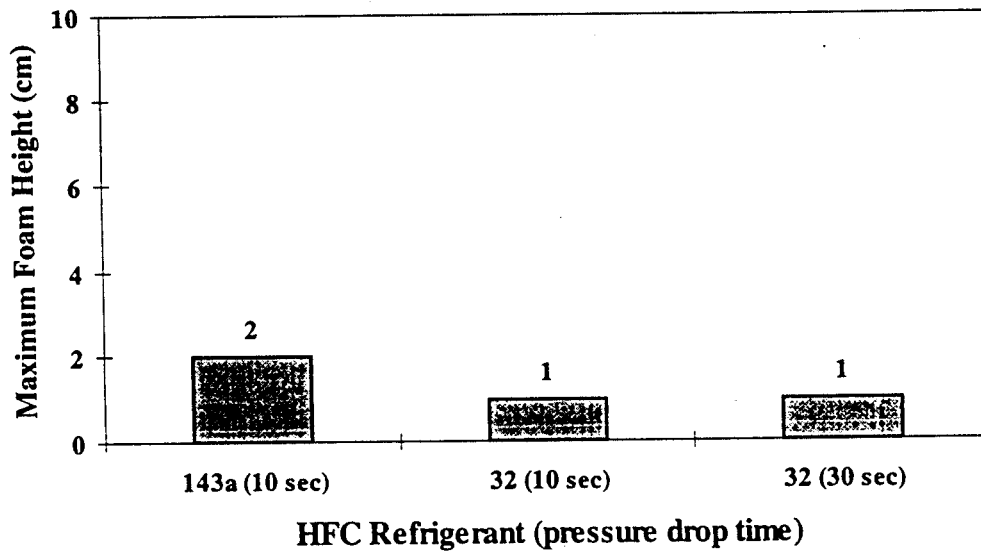


Figure 5.23 HFC pressure-release foaming for a 50 psi pressure drop (1:1 ratio)
 (Refer to [Table A5.3.8](#) in the [Appendix](#))



5.4 Desorption Rates

5.4.1 Background

In addition to the absorption rate data generated by the pressure vessel experiments, desorption rates of the various HFC/POE pairs were measured using the same apparatus as is pictured in [Figure 5.1](#), which was used to measure the foaming characteristics of the HFC/POE mixtures. In essence, at the conclusion of each foaming trial, two final steps were taken (after [step 13](#) in the experimental procedure of the HFC foaming, [Section 5.3.3](#)) to measure the amount of refrigerant desorbed out of the refrigerant/lubricant mixture. This weight-loss method takes into account the final mass of the refrigerant/lubricant mixture, and the time of the desired pressure drop for the given trial and produces a desorption rate value, in grams of refrigerant lost per second. Desorption rate values can also be calculated as mass lost per area per time by taking into account the cross-sectional area of the refrigerant/lubricant mixture surface.

5.4.2 Experimental Procedure

In short, the two steps taken to measure the desorption rates are listed below. They were performed upon the immediate completion of [step 13](#) in the HFC pressure-release foaming procedure.

After the foam has completely collapsed, the tube/valve A system is weighed on the balance. It is assumed at this point that none of the POE lubricant has left the mixture and only refrigerant has desorbed out of the mixture. The mass is recorded and subtracted

from the mass recorded in [Step 8](#). This results in the mass of refrigerant initially desorbed for the trial.

The final step allows the tube/valve system to rest on the balance with the valve open for approximately 15 minutes to measure any amount of refrigerant which further desorbs from the mixture. After 15 minutes, the mass is taken and subtracted from the value reported in [Step 8](#). This value is then reported as the total amount of refrigerant desorbed for the trial (i.e. "slow" desorption rate).

5.4.3 Results and Discussion

Desorption rates were taken for 18 of the 26 pressure-release foaming trials and their data is summarized in the [Appendix \(Table 5.4\)](#). Although "slow" desorption rates are reported in the tables associated with the specifics regarding individual trials ([Appendix Tables 5.3.1 through 5.3.7](#)), only *initial* ("fast") desorption rates, the more relevant parameter of the two, are compared and analyzed.

[Figure 5.24](#) shows the initial desorption rates for R-134a trials varying HFC:POE ratio and pressure drop time. Thirty second drop trials reveal somewhat of a linear trend as initial desorption rates increased slightly with increasing HFC:POE ratio. However, the ten second drop trials are somewhat inconsistent and seem to change dramatically with change in HFC:POE ratio. One source of error is the human error associated with regulating the transient valve on the pressure-release apparatus pictured in [Figure 5.19](#). It is estimated that the drop times reported are most likely within 1 (plus/minus) second of the correct value. In addition, a relative error of 0.05 g/sec for initial desorption rate has been reported based on the error associated with the weighing device.

Figure 5.24 Initial desorption rates for R-134a varying HFC:POE ratio and drop time
(Refer to [Table A5.4](#) in the [Appendix](#))

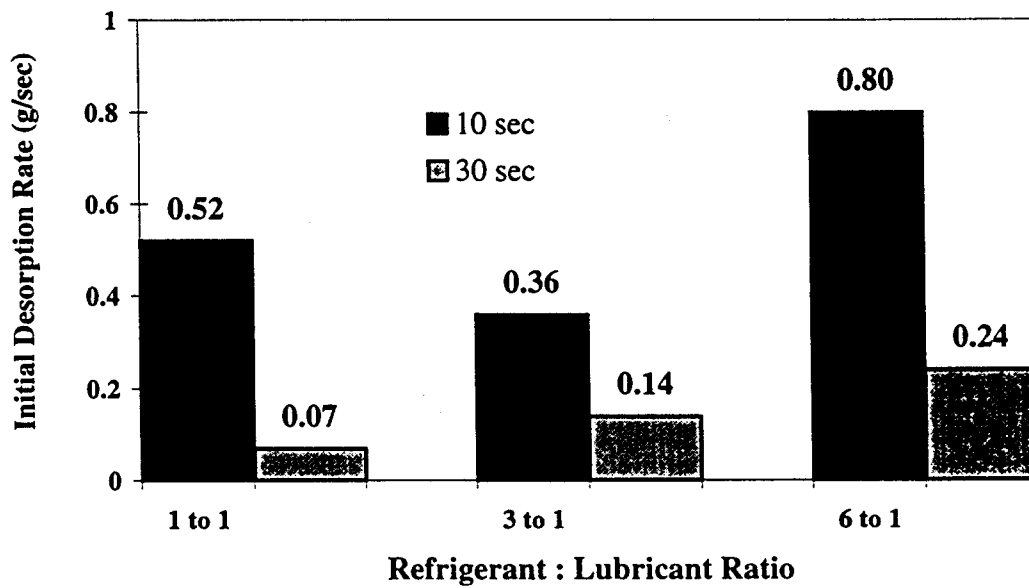
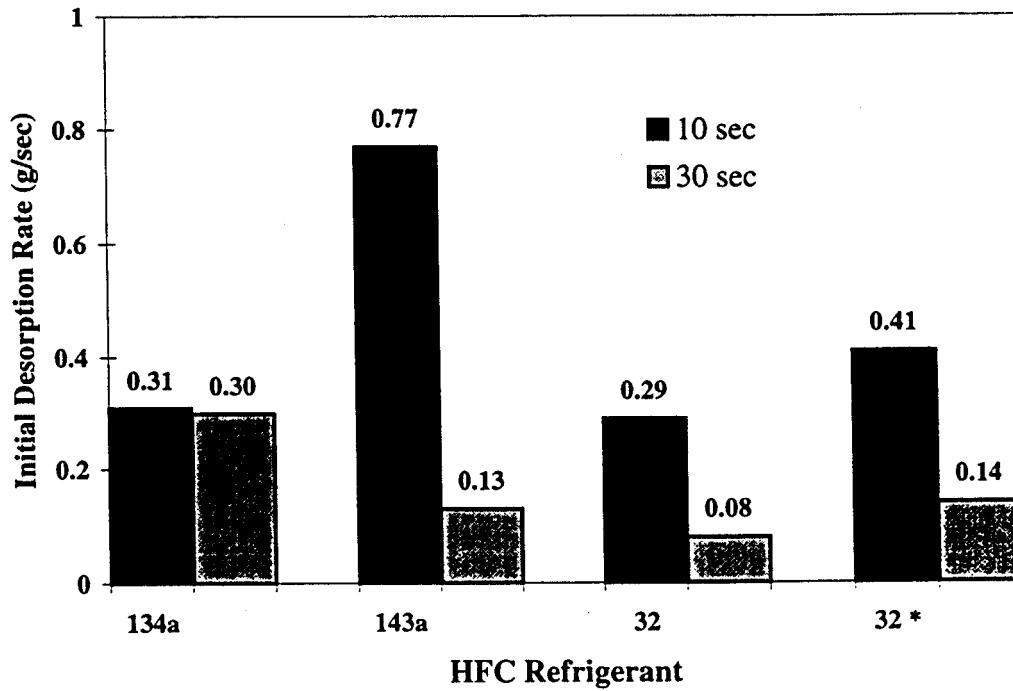


Figure 5.25 shows initial desorption rate data for trials conducted at 50 psi (R-134a, R-143a and R-32) and 70 psi (R-32 only) for both "fast" drop times. R-134a peculiarly had approximately the same initial desorption rate for a 10 second drop as it did for 30 second drop. However, one of the most significant observations is the relatively high desorption rate for R-143a (0.77 g/sec) compared with the other refrigerants at a drop time of 10 seconds. Recall that R-143a displayed the highest deviation *above* the dynamic interfacial tension curve for the air/POE system for both POEs (Figures 4.13 and 4.14) and especially, for the ICI polyolester (Figure 4.14), the lubricant that was used to conduct *all* the pressure-release foaming/desorption rate trials. In essence, the R-143a pairs have the least compatibility, in terms of foamability and initial desorption rate, with the HFCs tested in this study. Theoretically, it appears that the R-143a molecules are desorbing out of the mixture so rapidly that they fail to effectively interact with the refrigerant molecules. Recall that this interfacial interaction is required for interfaces to expand and thus, cause foaming to occur.

The other trials, aside from the 30 second R-134a trial, in Figure 5.25 appear to have similar desorption rates for both 10 and 30 second pressure drops. However, it is the R-143a "fast" desorption rate observation which supports previous findings that R-143a, among the other HFCs tested in this study, is the *least* favorable HFC to form foam with polyolester lubricant.

Figure 5.25 Initial desorption rates for HFCs subjected to a 50 psi pressure drop
* subjected to 70 psi pressure drop
(Refer to [Table A5.4](#) in the [Appendix](#))



5.5 ASTM Standard Test Method for Foaming Characteristics

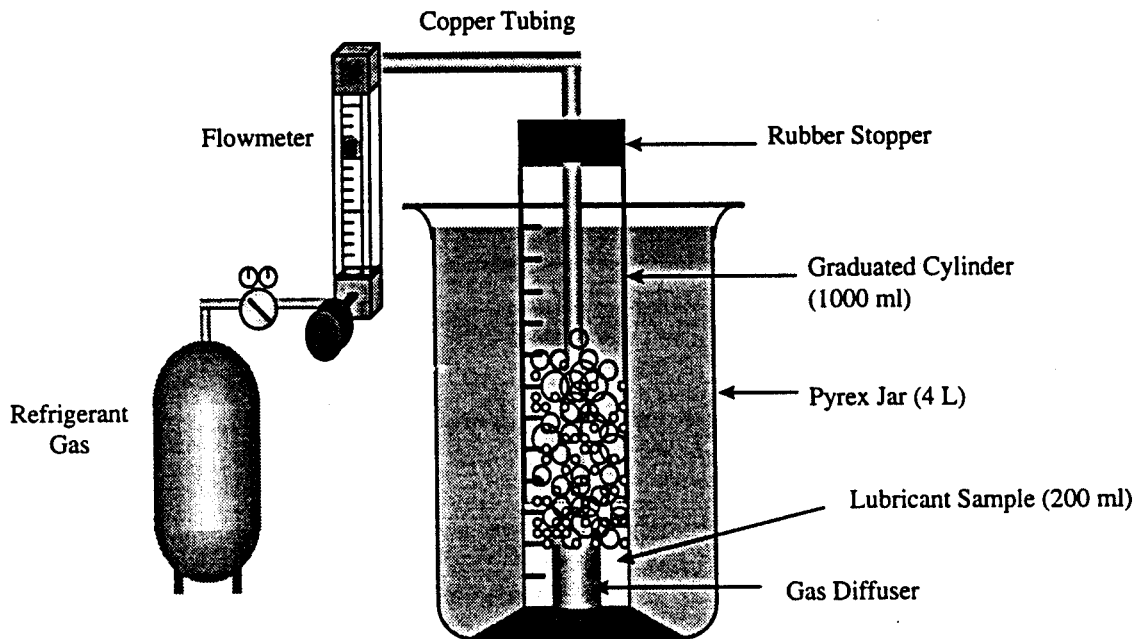
5.5.1 Introduction

The apparatus for the American Society of Testing Materials (ASTM) Standard Test Method for Foaming Characteristics of Lubricating Oils (method D 892 - IP 146 Alternative) was constructed for the purpose of reporting more standardized foaming data. The apparatus, which is shown in [Figure 5.26](#), was used to test the polyolesters with HFC and blended refrigerants in much of the same way that the baseline pairs were tested with the aeration column apparatus described in [section 5.2](#). Although both methods are expected to provide similar data, the D 892 test should yield more standardized data applicable to the area of refrigeration lubrication.

5.5.2 Experimental Design

The lubricant is placed in a 1000 ml graduated cylinder that has a flat-edged top (as opposed to ones with pour spouts). The cylinder is then placed in a temperature bath consisting of a clear Pyrex jar filled with water. The Pyrex jar must be large enough to permit the immersion of the cylinder at least to the 900 ml mark. The graduated cylinder is fitted with a lead ring at its base so as to overcome buoyancy when placed in the bath. A rubber stopper having a hole for the refrigerant-inlet tube is used to seal the top of the graduated cylinder. This inlet tube is connected to the refrigerant supply, located outside of the bath, and to a gas diffuser which is placed inside the cylinder so that it just touches the bottom and is approximately at the center of the circular cross section. The

Figure 5.26 ASTM Standard Test Method for Foaming Characteristics



refrigerant is regulated by a flowmeter and passed through the gas diffuser in the same way that refrigerant was passed through the fritted disk funnel in the aeration column.

The gas diffuser is a cylindrical metal diffuser (model no. M13-0653) purchased from Petrolab Corp. (Latham, NY) which is deemed suitable by ASTM Standards. Copper tubing, for chemical compatibility reasons, was used to connect the diffuser to the refrigerant supply.

5.5.3 Experimental Procedure

Sequence I

Approximately 200 ml of a lubricant sample, as received, is decanted into a beaker and heated to $120 \pm 5^{\circ}\text{F}$ and then allowed to cool to $75 \pm 5^{\circ}\text{F}$ for not more than 3 hours. The lubricant is then poured into the cylinder to approximately the 190 ml mark. The stopper, fitted with the required tubing, is then affixed to the top of the cylinder. The cylinder is then immersed into the temperature bath at least to the 900 ml mark. The initial foam test requires a temperature bath of $75 \pm 1^{\circ}\text{F}$. Once this is maintained, the refrigerant, regulated by a flowmeter at 94 ± 5 ml/min, is then passed through the diffuser into the lubricant solution for 5 minutes. After the 5 minute period, the foam is then allowed to settle for 10 minutes. Foam volume, measured from the top of the oil to the top of the foam height, is recorded at the end of both time periods.

Sequence II

A second lubricant sample is placed into a cleaned 1000 ml graduated cylinder until the lubricant level is at 180 ml. The cylinder is immersed as before into a bath which is maintained at $200 \pm 1^\circ\text{F}$. When the oil has reached a temperature of $199^\circ\text{F} \pm 2^\circ\text{F}$, a clean gas diffuser is inserted and the procedure then continues in the same fashion as in [Sequence I](#).

Sequence III

Any foam remaining from Sequence II is collapsed with a stirring rod. The sample is cooled to 110°F by allowing the cylinder to stand in room temperature conditions. The cylinder is then placed in a 75°F bath and the oil is allowed to reach the bath temperature. A clean diffuser is inserted and the foam volume testing continues as before.

5.5.4 Results and Discussion

Although this method probably would have been successful for the baseline pairs, this method did not prove to be suitable for alternative refrigerant pairs. Bubbles were formed from the gas diffuser, however, they merely broke at the air/lubricant interface. In short, no foaming was observed for any of the HFC/POE pairs mainly because the experiments were conducted at ambient pressure (i.e. *no* pressure drop). Although the temperature of the lubricant is a significant parameter for the ASTM method and is different than previous aeration and pressure-release trials, it seems that the absence of a pressure drop is the reason for the lack of foam formation.

6. ABSORPTION RATES

6.1 Introduction

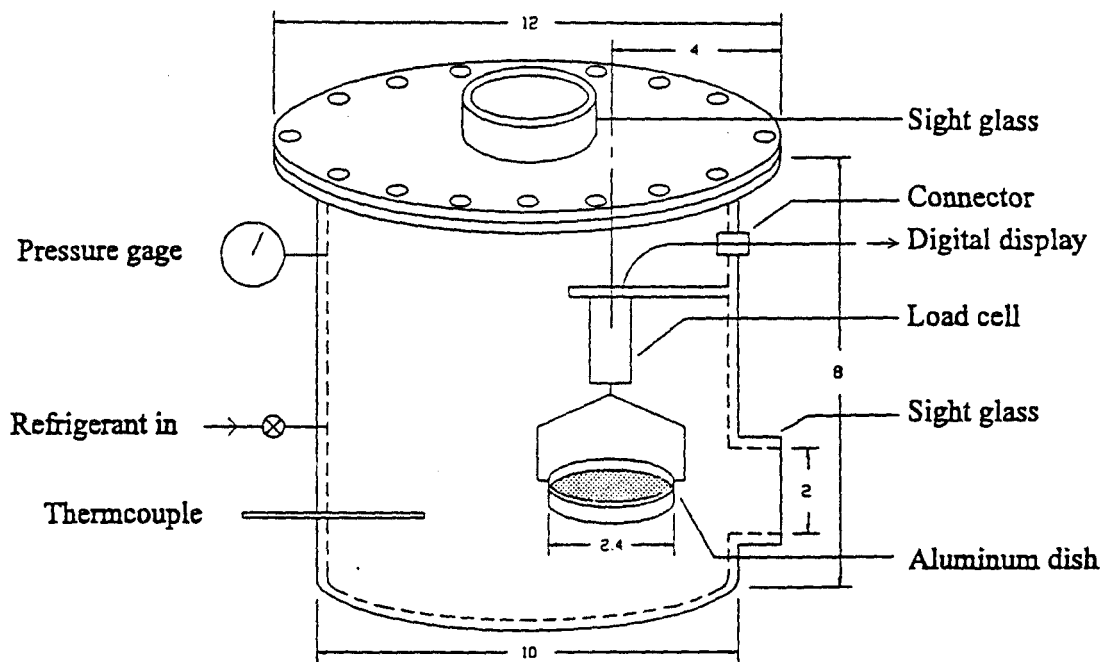
Absorption of refrigerant in the lubricant has been studied by a weight gain method. An open container of lubricant in a pressure vessel is continuously weighed by a force transducer when the vessel is filled with a known refrigerant under predetermined pressure and temperature conditions. The change in the weight is plotted as a function of time and absorption rate is calculated.

6.2 Apparatus

An apparatus to measure the absorption of refrigerant into the ICI polyolester is shown in [Figure 6.1](#). It consists of a 10 inch diameter flanged steel vessel with a height of 8 inches and a wall thickness of 0.25 inch. This vessel is fitted with two sight glasses, one close to the bottom of the vessel and another on the flange as shown in the figure. These sight glasses can withstand a pressure of 500 psig. A force transducer (from Cooper Instruments, model LPM620-30) is installed inside the vessel and is connected to a digital display through a connector. A pressure gauge and T-type thermocouple is fitted on the vessel to measure the pressure and temperature. An access port is fitted on the pressure vessel for charging the system with refrigerant. A copper coil (0.25 inches in diameter, not shown in figure) is installed inside the pressure vessel to vary the temperature of the vessel. The temperature inside the vessel is controlled by passing a fluid from a thermostat bath through the copper coil. Water is used for temperatures higher than 0°C and a 50-50 ethylene glycol and water is used for the temperature below

0°C. An aluminum dish of 57 mm diameter is used as a pan to hold the lubricant and is connected to the force transducer with stainless steel wires. This pressure vessel is insulated with 1 inch thick fiberglass to prevent heat loss.

Figure 6.1 Absorption rate test facility



6.3 Calibration

The force transducer is first calibrated with standard weights. A known standard weight is placed on the pan and weight measured by the force transducer is recorded. This force transducer is designed to measure the weight up to 30 grams, with an accuracy of $\pm 0.15\%$ of full scale. Typical calibration values are shown below:

Standard weight (g)	0.5	1	1.5	2	2.5	3	3.5	4
Weight measured by transducer (grams)	0.498	1.006	1.505	2.005	2.503	3.003	3.501	4.003

In this case the difference between standard weight and measured weight is at third decimal place and varies between -0.002 to +0.006 grams.

6.4 Procedure And Measurements

To measure the absorption rate and solubility of refrigerant in the lubricant two grams (± 0.001 g) of lubricant is weighed in the aluminum pan inside the pressure vessel. The pressure vessel is then sealed by closing the top with the flange using 12 nuts and bolts of 1/4 inch size. It is then evacuated close to 29 in Hg. with a vacuum pump. After the evacuation is complete the refrigerant to be tested is allowed to enter the pressure vessel through the access port until a predetermined pressure is reached. After waiting for about 30 to 40 seconds, the value of force transducer display unit is set to zero reading, so that the change in the values will directly give the weight gained by the lubricant. The weight gain is recorded as a function of time until no appreciable change in the weight is observed for about 10 to 15 minutes. This procedure is repeated a second

or third time to check the consistency of the results. The uncertainties in the measurements of pressure, temperature and weight are ± 0.5 psi, $\pm 0.2^\circ\text{C}$ and ± 0.045 grams, respectively. The absorption rates and solubility of HFC refrigerants namely, R-134a, R-143a, R-125, R-32 and their blends R-404A, R-407C and R-410A were studied at following temperature and pressure conditions:

- a. Refrigerant and lubricant are at room temperature (24°C)
- b. Lubricant is 10 degrees warmer than refrigerant.
- c. Lubricant is 20 degrees warmer than refrigerant.
- d. Lubricant and refrigerant are at 40°C
- e. Lubricant and refrigerant are at -10°C

6.5 Results And Discussion

The graphs are plotted between weight composition (x) of the refrigerant in the refrigerant/lubricant mixture as a function of time for different pressure and temperature conditions. Here x is given by the formula

$$x = 100 \cdot [m_r / (m_r + m_o)]$$

where m_r = mass of refrigerant in the mixture and m_o = mass of oil in the mixture.

By inspection it was found that the absorption data can be represented by the exponential function as:

$$x = X (1 - e^{-kt})$$

where X = solubility of refrigerant in the lubricant, k = absorption rate constant and t = time in minutes. The initial absorption rate (x_0) can be obtained from the equation:

$$x_0 = k X$$

The data of solubility, absorption rate, and initial rate absorption at 24°C are reported in the [Table 6.1](#) and plotted in [Figures 6.2 to 6.8](#). In these figures, experimental data is represented by the symbols and the data curve-fit is represented by solid lines. The solubility of R-134a and R-125 at 24°C measured in this study is compared with the solubility data published by Martz et al. (1996), ICI (1996), and Sibley (1993). The comparison of the solubility data is shown in [Figure 6.9](#). The difference in the results is mainly due to uncertainty error of $\pm 2\%$ in the measurements. Some of the refrigerants have very large solubility at -12°C, 20 psig. The reason is probably due to the fact that these refrigerants partially condense at that condition. This reason also explains this experiment cannot be conducted at -12°C and 50 psig.

Table 6.1 Experimental results of the absorption of HFC refrigerants and their blends in POE lubricant at room temperature (24°C)

Refrigerants	Pressure (psig)	Solubility, X (%)	Absorption rate, k (min ⁻¹)	Initial absorption rate (% / min ⁻¹)
R-32	20	1.597	0.06296	0.1005
	50	2.718	0.04905	0.1333
	70	6.697	0.06052	0.4053
R-125	20	6.749	0.09749	0.658
	50	10.6	0.05059	0.5363
	70	15.36	0.05203	0.7992
R-134a	20	8.063	0.05565	0.449
	30	12.52	0.05098	0.6383
	50	21.09	0.06617	1.396
R-143a	20	2.125	0.05087	0.1081
	50	5.233	0.02898	0.1517
	70	7.514	0.03793	0.285
R-404A	20	2.2	0.02113	0.0465
	50	6.74	0.02809	0.1893
	70	10.99	0.03286	0.3611
R-407C	20	4.926	0.01659	0.0817
	50	11.58	0.0581	0.6728
	70	21.49	0.08866	1.905
R-410A	20	2.936	0.1614	0.4739
	50	7.07	0.07812	0.5523
	70	16.3	0.169	2.755

Table 6.2 Experimental results of the absorption of HFC refrigerants
and their blends in POE lubricant at 34°C

Refrigerants	Pressure (psig)	Solubility, X (%)	Absorption rate, k (min ⁻¹)	Initial absorption rate (% / min ⁻¹)
R-32	20	0.9159	0.1084	0.0993
	50	2.0895	0.1056	0.2207
R-125	20	2.917	0.1849	0.5394
	50			
R-134a	20	8.2764	0.2049	1.6958
	50	18.5744	0.1820	3.3805
R-143a	20	3.4023	0.5941	2.0213
	50	9.1437	0.5789	5.2933
R-404A	20	4.6490	0.2162	1.0051
	50	11.9337	0.1817	2.1684
R-407C	20	6.0516	0.0739	0.4472
	50			
R-410A	20	1.7205	0.1402	0.2412
	50			

Table 6.3 Experimental results of the absorption of HFC refrigerants
and their blends in POE lubricant at 44°C

Refrigerants	Pressure (psig)	Solubility, X (%)	Absorption rate, k (min ⁻¹)	Initial absorption rate (% / min ⁻¹)
R-32	20	2.3583	0.1258	0.2967
	50	3.6171	0.1132	0.4095
R-125	20			
	50			
R-134a	20	7.1739	0.2202	1.5797
	50	17.5541	0.2456	4.3113
R-143a	20	3.4946	0.7792	2.7230
	50	9.0548	0.7765	7.0311
R-404A	20	2.9324	0.2257	0.6618
	50	4.7034	0.1208	0.5682
R-407C	20	2.8044	0.0917	0.2572
	50	5.0879	0.1049	0.5337
R-410A	20	1.5083	0.0677	0.1021
	50	3.8351	0.0723	0.2773

Table 6.4 Experimental results of the absorption of HFC refrigerants
and their blends in POE lubricant at -12°C

Refrigerants	Pressure (psig)	Solubility, X (%)	Absorption rate, k (min ⁻¹)	Initial absorption rate (% / min ⁻¹)
R-32	20	3.9364	0.2462	0.9691
R-125	20			
R-134a	20			
R-143a	20	13.8390	0.1303	1.8032
R-404A	20	18.0217	0.0960	1.7301
R-407C	20	21.5475	0.0660	1.4221
R-410A	20	3.8852	0.0730	0.2836

Figure 6.2 Absorption of R-32 in POE at room temperature (24°C)

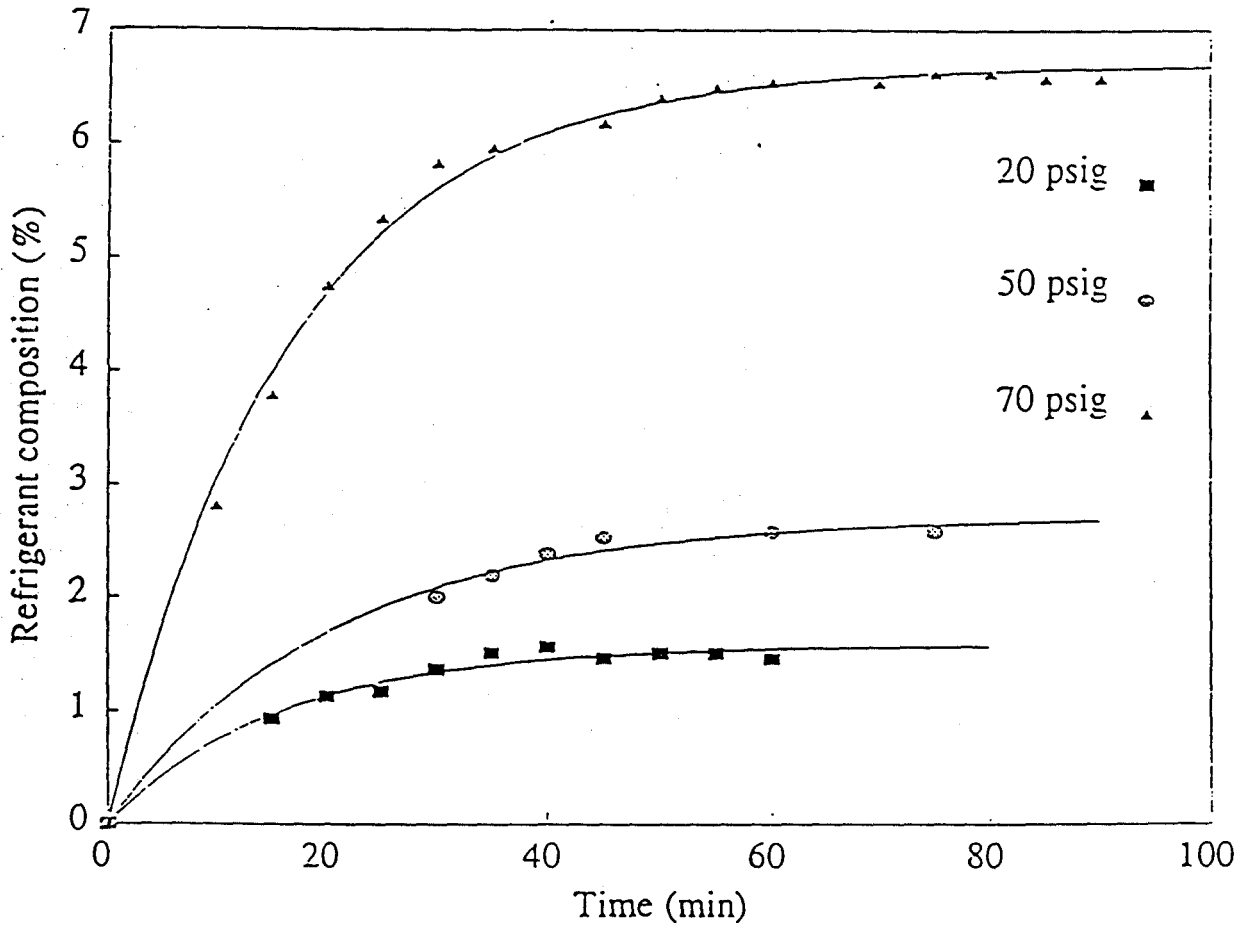


Figure 6.3 Absorption of R-125 in POE at room temperature (24°C)

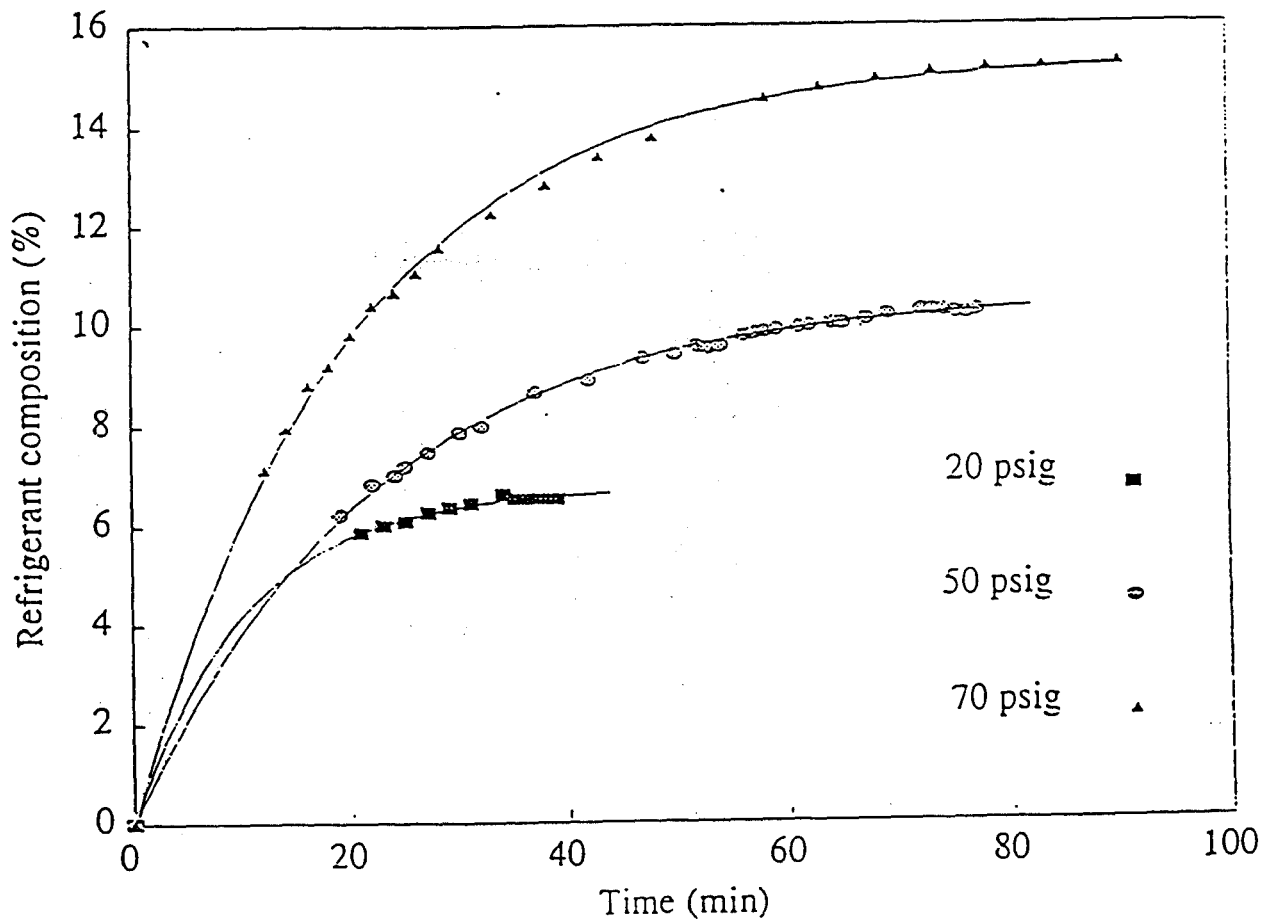


Figure 6.4 Absorption of R-134a in POE at room temperature (24°C)

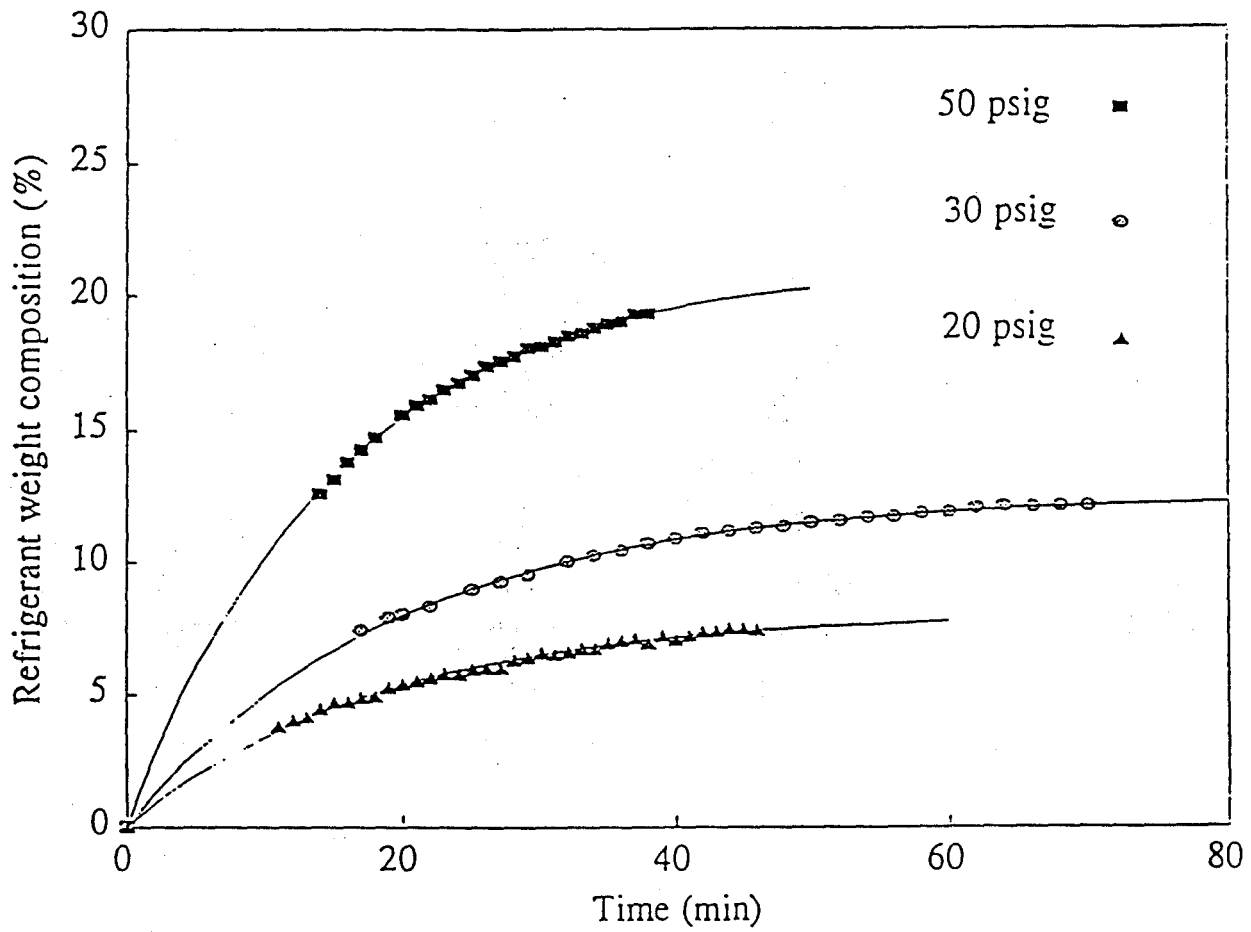


Figure 6.5 Absorption of R-143a in POE at room temperature (24°C)

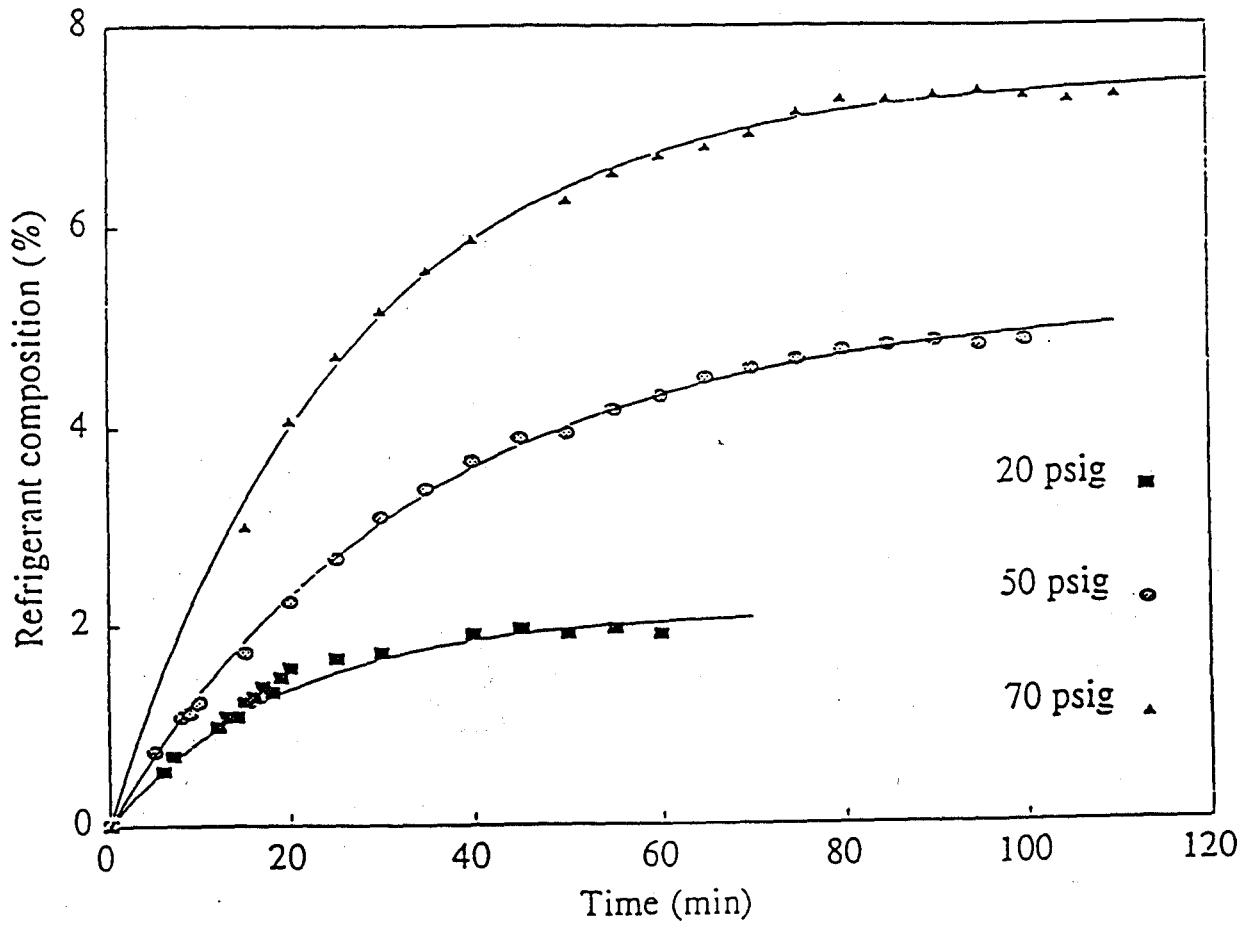


Figure 6.6 Absorption of R-404A in POE at room temperature (24°C)

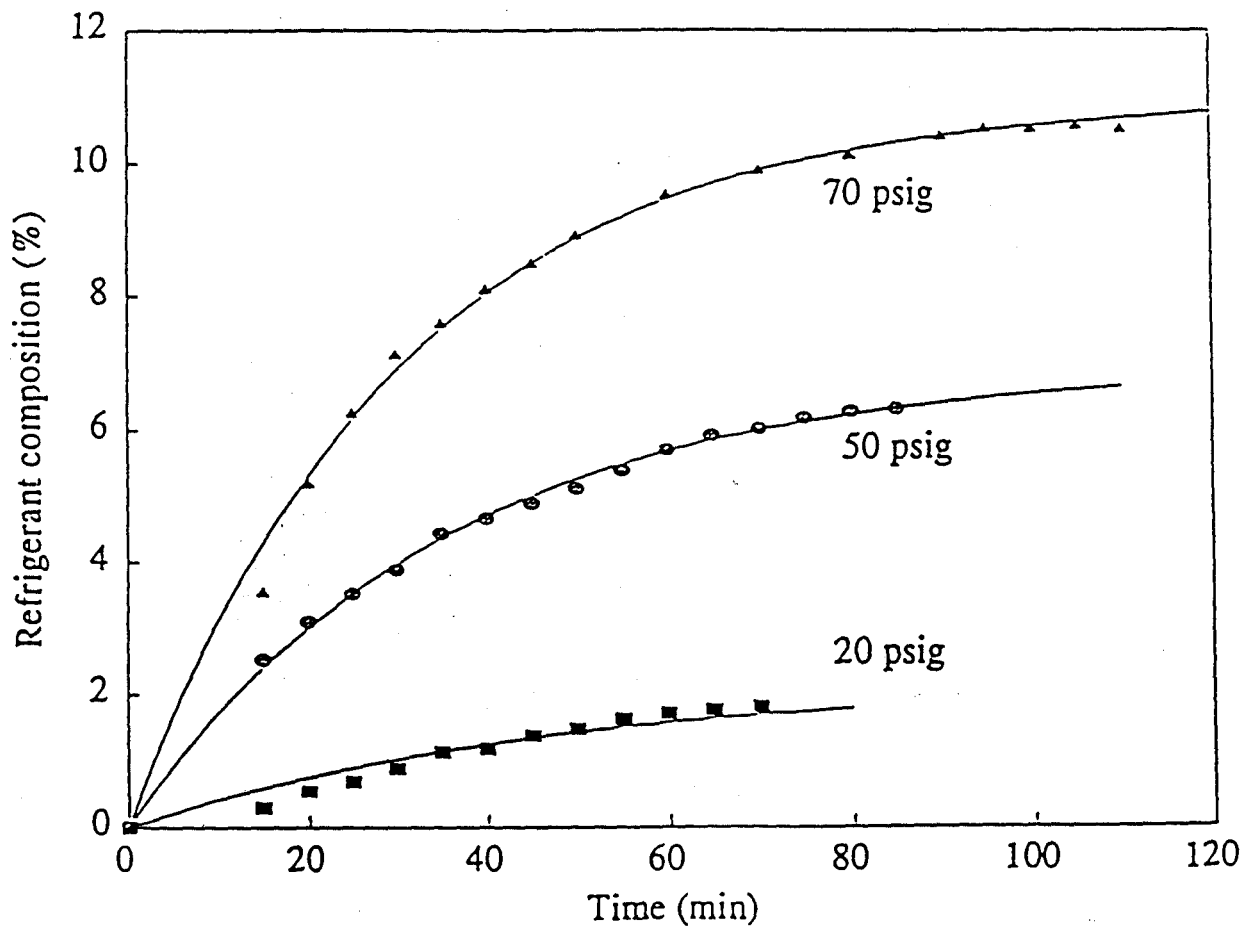


Figure 6.7 Absorption of R407C in POE at room temperature (24°C)

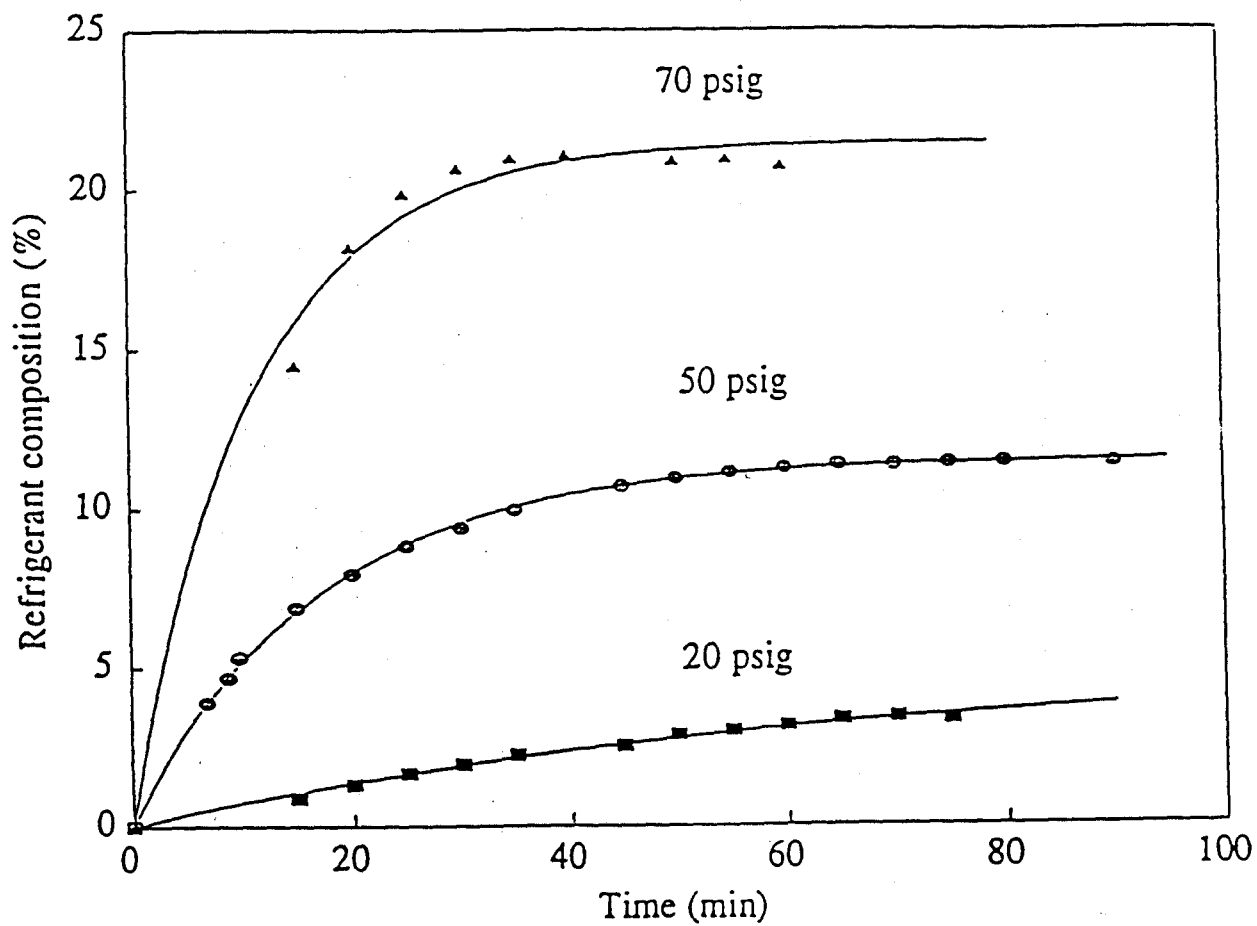


Figure 6.8 Absorption of R-410A in POE at room temperature (24°C)

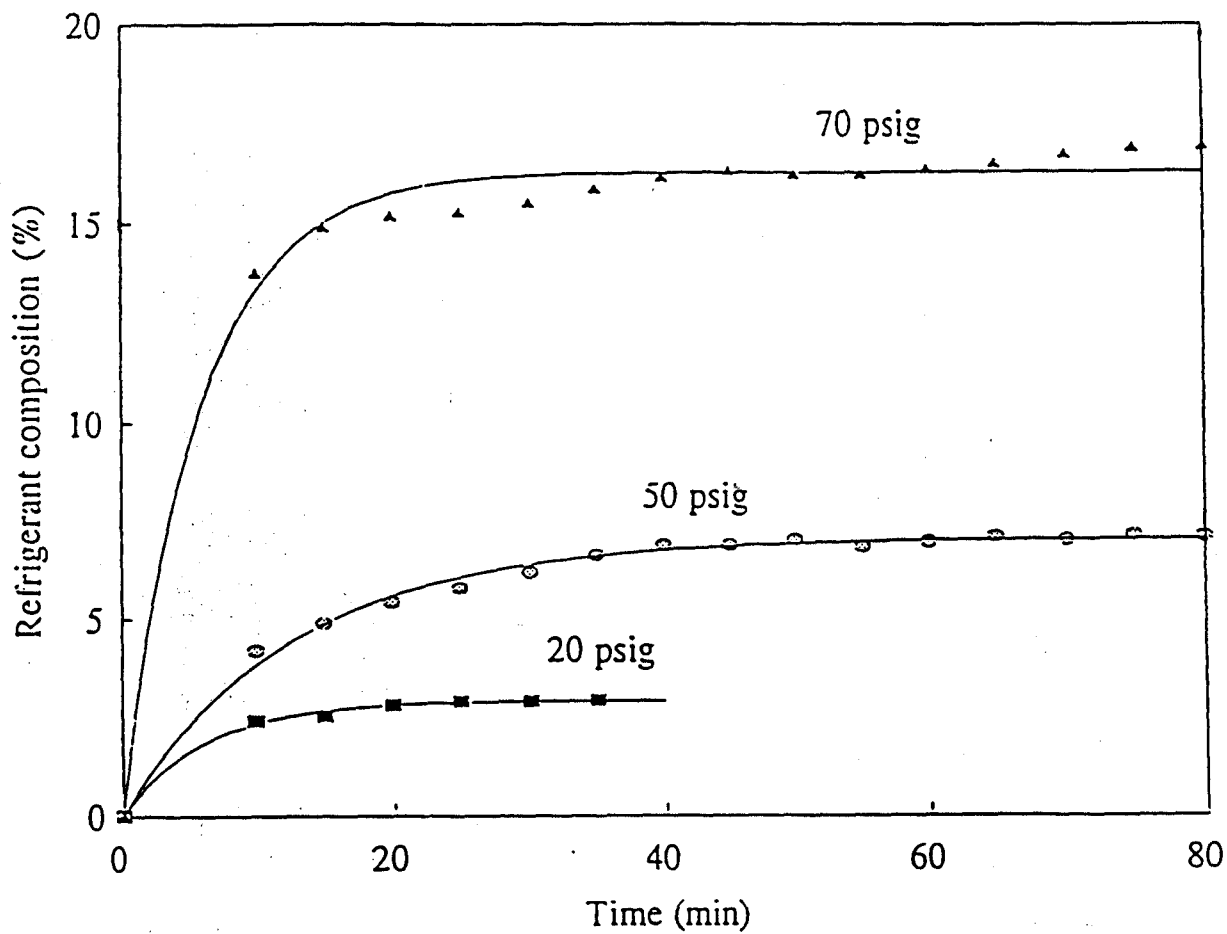


Figure 6.9 Comparison of experimental data with published values

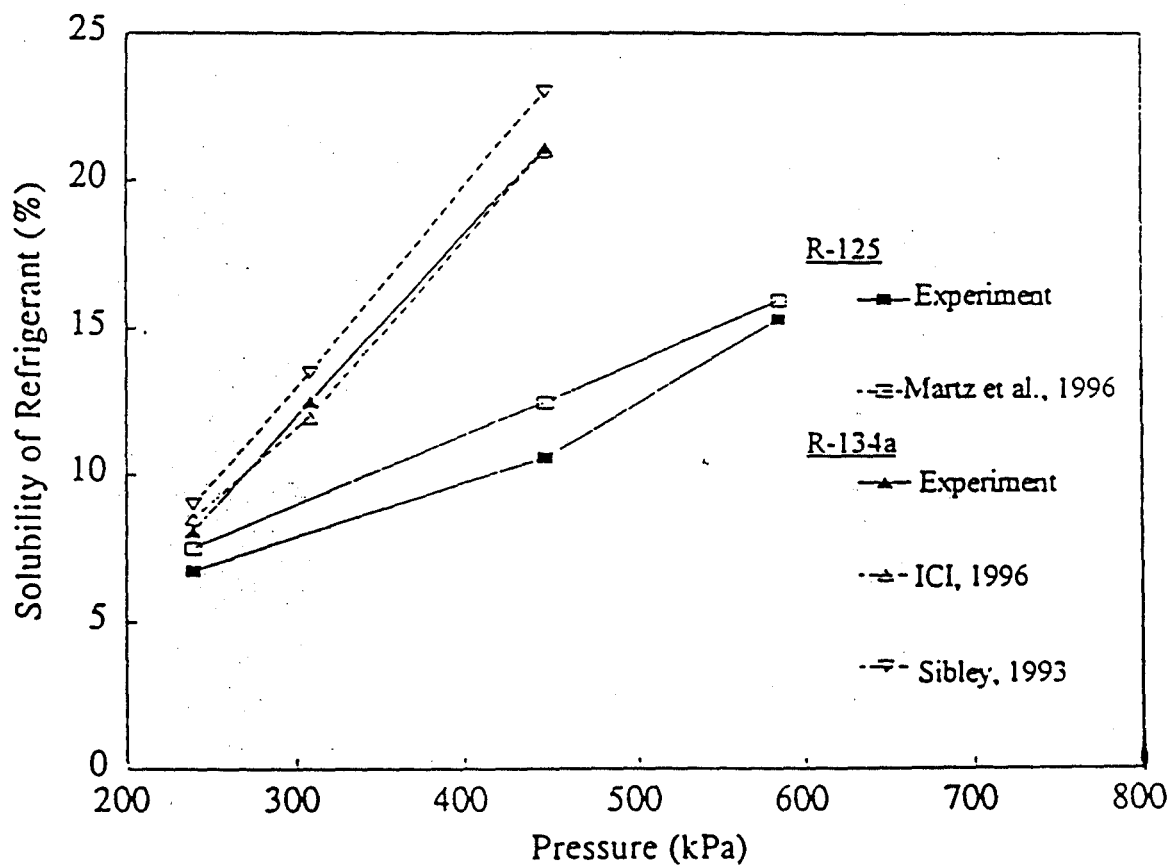


Figure 6.10 Absorption of R-32 in POE at 34°C

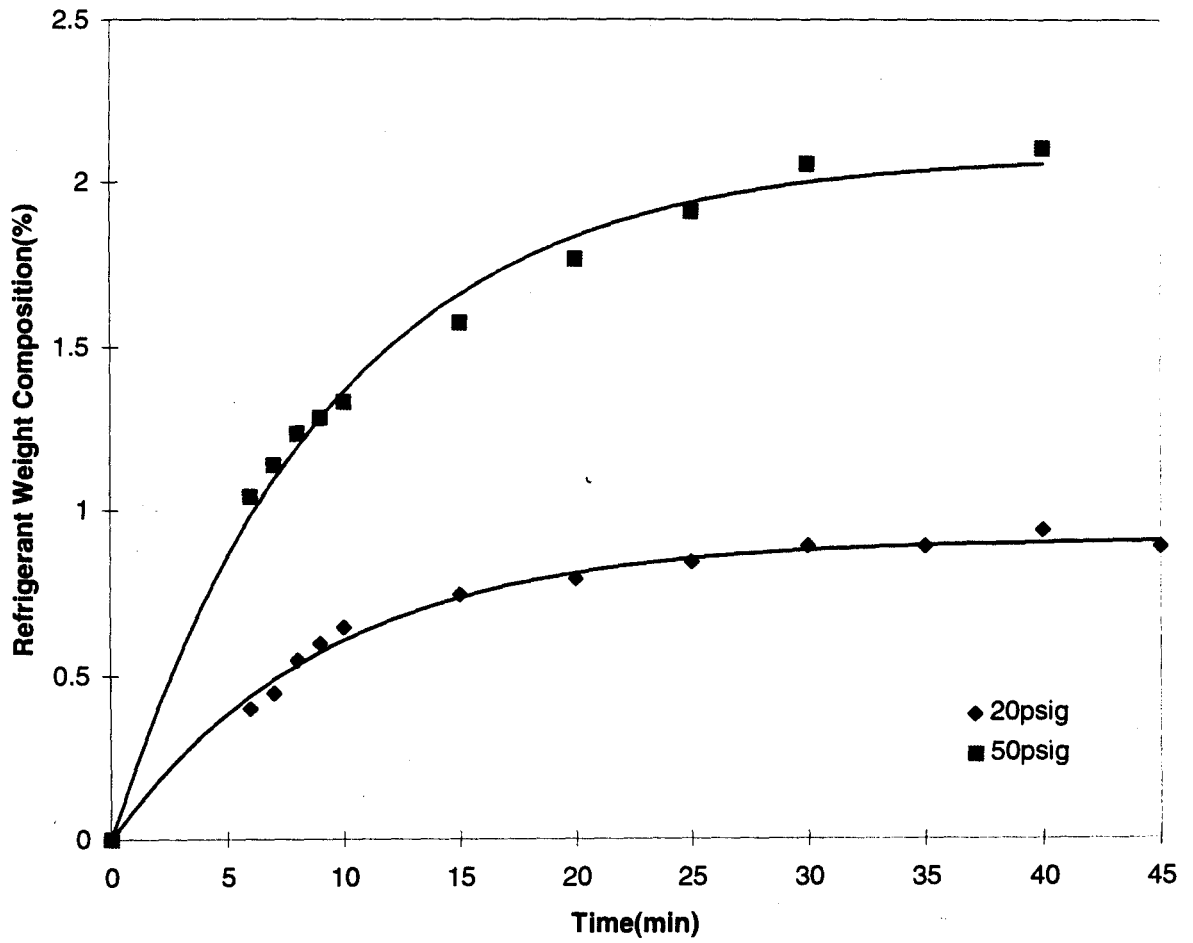


Figure 6.11 Absorption of R-125 in POE at 34°C

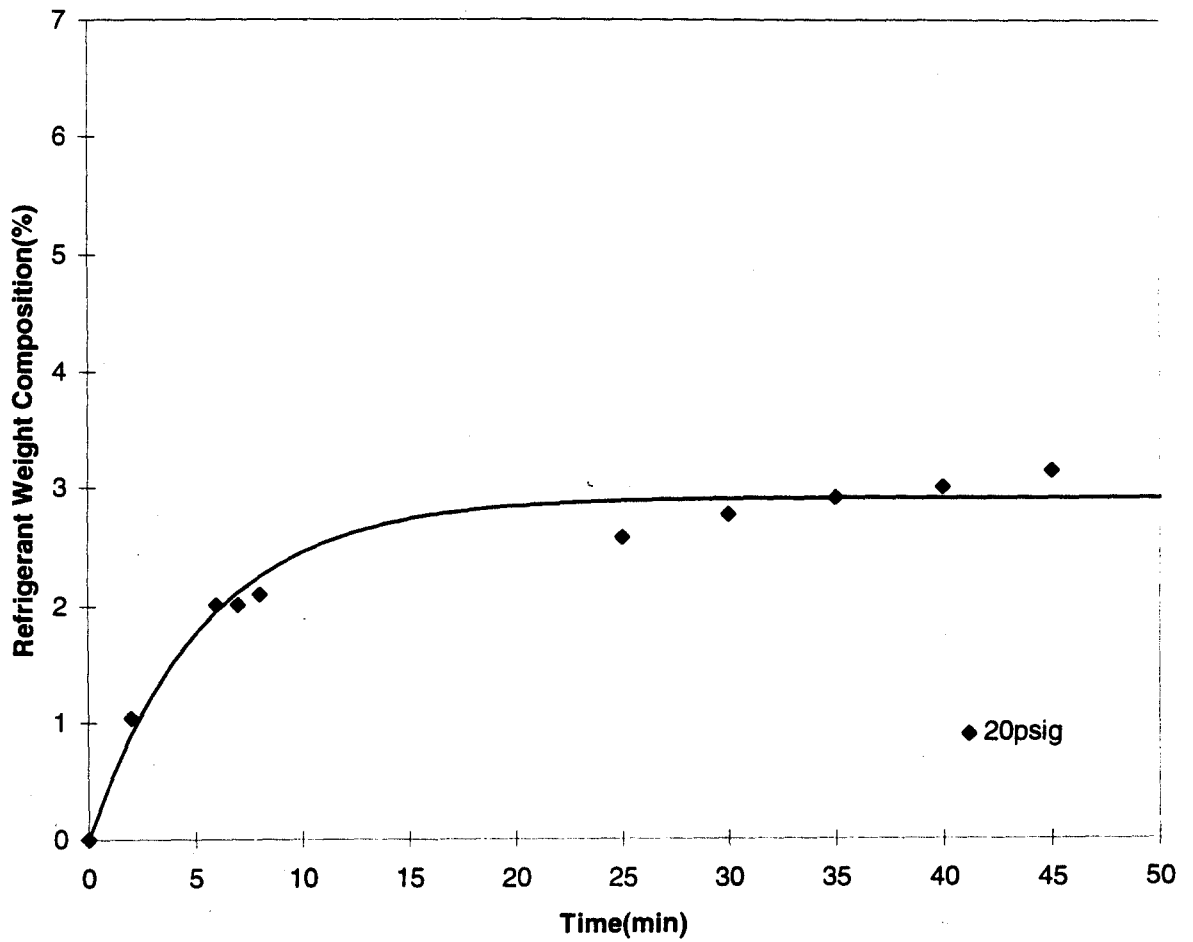


Figure 6.12 Absorption of R-134a in POE at 34°C

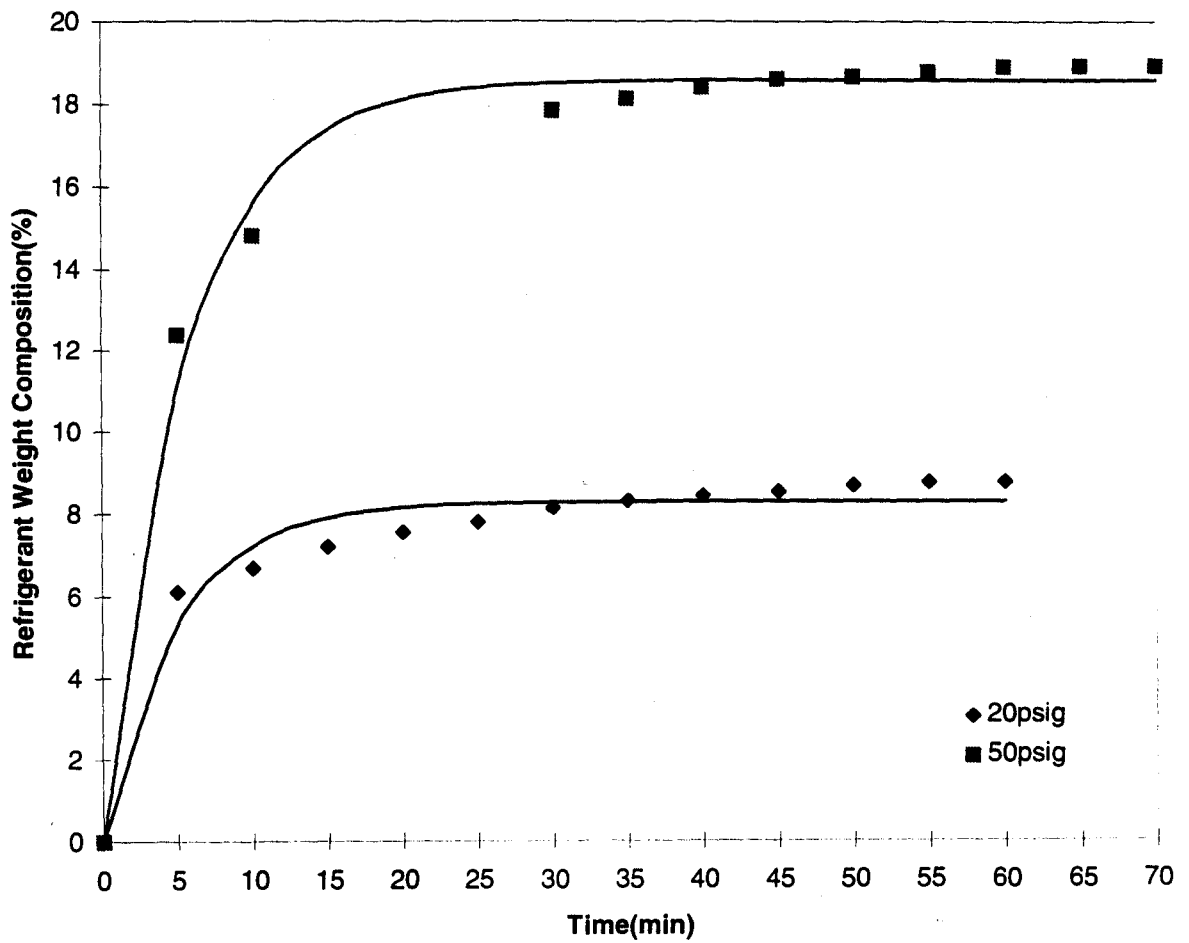


Figure 6.13 Absorption of R-143a in POE at 34°C

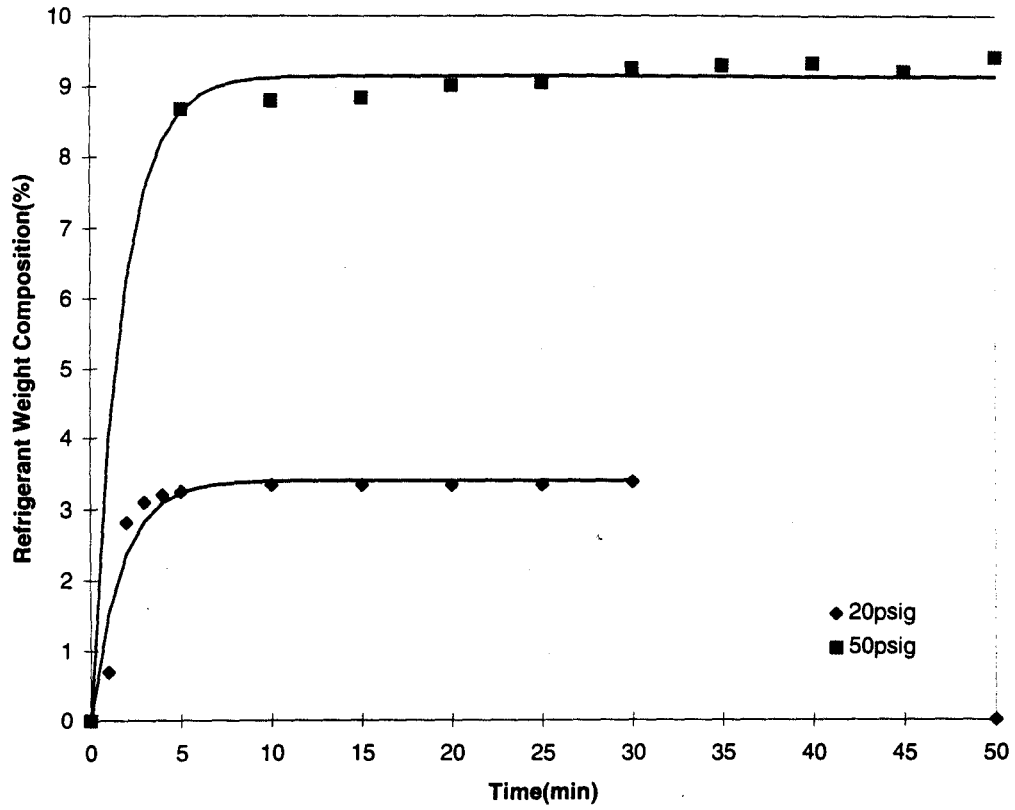


Figure 6.14 Absorption of R-404A in POE at 34°C

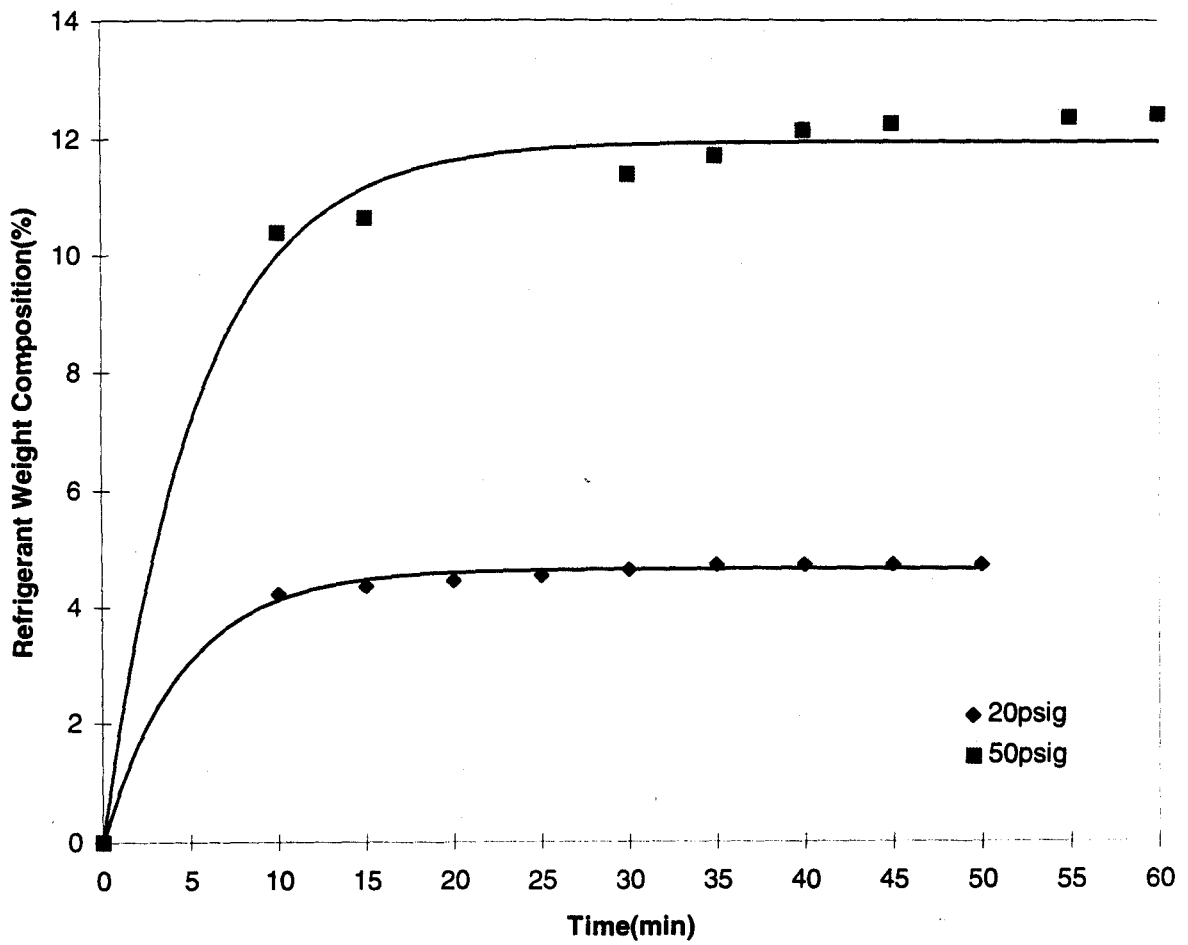


Figure 6.15 Absorption of R-407C in POE at 34°C

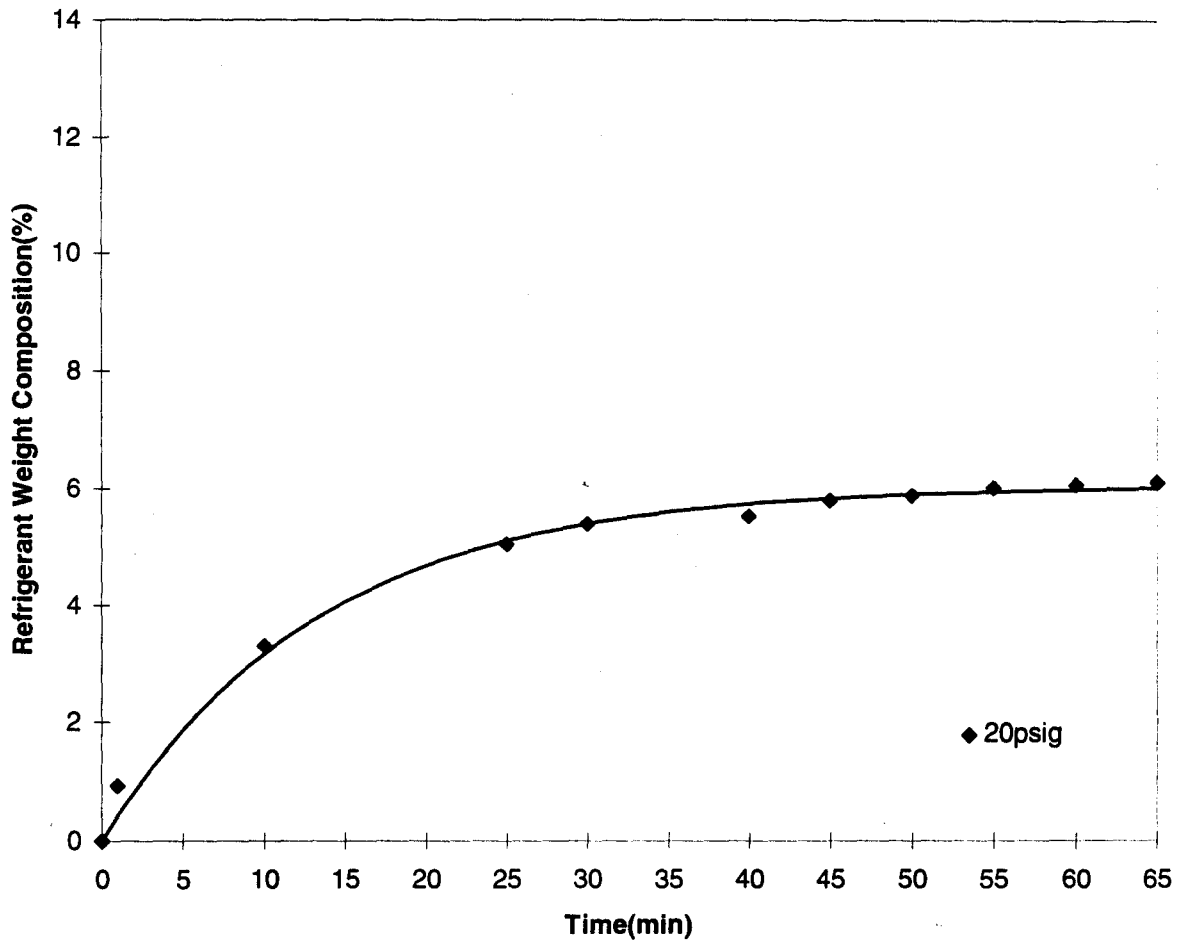


Figure 6.16 Absorption of R-410A in POE at 34°C

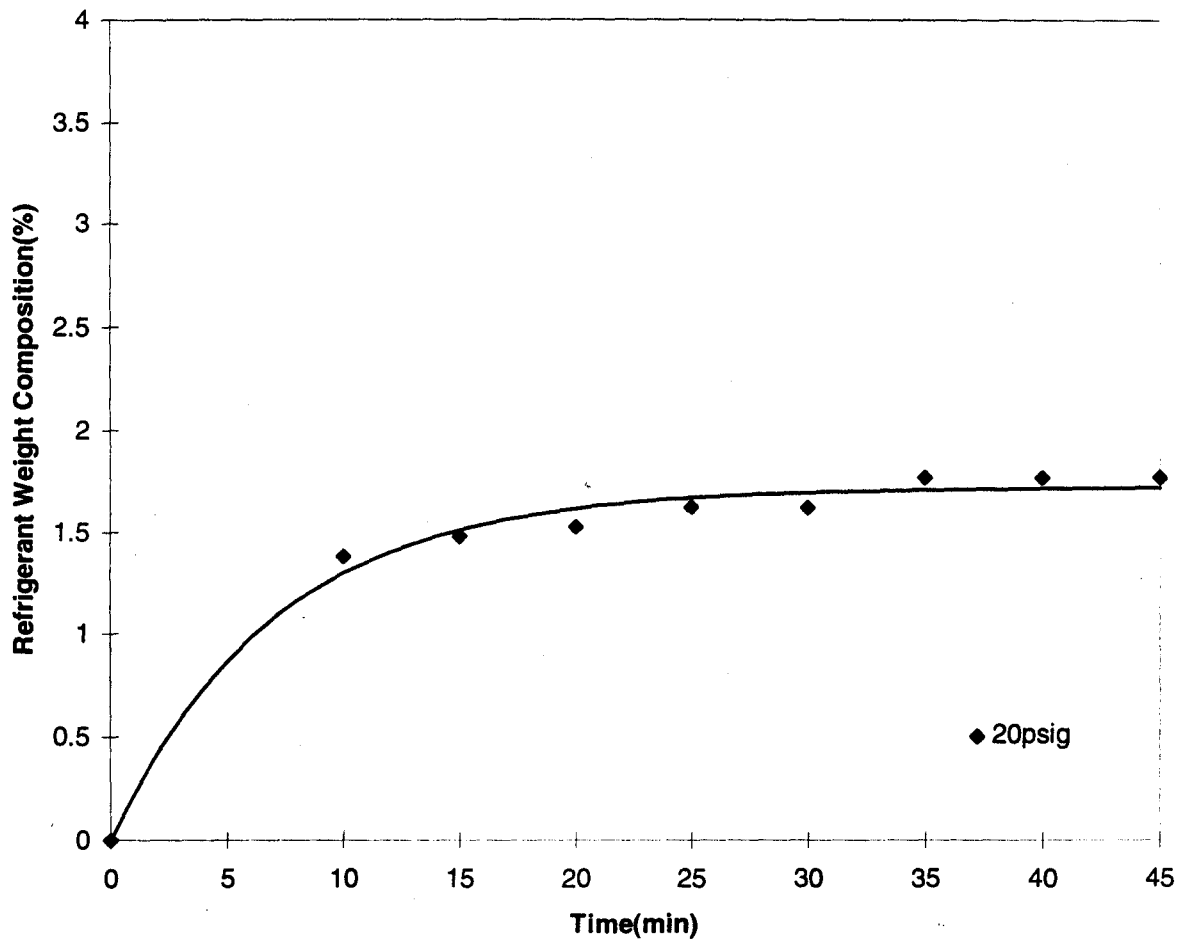


Figure 6.17 Absorption of R-32 in POE at 44°C

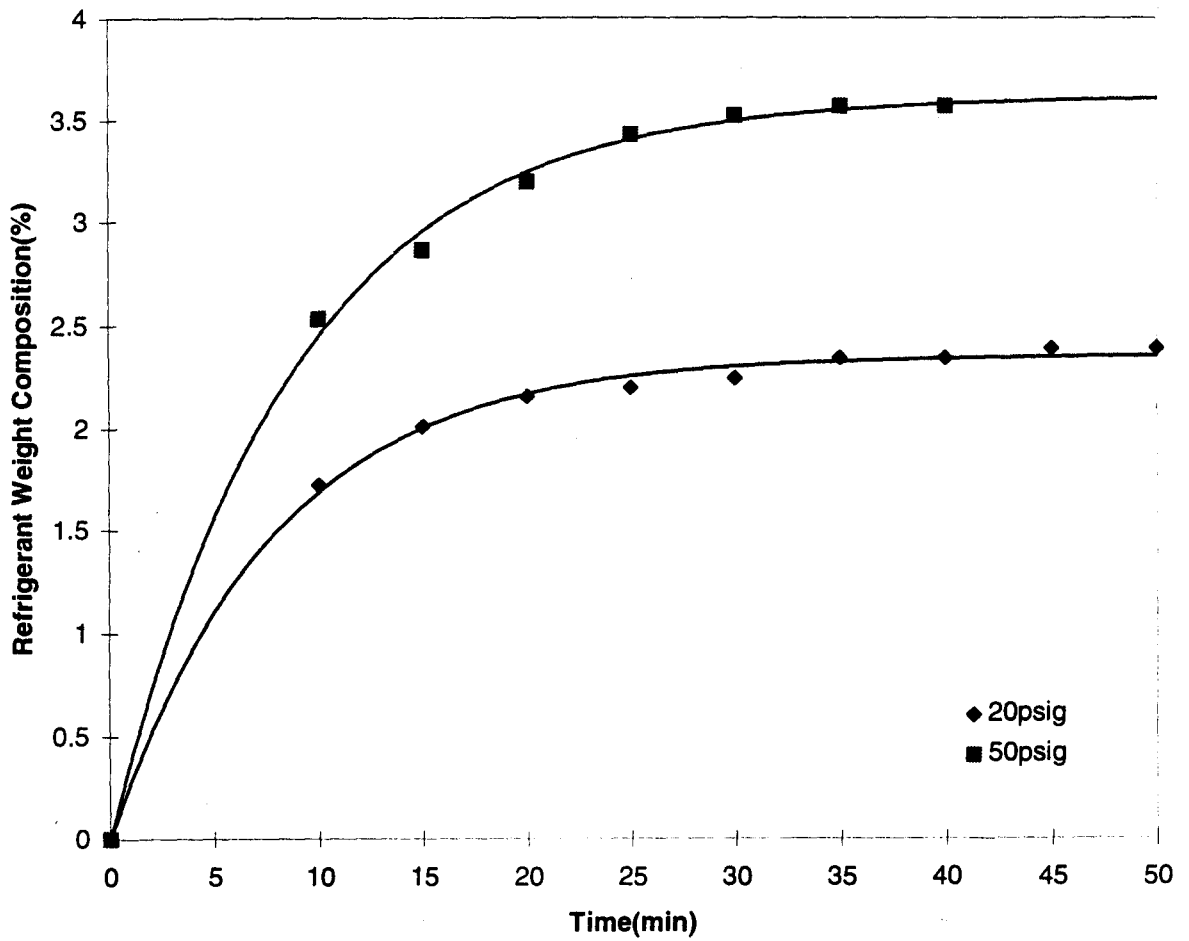


Figure 6.18 Absorption of R-134a in POE at 44°C

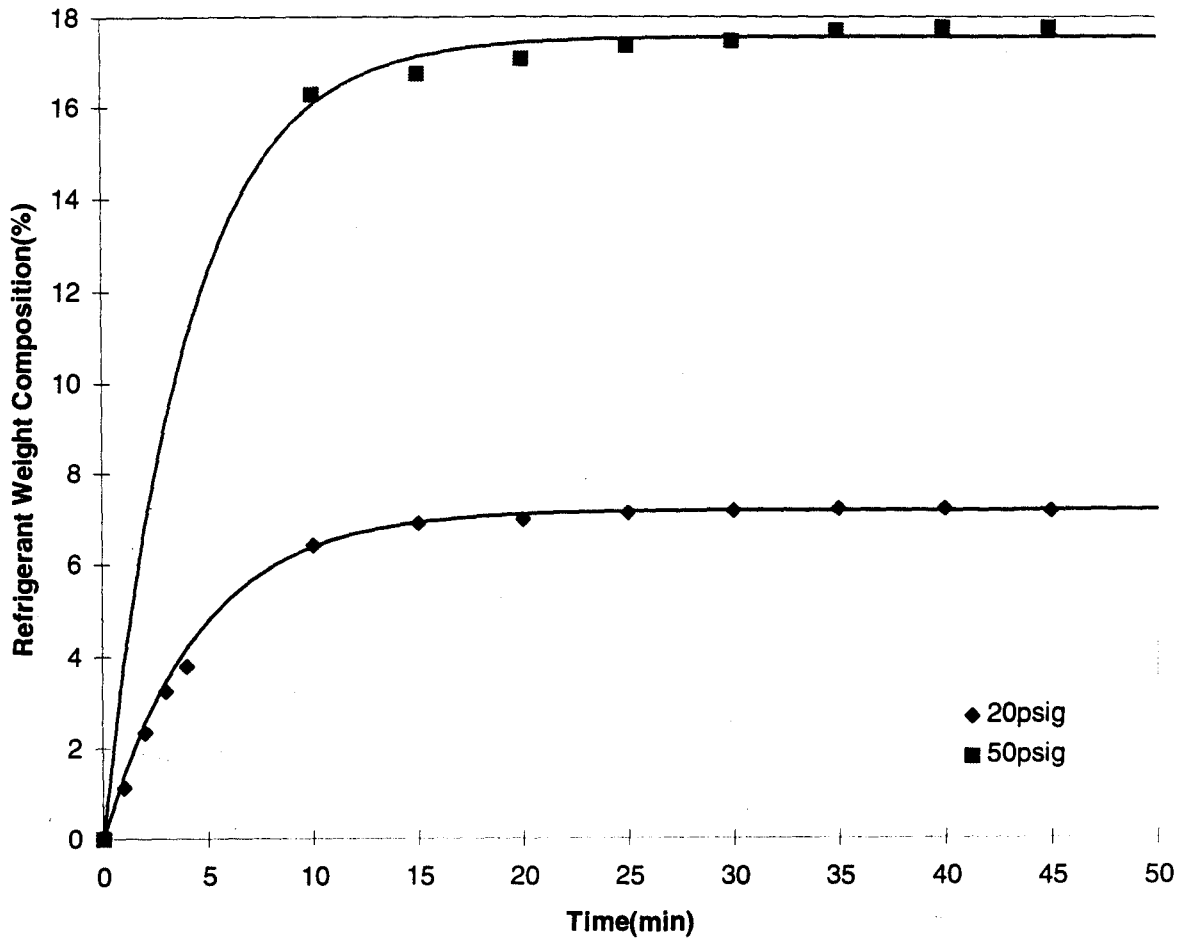


Figure 6.19 Absorption of R-143a in POE at 44°C

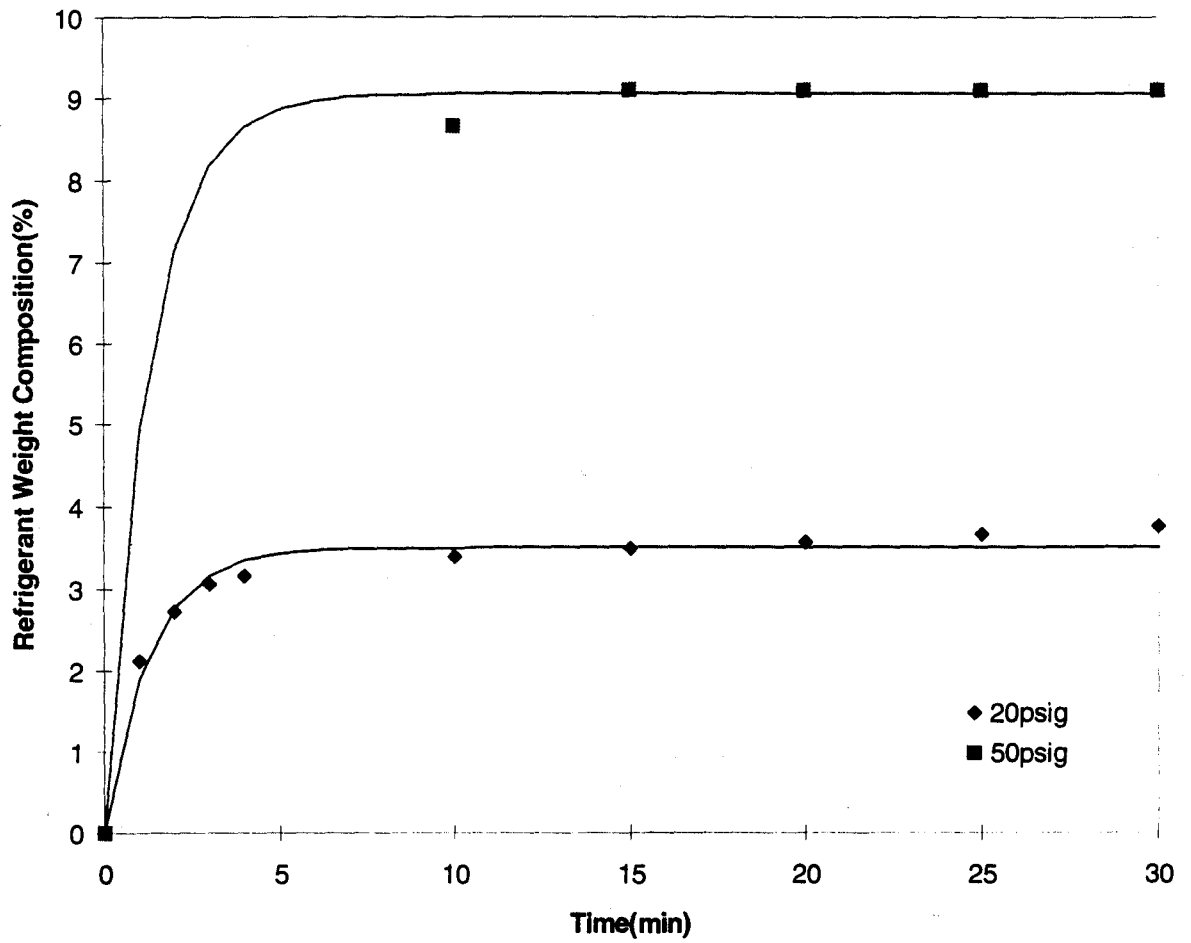


Figure 6.20 Absorption of R-404A in POE at 44°C

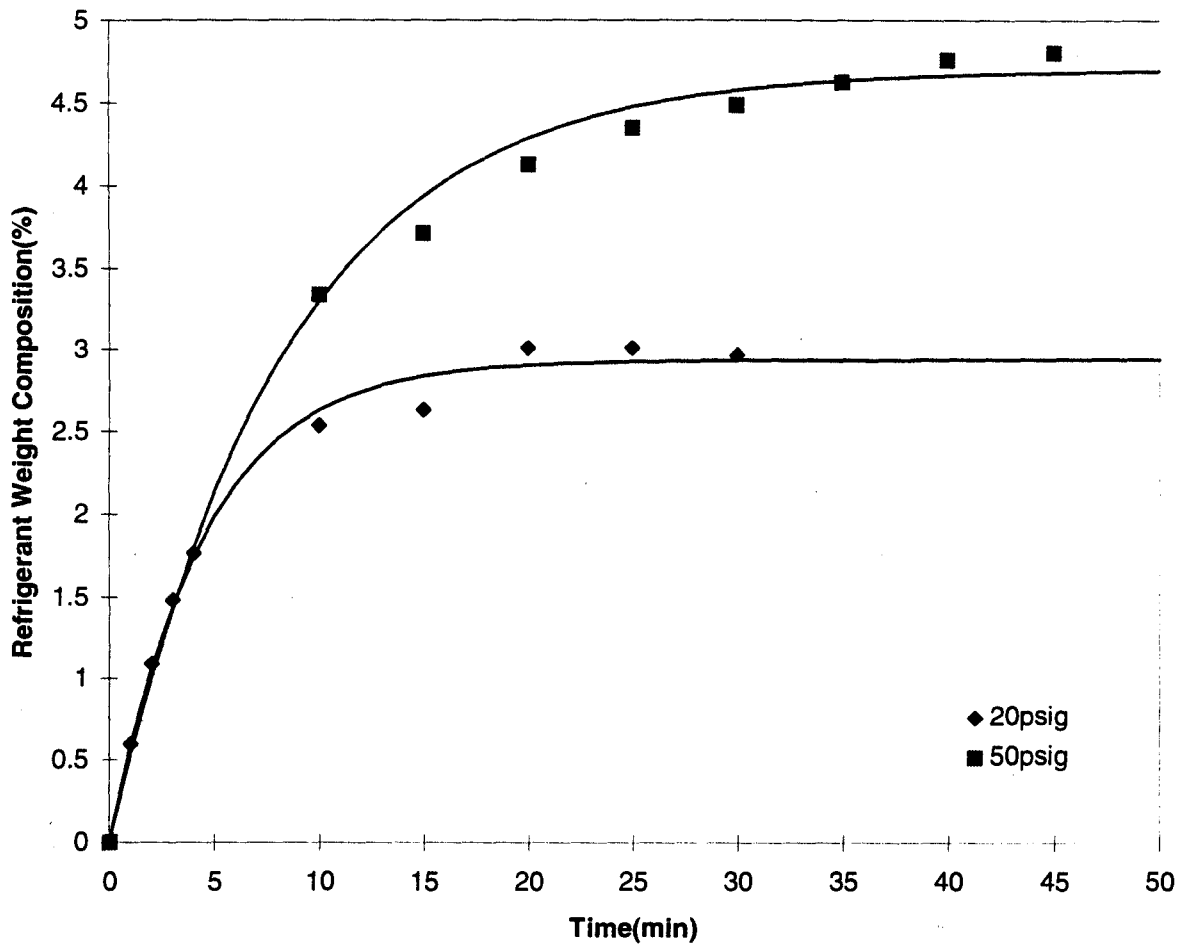


Figure 6.21 Absorption of R-407C in POE at 44°C

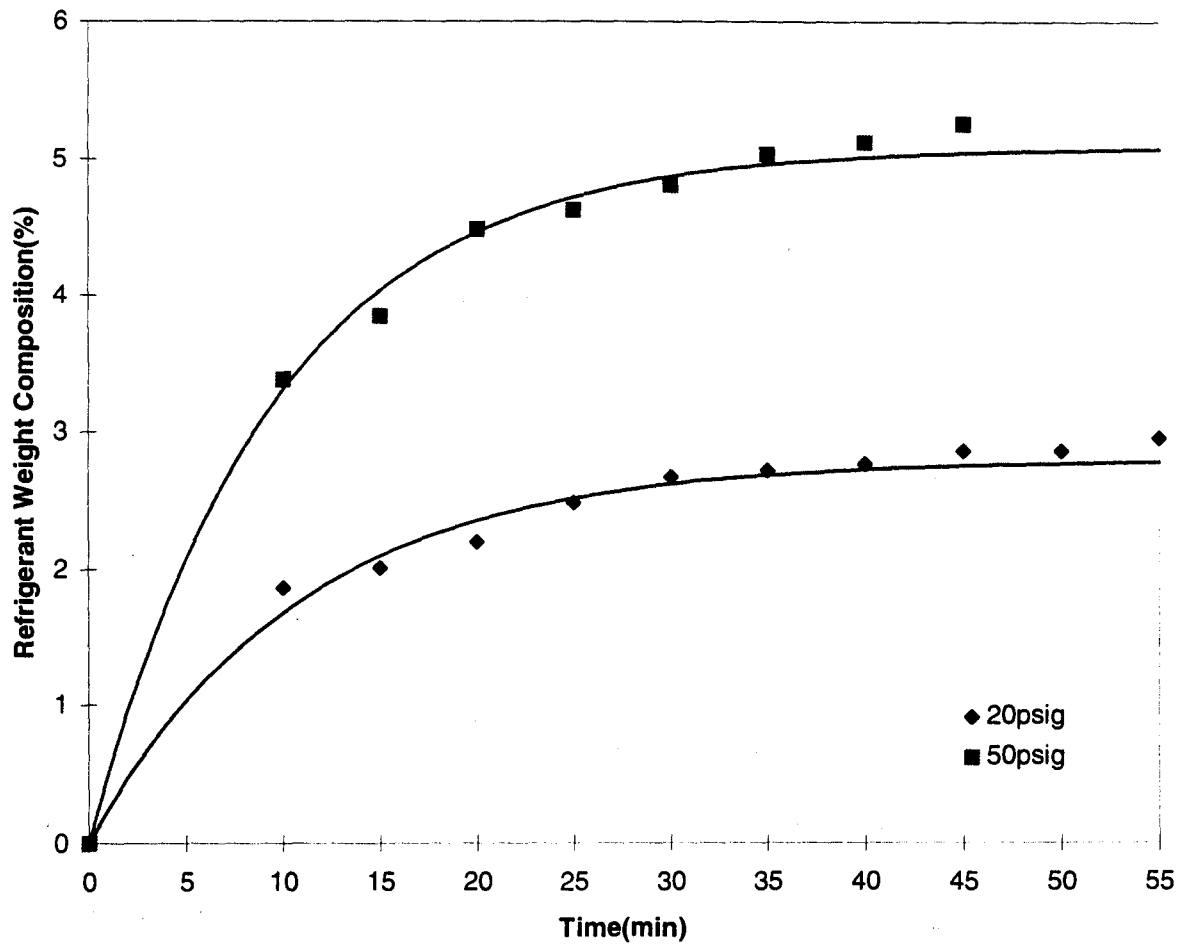


Figure 6.22 Absorption of R-410A in POE at 44°C

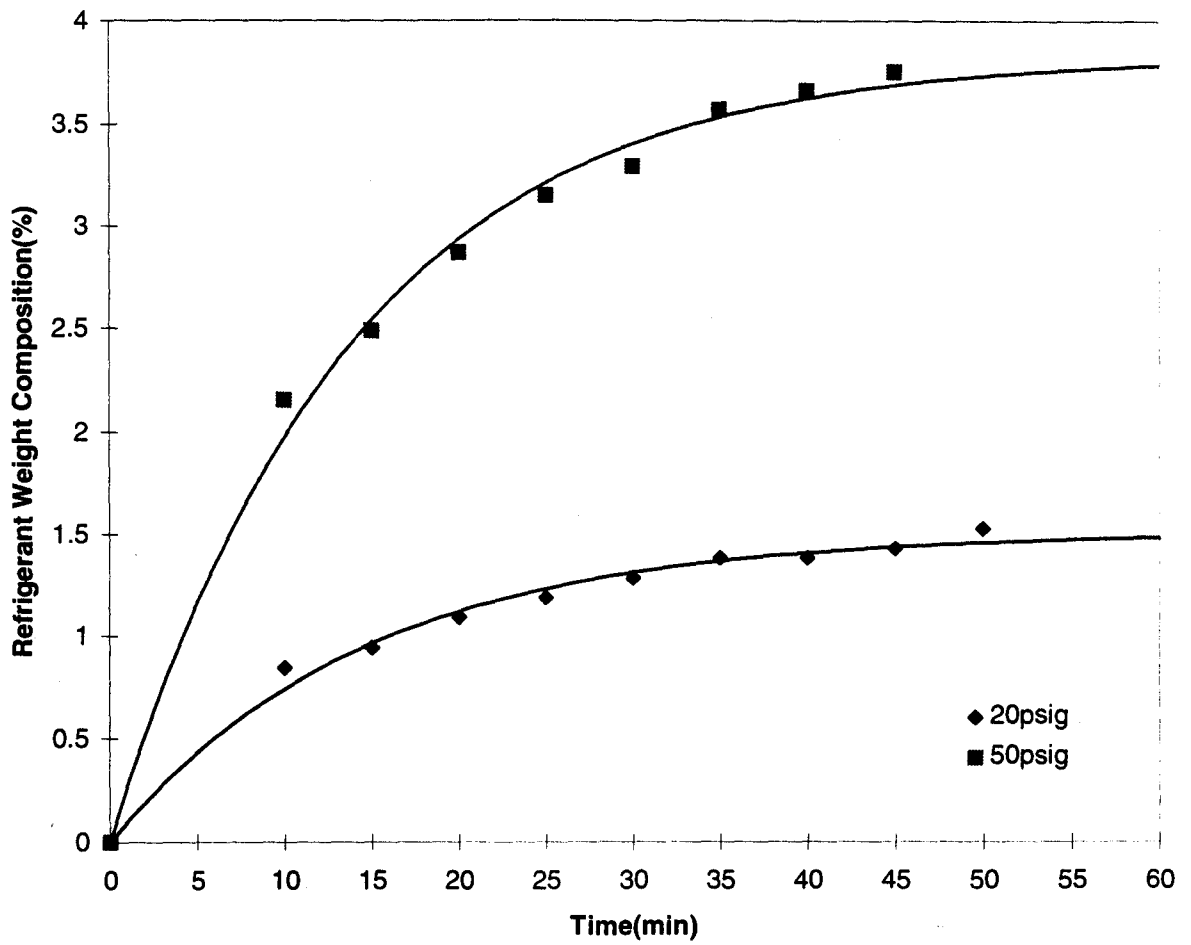


Figure 6.23 Absorption of R-32 in POE at -12°C

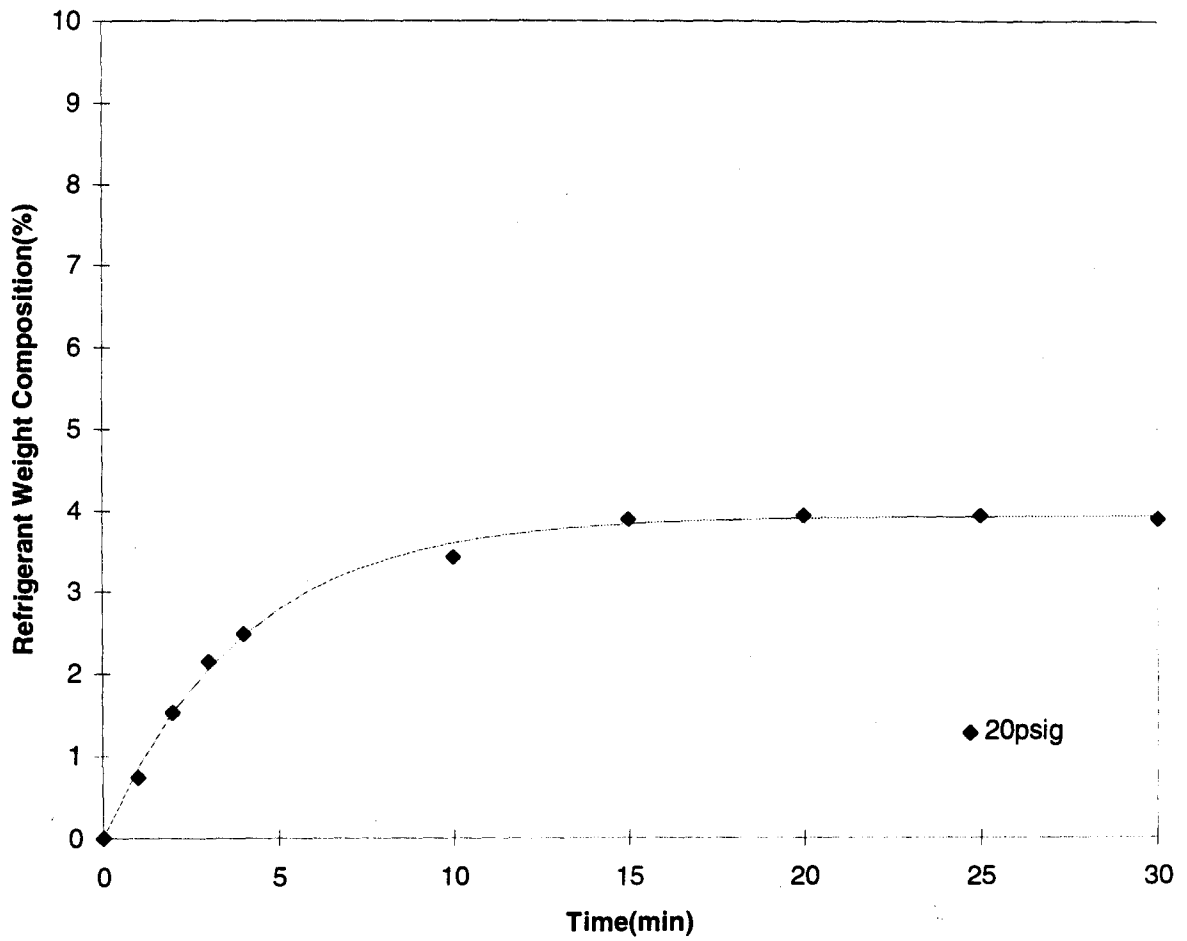


Figure 6.24 Absorption of R-143a in POE at -12°C

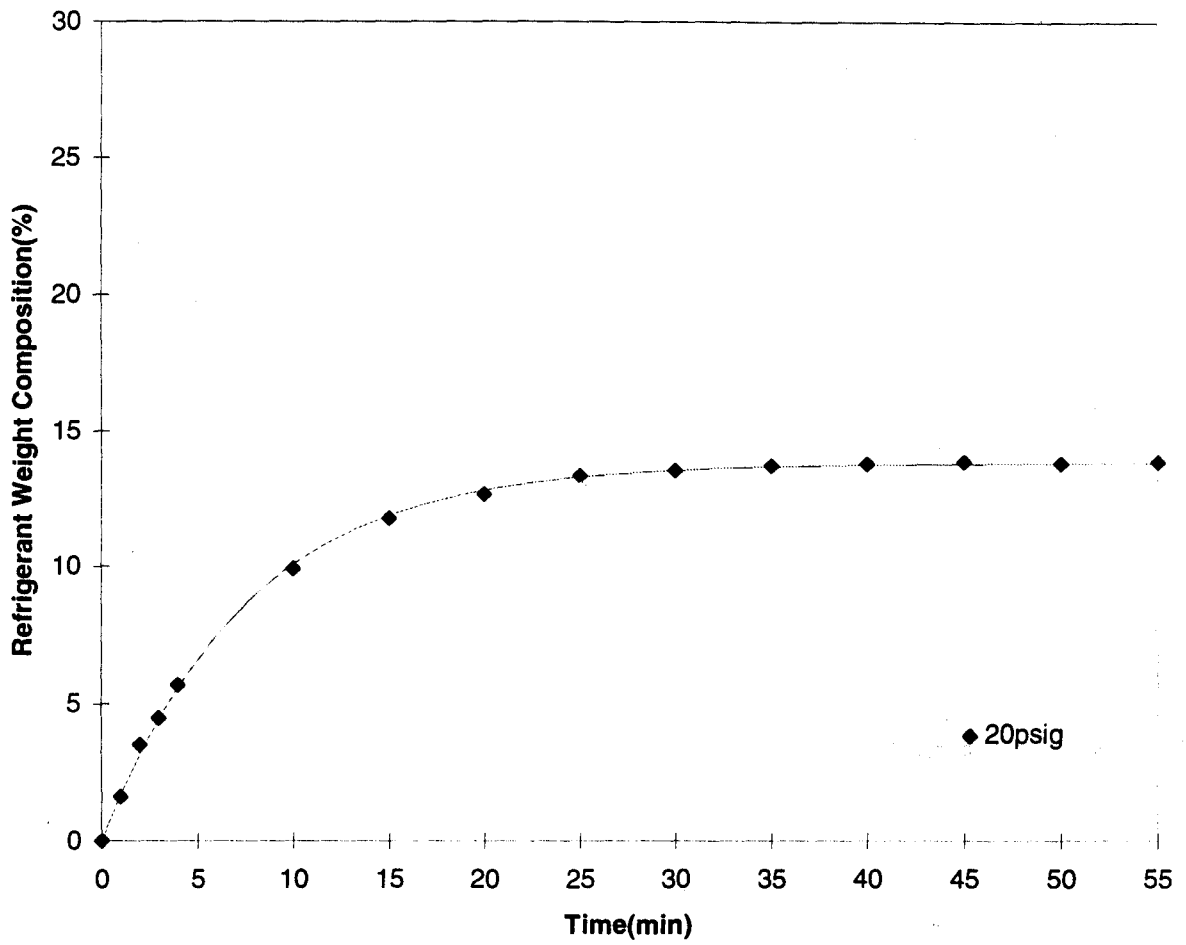


Figure 6.25 Absorption of R-404A in POE at -12°C

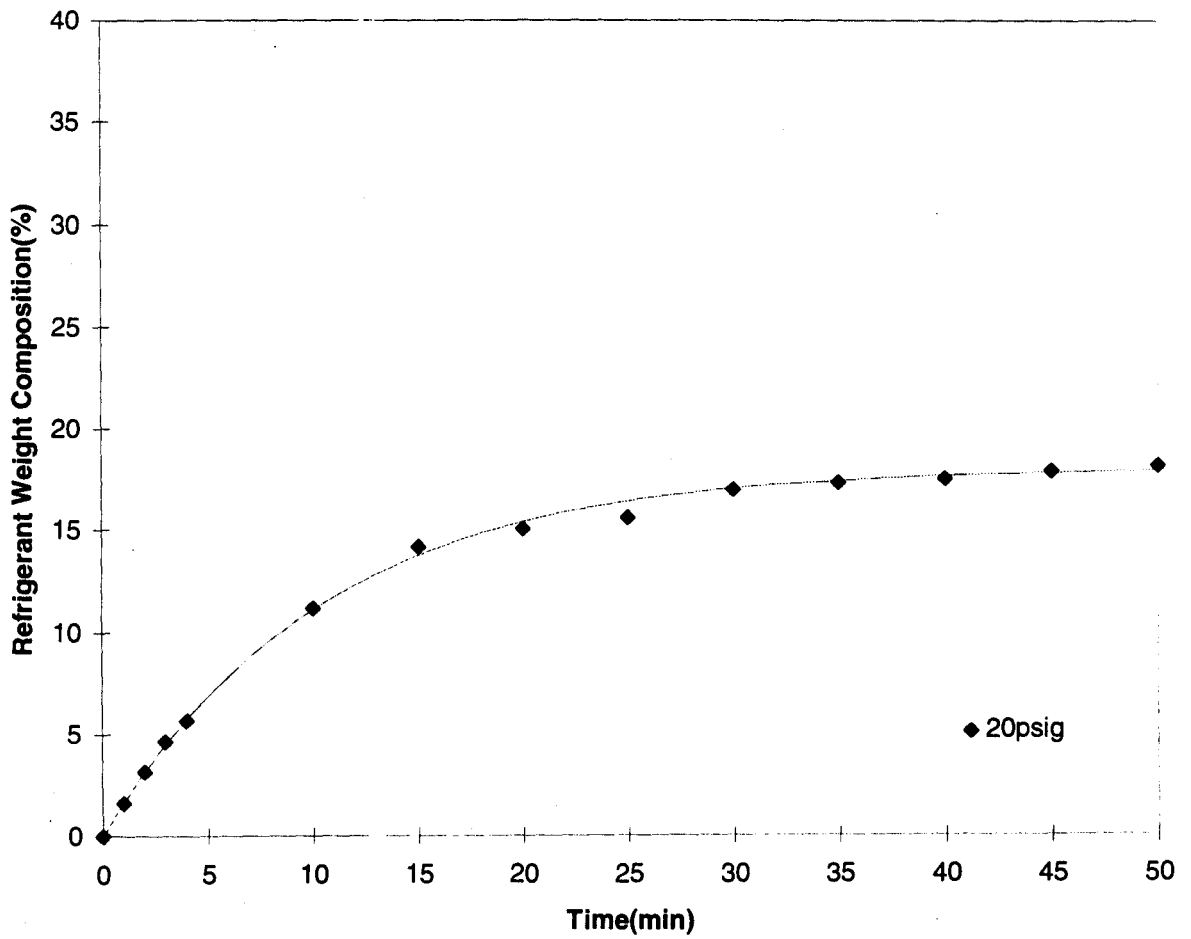


Figure 6.26 Absorption of R-407C in POE at -12°C

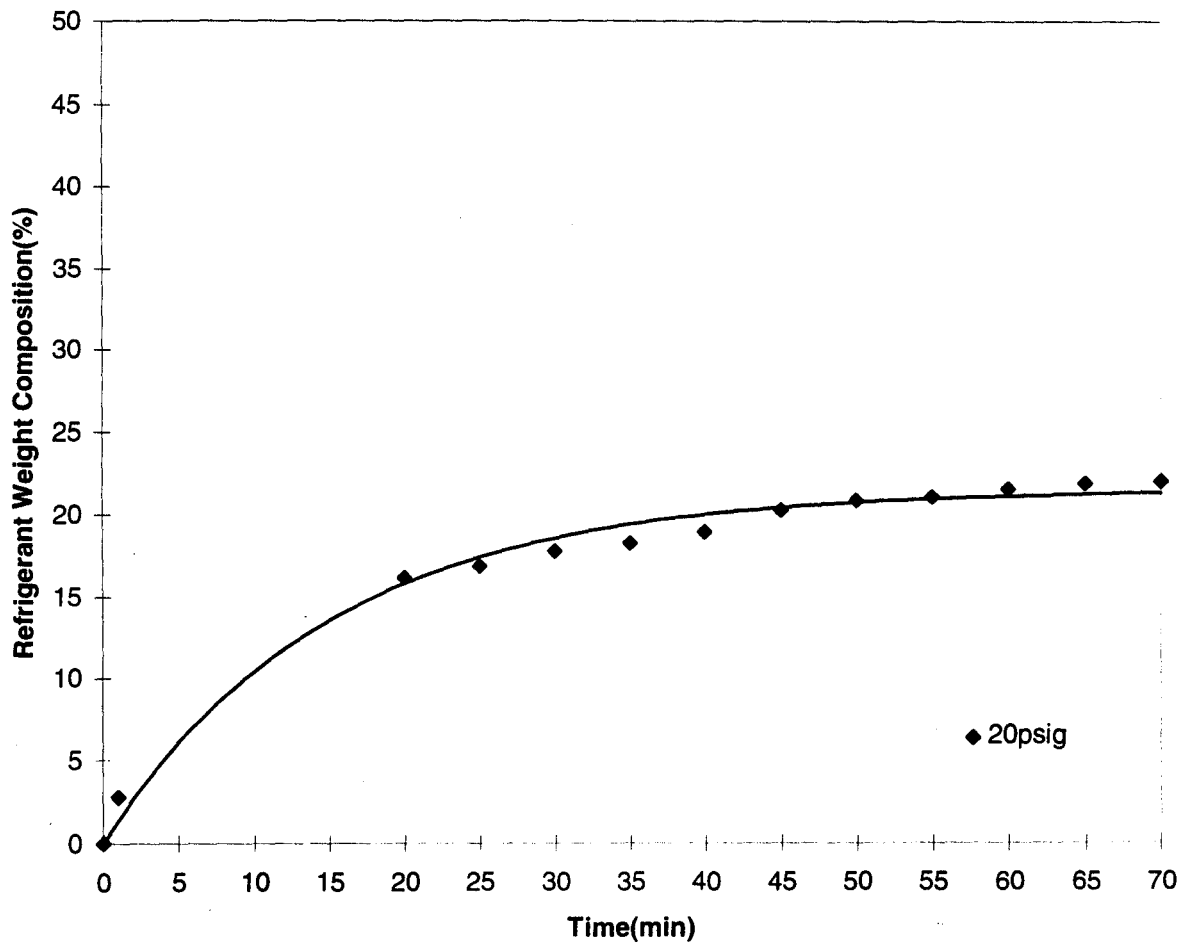
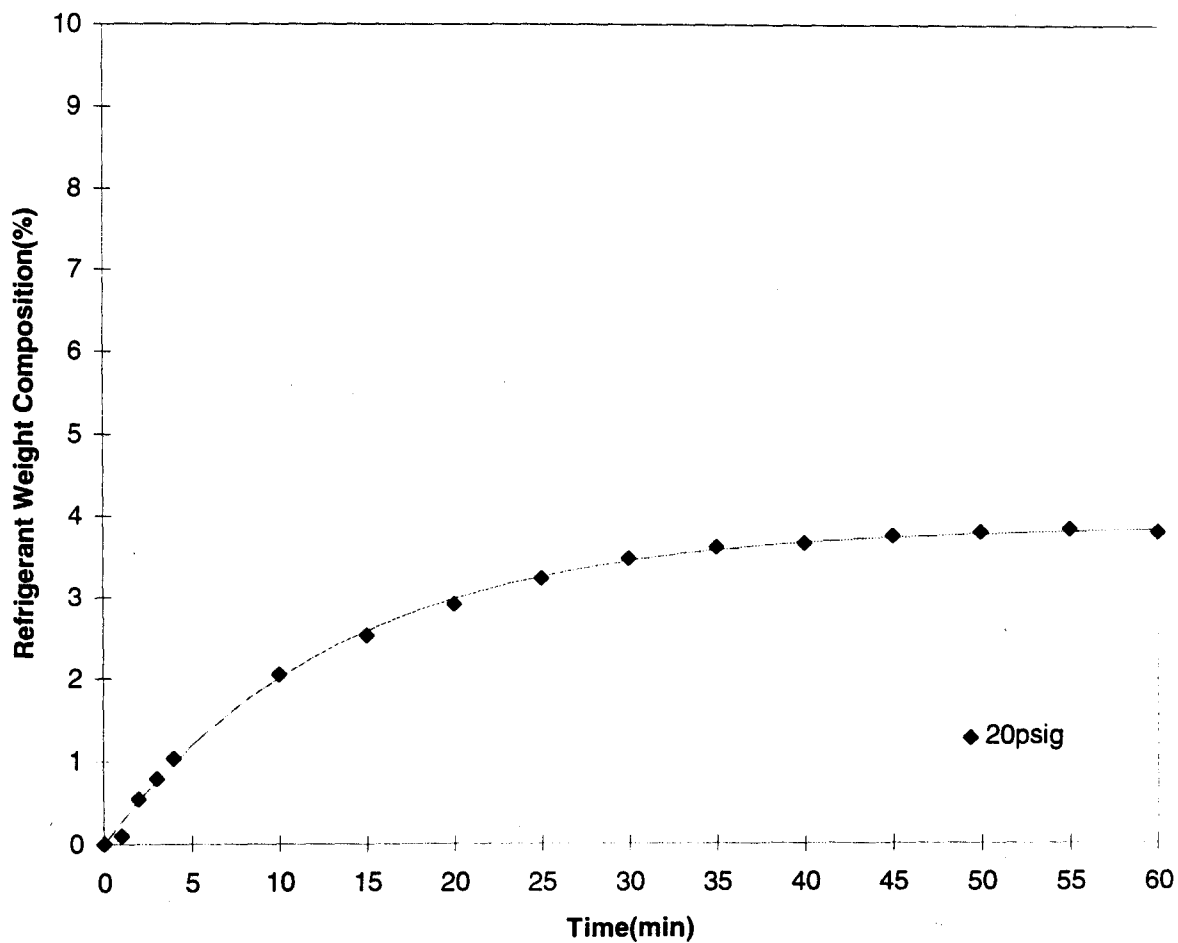


Figure 6.27 Absorption of R-410A in POE at -12°C

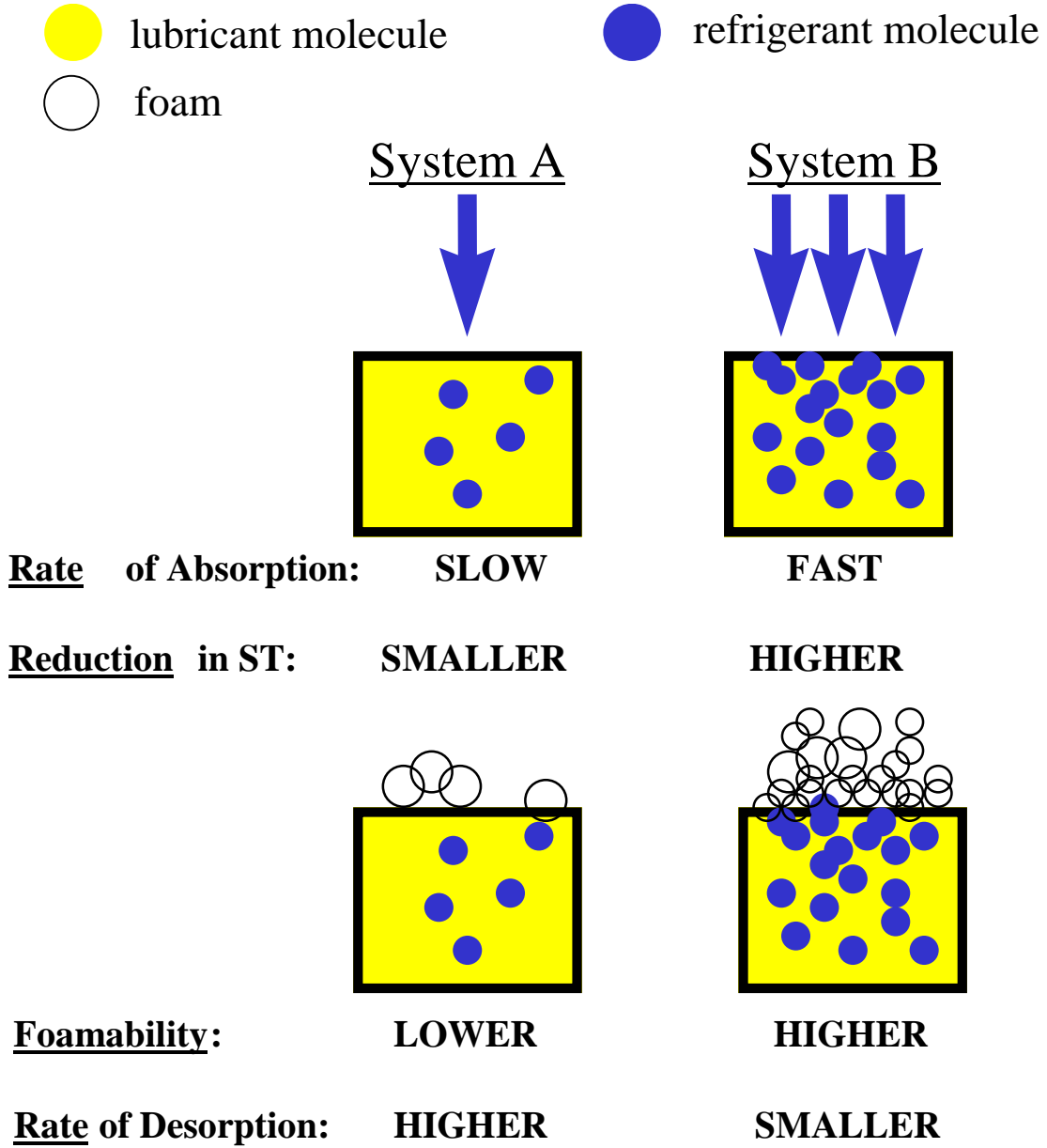


7. SUMMARY & CONCLUSIONS

7.1 The Correlation and Significance of the Properties Measured

Recall that the greater the reduction in the dynamic surface tension curve, the easier it is for a refrigerant/lubricant mixture to form foam. The reasoning behind this statement lies in the fact that, in order to expand an interface (i.e. make foam bubbles), work must be done *on* that interface. Decreasing the dynamic surface (interfacial) tension curve implies that refrigerant molecules are concentrated enough at the refrigerant/lubricant interface to reduce the surface tension at any given surface lifetime. Thus, for foam production, refrigerants and lubricants must be compatible as such so as to yield a *lowering* of the dynamic surface tension curve. Thus, it is important for refrigerant molecules to absorb into the lubricant. The faster the absorption rate, the faster the refrigerant molecules can affect the interfacial properties, namely dynamic interfacial tension. However, desorption rates must also be considered. If a refrigerant desorbs out of a refrigerant/lubricant mixture at a fast rate, it will have less of an effect on the mixture's dynamic surface tension (and hence, foaming capability) than a refrigerant with a slow desorption rate. In short, all the properties measured in this study are inherently related and are essential for examining the foaming potential of various refrigerant/lubricant mixtures. A schematic representation of this statement appears in [Figure 7.1](#).

Figure 7.1 Schematic representation of the correlation between the relevant surface properties of refrigerant/lubricant mixtures.



7.2 Significance of Baseline Tests

The experiments involving the (H)CFC/mineral oil pairs revealed the convincing foaming potential of the pre-HFC refrigerant/lubricant system. Both foamability and foam stability tests proved that the 4GS/R-22 system to produce the most foam, both in terms of quantity *and* persistence, respectively. However, in addition to the foaming properties such as foamability, foam stability and bubble size, other surface-science related properties support the foaming data, the most noteworthy of these properties being dynamic surface tension. While static surface tension experiments, performed with the Wilhelmy plate apparatus, were used to establish benchmark values for the 3GS and 4GS mineral oils, it was the dynamic *surface* (lubricants and mixtures injected with air) and *interfacial* (lubricants injected with refrigerant gas) tension experiments (performed with the maximum bubble pressure apparatus) that validated the foaming results as R-22 refrigerant reduced the dynamic surface tension curve the greatest. In short, the greatest lowering of dynamic surface tension correlated to the most foam formed and most persistent foam formed. Most importantly however, the baseline tests affirmed that the surface tension and foaming methods used can be *cohesively* applied to foaming characteristics of refrigerant/lubricant mixtures.

7.3 Alternative Refrigerant/Lubricant Mixtures

While all of the baseline tests were performed at room conditions *without* the induction of a pressure drop, the experiments (absorption, desorption and foaming) involving the HFC/polyolester mixtures were conducted with pressure drops.

Foamability and foam stability experiments were performed at ambient pressure using the aeration column (also used for the baseline study) and the ASTM standard test method foaming characteristics of lubricating oils; however, it was emphatically concluded that HFC/POE mixtures do *not* form foam under conditions without a rapid pressure drop.

Although the HFC/POE pairs were successfully tested with the maximum bubble pressure apparatus at room conditions without a pressure drop, a pressure-release foaming apparatus was constructed to perform the foaming tests. This apparatus was also used to measure desorption rates of HFCs from the refrigerant/lubricant mixtures. A pressure vessel apparatus was constructed to perform the absorption rate study. In terms of the results, which are displayed in [Table 7.1](#), R-134a was the most stable and most foamable with POE lubricants, while R-143a was one of the least stable and foamable. Although HFC/POE mixtures produce *considerably* less foam than (H)CFC/mineral oil mixtures, even under pressure drop conditions, it should be noted that the major difference between the two types of refrigerant/lubricant systems is that the HFC/POE mixtures exhibited *no* foam stability whatsoever. It appears that the experimental data correlates rather well with regards to surface properties and foaming characteristics.

7.4 Comparison of (H)CFC Pairs with HFC Pairs

In terms of comparing the baseline pairs with the HFC/POE pairs, R-134a was the only HFC that exhibited any kind of similarity in terms of dynamic interfacial tension reduction. Foamability and foam stability tests were all considerably greater for the baseline tests, albeit for a completely different method for foam production. In terms of

the major foaming characteristics and dynamic surface tension reduction, relevant comparisons between R-12 and R-134a as well as R-22 with both R-407C and R-410A are made in Table 7.1.

Table 7.1 Comparisons of interest.
(H)CFCs with mineral oils and HFCs with POEs.

<i>Dynamic Surface Tension Reduction</i>
R-12/3GS ~ R-22/3GS R-12/4GS ~ R-22/4GS
R-12/4GS ~ R-134a/POE R-22/4GS > R-407C/POE R-22/4GS > R-410A/POE

Foamability
R-12/3GS ~ R-22/3GS R-12/4GS ~ R-22/4GS
R-12/4GS > R-134a/POE R-22/4GS >> R-407C/POE R-22/4GS >> R-410A/POE

Foam Stability
R-12/3GS ~ R-22/3GS R-12/4GS < R-22/4GS
R-12/4GS > R-134a/POE R-22/4GS >> R-407C/POE R-22/4GS >> R-410A/POE

REFERENCES

1. ASTM D-892, Foaming Characteristics of Lubricating Oils
2. Bayani, A., Thome, J.R., and Favrat, D., "Online Measurement of Oil Concentrations of R-134a/Oil Mixtures with a Density Flowmeter," *HVAC&R Research*, July, 232-241 (1995).
3. Blute, I., Jansson, M., Oh, S.G., and Shah, D.O., "The Molecular Mechanism for Destabilization of Foams by Organic Ions," *JAOCS* **71**, No. 1, January, 41-46 (1994).
4. Chang, Y.N. and Nagashima, A., "Effect of Dissolved Lubricating Oils on the Viscosity of Alternative Refrigerants," *International Journal of Thermophysics* **14**, No. 5, 1007-1019 (1993).
5. Gilman, L.B., "A Review of Instruments for Static and Dynamic Surface Tension Measurement," *Presented at the 84th AOCS Annual Meeting and Expo*, 1-18 (1993).
6. Komatsuzaki, S., Homma, Y., Itoh, Y., Kawashima, K., and Iizuka, T., "Polyol Esters as HFC-134a Compressor Lubricants," *Lubrication Eng.* **50**, No. 10, 801-807 (1994).
7. Komatsuzaki, S. Homma, Y., Kawashima, K., and Itoh, Y., "Polyalkylene Glycol as Lubricant for HFC-134a Compressors," *Lubrication Eng.* **47**, No. 12, 1018-1025 (1991).
8. Sharma, M.K. and Shah, D.O., "Effect of Oil Viscosity on Recovery Processes in Relation to Foam Flooding," *JAOCS* **61**, 585-590 (1984).
9. Short, G.D., "Synthetic Lubricants and Their Refrigeration Applications," *Lubrication Eng.* **46**, No. 4, 239-247 (1989).
10. Sibley, H.M., "Oil Foaming Characteristics: The Forgotten Design Parameter with HFC-134a," *Japanese Association of Refrigeration, Tokyo, Japan, paper 5.4*, 101-104 (1993).
11. Suzuki, S., Fujisawa, Y., Nakazawa, S., and Matsouka, M., "Measuring Method of Oil Circulation Ratio Using Light Absorption," *ASHRAE Trans.* **99**, No. 1, 413-421 (1993).

12. Van Gaalen, N.A., Zoz, S.C., and Pate, M.B., "The solubility and Viscosity of Solutions of HCFC-22 in a Napthenic Oil and in an Alkylbenzene at High Pressures and Temperatures," *ASHRAE Trans.* **97**, No. 1, 100-108 (1991a).
13. Van Gaalen, N.A., Zoz, S.C., and Pate, M.B., "The solubility and Viscosity of Solutions of R-502 in a Napthenic Oil and in an Alkylbenzene at High Pressures and Temperatures," *ASHRAE Trans.* **97**, No. 2, 285-292 (1991b).
14. Yanagisawa, T. and Shimizu, T., "Foaming of a Refrigeration Oil in a Rolling Piston Type Rotary Compressor," *Rev. Int. Froid.* **9**, 17-20 (1986).
15. Yanagisawa, T. Shimizu and M. Fukuta, "Foaming Characteristics of an Oil-Refrigerant Mixture," *Int. J. of Refrig.* **14**, No. 3, 132-136 (1991).
16. Zoz, L.J. Berkenbosch and M.B. Pate, "Miscibility of Seven Different Lubricants with Ten Different Non-CFC Refrigerants," *ASHRAE Transactions* **100**, Part 2, 197-207 (1994).

APPENDIX
OF
EXPERIMENTAL DATA

TABLE A3.1
Lubricant Densities

Conditions:

Temp = 25° C

Pressure = 1 atm

Mass of container = 30.33 grams

<i>Type (name)</i>	Container + Lub (grams)	Mass of Lub (grams)	Volume of Lub (ml)	Density (g/ml)	Reported Density (g/ml)
<i>Mineral Oils</i>					
Witco 4GS	42.64	12.31	15.1	0.82	0.8
Witco 3GS	42.12	11.79	15.2	0.78	0.8
<i>Polyolesters</i>					
Witco SL68	43.61	13.28	15.0	0.89	0.9
ICI RL68H	43.62	13.29	15.1	0.88	0.9

TABLE A3.2

Lubricant Viscosities

Conditions:*Temp = 25° C**Pressure = 1 atm***Units:***All shear rates in sec⁻¹**All viscosities in centipoise***TABLE A3.2.1 ICI RL68H**

shear rate	trial 1 viscosity	trial 2 viscosity	trial 3 viscosity
40	91.5	92.5	109
100	91.6	87.8	109
200	91.3	86.8	109
Averages:	91.5	89.0	109.0

Statistical Data:

	all three	best two
<i>Mean</i>	96.5	90.3
<i>St. Dev.</i>	9.6	2.3

TABLE A3.2.2 Witco SL68

shear rate	trial 1 viscosity	trial 2 viscosity	trial 3 viscosity
40	114	108	112
100	112	104	109
200	112	104	108
Averages:	112.7	105.2	109.7

	all three	best two
<i>Mean</i>	109.2	111.2
<i>St. Dev.</i>	3.7	2.2

TABLE A3.2.3 Witco 4GS

shear rate	trial 1 viscosity	trial 2 viscosity	trial 3 viscosity
40	93.0	88.5	94.0
100	88.4	84.8	91.0
200	87.7	84.1	90.8
Averages:	89.7	85.8	91.9

	all three	best two
<i>Mean</i>	89.1	90.8
<i>St. Dev.</i>	3.4	2.5

TABLE A3.2

Lubricant Viscosities

TABLE A3.2.4**Witco 3GS**

shear rate	<i>trial 1</i> viscosity	<i>trial 2</i> viscosity	<i>trial 3</i> viscosity
100	46.0	49.6	53.4
200	45.4	49.0	50.9
Averages:	30.5	32.9	34.8

	<i>all three</i>	<i>best two</i>
<i>Mean</i>	49.1	47.5
<i>St. Dev.</i>	3.0	2.1

TABLE A3.2.5

Data Summary

Lubricant Type	Viscosity at 40°C	Viscosity at 25°C	Standard Deviation
ICI RL68H	68	90.3	2.3
Witco 4GS	68	90.8	2.5
Witco 3GS	32	47.5	2.1
Witco SL68	68	111.2	2.2

TABLE A3.3

Lubricant Static Surface Tension

Conditions:*Temp = 25° C**Pressure = 1 atm***Units:***All converted values in dynes/cm***TABLE A3.3.1****Unconverted Values (set #1)**

Trial Number	Calibration		Lubricant samples		
	Water	Methanol	Witco 4GS	Witco 3GS	ICI
1	389.0	120.0	172.2	171.6	153.2
2	389.8	121.0	171.4	169.6	152.9
3	389.0	121.4	170.6	169.6	152.8
4	390.0	121.4	169.8	169.5	152.4
5	398.7	122.2	170.0	169.8	153.0
6		120.9	171.2	169.0	
7		121.6	169.2		
8		121.4	171.2		
9		121.4	170.0		
Average	391.3	121.3	170.6	169.9	152.9
CRC value	72.74	22.61			
Conversion	5.38	5.36			

TABLE A3.3.2**Unconverted Values (set #2)**

Trial Number	Calibration		Lubricant samples			
	Water	Acetone	Witco 4GS	Witco 3GS	Witco SL68	ICI
1	390.6	126.8	170.8	170.5	156.2	152.3
2	390.8	126.4	170.2	170.0	156.0	151.5
3	391.2	126.0	170.0	170.0	155.4	152.0
4			170.1	170.0	156.0	152.4
5			170.0	169.8	156.0	152.6
Average	390.9	126.4	170.2	170.1	155.9	152.2
CRC value	72.43	23.44				
Conversion	5.40	5.39				

TABLE A3.3

Lubricant Static Surface Tension

TABLE A3.3.3**Converted Values (set #1)**

Trial Number	Calibration		Lubricant samples		
	Water	Methanol	Witco 4GS	Witco 3GS	ICI
1	72.3	22.4	32.0	31.9	28.5
2	72.5	22.6	31.9	31.5	28.4
3	72.3	22.6	31.7	31.5	28.4
4	72.5	22.6	31.6	31.5	28.3
5	74.1	22.8	31.6	31.6	28.4
6		22.6	31.8	31.4	
7		22.7	31.4		
8		22.6	31.8		
9		22.6	31.6		
Average	72.7	22.6	31.7	31.6	28.4

TABLE A3.3.4**Converted values (set #2)**

Trial Number	Calibration		Lubricant samples			
	Water	Acetone	Witco 4GS	Witco 3GS	Witco SL68	ICI
1	72.3	23.5	31.6	31.6	28.9	28.2
2	72.4	23.5	31.5	31.5	28.9	28.1
3	72.4	23.4	31.5	31.5	28.8	28.1
4			31.5	31.5	28.9	28.2
5			31.5	31.4	28.9	28.3
Average	72.4	23.5	31.5	31.5	28.9	28.2

TABLE A3.3.5

Data Summary

Lubricant Type	Surface Tension	Standard Deviation
Witco 4GS	31.6	0.17
Witco 3GS	31.5	0.13
Witco SL68	28.9	0.14
ICI RL68H	28.6	0.06

Table A4.1

Static Surface Tension vs. Refrigerant/Lubricant Composition

Conditions:

Temp = 25°C

Pressure = 1 atm

Materials:

Lubricants: Witco 3GS & 4GS mineral oils

Refrigerants: (CFC) R-12, (HCFC) R-22

Variable (units):

Surface tension (dynes/cm)

Table A4.1.1 **Calibration**

Trial	Units	DI Water	3GS
1	scale values	95.0	42.0
2	scale values	96.0	42.4
3	scale values	96.0	41.6
Average	dynes/cm	95.7	42.0
Recorded	dynes/cm	72.4	31.5
Factor		1.32	1.33

Table A4.1.2

3GS & R-12

% Lub	Trial 1	Trial 2	Trial 3	Average	ST (dynes/cm)
100	42.0	42.2	42.0	42.1	31.6
99	42.0	42.0	42.0	42.0	31.6
97	41.2	42.0	41.5	41.6	31.3
95	41.0	42.0	41.4	41.5	31.2
92	41.6	41.2	41.6	41.5	31.2
90	41.0	41.8	41.4	41.4	31.1

Table A4.1
Static Surface Tension vs. Refrigerant/Lubricant Composition

Table A4.1.3 **4GS & R-12**

% Lub	Trial 1	Trial 2	Trial 3	Average	ST (dynes/cm)
100	42.2	41.2	42.2	41.9	31.5
99	42.0	42.2		42.1	31.7
97	41.8	41.8		41.8	31.4
95	41.0	41.2		41.1	30.9
92	41.4	40.8		41.1	30.9
90	40.0	40.0		40.0	30.1

Table A4.1.4 **3GS & R-22**

% Lub	Trial 1	Trial 2	Trial 3	Average	ST (dynes/cm)
100	41.8	42.0		41.9	31.5
99	41.8	41.0	42.0	41.6	31.3
97	41.8	42.0	41.4	41.7	31.4
95	41.4	41.8	41.4	41.5	31.2
92	41.6	41.0	41.2	41.3	31.0
90	40.0	40.0	40.6	40.2	30.2

Table A4.1.5 **4GS & R-22**

% Lub	Trial 1	Trial 2	Trial 3	Average	ST (dynes/cm)
100	41.6	42.0		41.8	31.4
99	41.4	41.8	42.0	41.7	31.4
97	41.8	41.4	41.6	41.6	31.3
95	41.6	41.6	41.4	41.5	31.2
92	41.8	41.4	41.8	41.7	31.3
90	41.6	41.2	41.0	41.3	31.0

Table A4.2

Dynamic Surface Tension: Pure Lubricants Trial 1

Equations relating temperature of standard liquids to surface tension.

Data from CRC Handbook of Chemistry & Physics

Water/Air Interface

$$ST = -0.1544T[^\circ\text{C}] + 75.823$$

Methanol/Air Interface

$$ST = -0.094T[^\circ\text{C}] + 24.490$$

Calibration Data

Temperature [$^\circ\text{F}$]	72
Temperature [$^\circ\text{C}$]	22.22
Surface tension of water [dyn/cm, CRC]	72.39
Surface tension of methanol [dyn/cm, CRC]	22.40
Voltage output for water [volts, transducer]	3.49
Voltage output for methanol [volts, transducer]	1.25

Standard	Methanol	Water
Voltage	1.25	3.49
ST (dyn/cm)	22.4	72.4

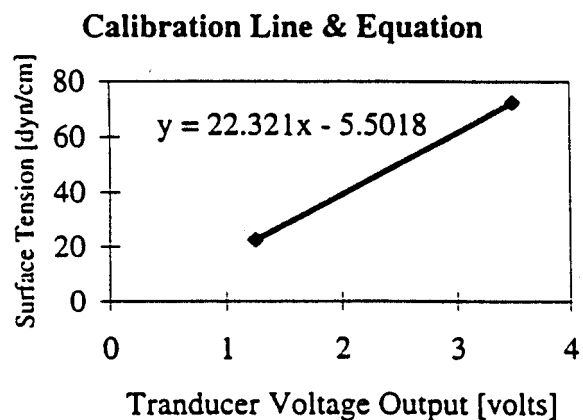


Table A4.2.1

Pure Lubricant Samples: Trial 1

Lubricant Sample	Transducer:		Oscilloscope:		Experimental values:	
	Input (V)	Output (V)	divisions	sec/div	Bubble freq (Hz)	ST (dynes/cm)
Witco 4GS	8.86	1.68	2.20	0.2	2.3	32.0
	8.86	1.71	1.30	0.2	3.8	32.7
	8.86	1.72	0.90	0.2	5.6	32.9
	8.87	1.73	0.80	0.2	6.3	33.1
	8.87	1.76	1.00	0.1	10.0	33.8
	8.87	1.79	0.80	0.1	12.5	34.5
Witco 3GS	8.88	1.63	1.95	0.2	2.6	30.9
	8.88	1.64	1.90	0.2	2.6	31.1
	8.87	1.65	1.80	0.2	2.8	31.4
	8.88	1.67	2.15	0.1	4.7	31.8
	8.88	1.69	0.95	0.1	10.5	32.3
	8.85	1.71	0.65	0.1	15.4	32.7
Witco SL68	8.85	1.53	3.35	0.2	1.5	28.7
	8.85	1.53	2.75	0.2	1.8	28.7
	8.86	1.55	2.80	0.2	1.8	29.1
	8.86	1.55	2.50	0.2	2.0	29.1
	8.85	1.57	1.60	0.2	3.1	29.6
	8.87	1.60	1.25	0.2	4.0	30.2
	8.87	1.65	1.30	0.1	7.7	31.4
	8.87	1.69	0.80	0.1	12.5	32.3
	8.85	1.74	0.60	0.1	16.7	33.4
ICI RL68H	8.86	1.53	3.00	0.2	1.7	28.7
	8.86	1.54	2.20	0.2	2.3	28.9
	8.87	1.55	1.90	0.2	2.6	29.1
	8.87	1.65	0.70	0.2	7.1	31.4
	8.88	1.68	0.45	0.2	11.1	32.0
	8.88	1.71	0.85	0.1	11.8	32.7

Table A4.2

Dynamic Surface Tension
Pure Lubricants Trial 2

Table A4.3

Dynamic Surface Tension
Lubricants with 10% Refrigerant Part 1

Equations relating temperature of standard liquids to surface tension

Data from CRC Handbook of Chemistry & Physics

Water/Air Interface

$$ST = -0.1544T[^\circ\text{C}] + 75.823$$

Methanol/Air Interface

$$ST = -0.094T[^\circ\text{C}] + 24.490$$

Calibration Data

Temperature [$^\circ\text{F}$]	72.51
Temperature [$^\circ\text{C}$]	22.50
Surface tension of water [dyn/cm, CRC]	72.35
Surface tension of methanol [dyn/cm, CRC]	22.38
Voltage output for water [volts, transducer]	3.58
Voltage output for- methanol [volts, transducer]	1.26

Standard	Methanol	Water
Voltage	1.26	3.58
ST (dyn/cm)	22.5	72.3

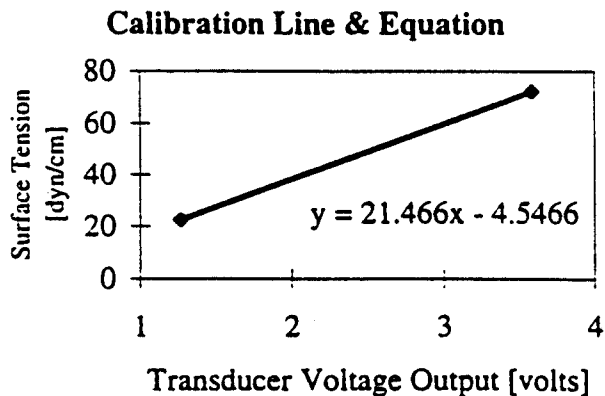


Table A4.2.2
Pure Lubricant Samples: Trial 2

Lubricant Sample	Transducer:		Oscilloscope:		Experimental values:	
	Input (V)	Output (V)	divisions	sec/div	Bubble freq (Hz)	ST (dynes/cm)
Witco 4GS	8.82	1.76	1.60	0.2	3.1	33.0
	8.82	1.80	0.85	0.2	5.9	33.7
	8.82	1.82	1.00	0.1	10.0	34.3
	8.82	1.86	0.70	0.1	14.3	35.1
	8.82	1.87	0.65	0.1	15.4	35.3
	8.82	1.93	0.40	0.1	25.0	36.6
	8.82	2.07	0.60	0.05	33.3	39.6
	8.82	2.22	0.30	0.1	33.3	42.8
Witco 3GS	8.83	1.72	1.85	0.2	2.7	32.0
	8.83	1.73	1.10	0.2	4.5	32.2
	8.83	1.76	0.40	0.2	12.5	32.9
	8.83	1.84	0.35	0.1	28.6	34.6
	8.83	1.87	0.50	0.05	40.0	35.3
	8.83	1.94	0.40	0.05	50.0	36.7
	8.83	2.06	0.15	0.1	66.7	39.3
Witco SL68	8.83	1.63	1.40	0.2	3.6	30.2
	8.83	1.65	1.10	0.2	4.5	30.6
	8.83	1.66	1.00	0.2	5.0	30.8
	8.83	1.69	0.60	0.2	8.3	31.5
	8.83	1.71	0.50	0.2	10.0	31.8
	8.83	1.73	0.40	0.2	12.5	32.2
	8.83	1.75	0.35	0.2	14.3	32.8
	8.83	1.79	0.55	0.1	18.2	33.5
	8.83	1.84	0.45	0.1	22.2	34.7
	8.83	2.02	0.30	0.1	33.3	38.6
ICI RL68H	8.84	1.60	1.00	0.5	2.0	29.6
	8.84	1.63	1.10	0.2	4.5	30.1
	8.84	1.64	1.00	0.2	5.0	30.3
	8.84	1.67	0.60	0.2	8.3	31.1
	8.84	1.69	0.50	0.2	10.0	31.4
	8.84	1.72	0.70	0.1	14.3	32.1
	8.84	1.76	0.50	0.1	20.0	33.0
	8.84	1.81	0.45	0.1	22.2	34.0
	8.84	1.87	0.40	0.1	25.0	35.2
	8.85	2.00	0.30	0.1	33.3	38.1
	8.85	2.10	0.30	0.1	33.3	40.2

Table A4.3.1

Lubricants with 10% Refrigerant: Part 1

Lubricant Sample	<i>Transducer:</i>		<i>Oscilloscope:</i>		<i>Experimental values:</i>	
	Input (V)	Output (V)	divisions	sec/div	Bubble freq(Hz)	ST (dynes/cm)
ICI / R-22	8.85	1.63	1.45	0.1	6.9	30.2
	8.85	1.64	1.20	0.1	8.3	30.3
	8.85	1.65	0.75	0.1	13.3	30.6
	8.85	1.67	0.60	0.1	16.7	31.1
	8.85	1.69	0.50	0.1	20.0	31.5
	8.85	1.71	0.35	0.1	28.6	31.9
	8.85	1.73	0.30	0.1	33.3	32.3
ICI / R-12	8.85	1.61	1.30	0.2	3.8	29.8
	8.85	1.66	0.40	0.2	12.5	30.8
	8.85	1.70	0.25	0.2	20.0	31.7
	8.85	1.72	0.45	0.1	22.2	32.1
	8.85	1.75	0.40	0.1	25.0	32.8
	8.85	1.78	0.35	0.1	28.6	33.4
	8.85	1.87	0.25	0.1	40.0	35.2
	8.85	1.91	0.25	0.1	40.0	36.1

Table A4.3

Dynamic Surface Tension

Lubricants with 10% Refrigerant Part 2

Equations relating temperature of standard liquids to surface tension

Data from CRC Handbook of Chemistry & Physics

Water/Air Interface

$$ST = -0.1544T[^\circ\text{C}] + 75.823$$

Methanol/Air Interface

$$ST = -0.094T[^\circ\text{C}] + 24.490$$

Calibration Data

Temperature [°F]	72.5
Temperature [°C]	22.50
Surface tension of water [dyn/cm, CRC]	72.35
Surface tension of methanol [dyn/cm, CRC]	22.38
Voltage output for water [volts, transducer]	3.58
Voltage output for methanol [volts, transducer]	1.26

Standard	Methanol	Water
Voltage	1.29	3.46
ST (dyn/cm)	22.2	72.0

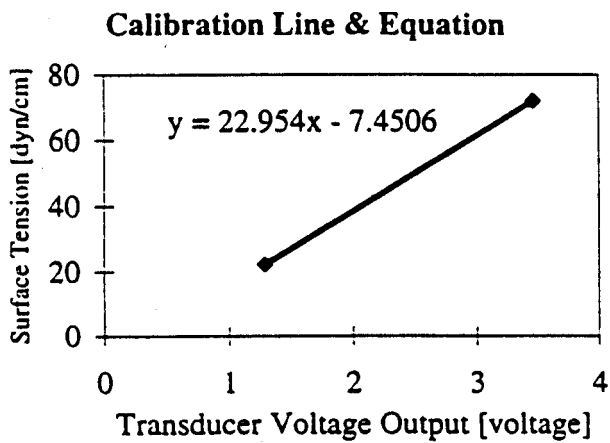


Table A4.3.2
Lubricants with 10% Refrigerant: Part 2

Lubricant Sample	Transducer:		Oscilloscope:		Experimental values:	
	Input (V)	Output (V)	divisions	sec/div	Bubble freq (Hz)	ST (dynes/cm)
ICI / R-22	8.58	1.580	1.40	0.2	3.6	28.8
	8.58	1.605	0.65	0.2	7.7	29.4
	8.58	1.640	0.65	0.1	15.4	30.2
	8.58	1.665	0.55	0.1	18.2	30.8
	8.58	1.700	0.40	0.1	25.0	31.6
	8.58	1.720	0.30	0.1	33.3	32.0
	8.58	1.760	0.20	0.1	50.0	32.9
ICI / R-12	8.54	1.570	1.20	0.2	4.2	28.6
	8.54	1.585	0.90	0.2	5.6	28.9
	8.54	1.595	0.75	0.2	6.7	29.2
	8.54	1.625	0.45	0.2	11.1	29.8
	8.54	1.640	0.75	0.1	13.3	30.2
	8.54	1.700	0.40	0.1	25.0	31.6
	8.54	1.805	0.30	0.1	33.3	34.0
	8.54	1.870	0.25	0.1	40.0	35.5
	8.54	2.080	0.20	0.1	50.0	40.3
SL68 / R-22	8.66	1.6	1.7	0.2	2.9	28.9
	8.66	1.615	1.6	0.2	3.1	29.2
	8.66	1.65	0.6	0.2	8.3	30.0
	8.66	1.69	0.35	0.2	14.3	30.8
	8.66	1.71	0.25	0.2	20.0	31.2
	8.66	1.75	0.4	0.1	25.0	32.1
	8.66	1.82	0.25	0.1	40.0	33.6
	8.66	1.89	0.2	0.1	50.0	35.1
SL68 / R-12	8.56	1.595	1.0	0.2	5.0	28.8
	8.56	1.605	0.75	0.2	6.7	29.0
	8.56	1.64	0.45	0.2	11.1	29.7
	8.56	1.665	0.3	0.2	16.7	30.3
	8.56	1.685	0.25	0.2	20.0	30.7
	8.56	1.7	0.5	0.1	20.0	31.0
	8.56	1.735	0.35	0.1	28.6	31.8
	8.56	1.84	0.25	0.1	40.0	34.0
	8.56	1.985	0.2	0.1	50.0	37.1

Table A4.3.2
Lubricants with 10% Refrigerant: Part 2

Lubricant Sample	Transducer:		Oscilloscope:		Experimental values:	
	Input (V)	Output (V)	divisions	sec/div	Bubble freq (Hz)	ST (dynes/cm)
4GS / R-22	8.52	1.67	1.00	0.2	5.0	30.8
	8.52	1.69	0.70	0.2	7.1	31.2
	8.52	1.70	0.50	0.2	10.0	31.6
	8.52	1.74	0.40	0.2	12.5	32.4
	8.52	1.75	0.30	0.2	16.7	32.6
	8.52	1.78	0.50	0.1	20.0	33.3
	8.52	1.79	0.45	0.1	22.2	33.6
	8.54	1.82	0.40	0.1	25.0	34.2
	8.55	1.92	0.25	0.1	40.0	36.5
4GS / R-12	8.57	1.70	1.55	0.2	3.2	31.5
	8.57	1.71	0.75	0.2	6.7	31.8
	8.57	1.75	0.40	0.2	12.5	32.6
	8.57	1.77	0.30	0.2	16.7	33.2
	8.58	1.79	0.55	0.1	18.2	33.5
	8.58	1.82	0.35	0.1	28.6	34.3
	8.60	1.85	0.30	0.1	33.3	34.9
	8.60	1.94	0.25	0.1	40.0	37.1
	8.60	2.08	0.20	0.1	50.0	40.2
3GS / R-22	8.58	1.67	0.90	0.2	5.6	30.9
	8.58	1.69	0.60	0.2	8.3	31.2
	8.58	1.70	0.40	0.2	12.5	31.6
	8.58	1.72	0.30	0.2	16.7	31.9
	8.60	1.75	0.40	0.1	25.0	32.7
	8.58	1.77	0.30	0.1	33.3	33.2
	8.60	1.85	0.25	0.1	40.0	35.0
	8.60	1.88	0.20	0.1	50.0	35.7
3GS / R-12	8.62	1.71	0.90	0.5	2.2	31.1
	8.62	1.71	0.60	0.5	3.3	31.2
	8.62	1.73	0.40	0.2	12.5	31.7
	8.62	1.77	0.25	0.2	20.0	32.5
	8.62	1.78	0.20	0.2	25.0	32.7
	8.65	1.89	0.20	0.1	50.0	35.0

Table A4.4

Dynamic Interfacial Tension: Baseline Pairs

Equations relating temperature of standard liquids to surface tension

Data from CRC Handbook of Chemistry & Physics

Water/Air Interface

$$ST = -0.1544T[^\circ\text{C}] + 75.823$$

Methanol/Air Interface

$$ST = -0.094T[^\circ\text{C}] + 24.490$$

Calibration Data

Temperature [$^\circ\text{F}$]	77.5
Temperature [$^\circ\text{C}$]	25.28
Surface tension of water [dyn/cm, CRC]	71.92
Surface tension of methanol [dyn/cm, CRC]	22.11
Voltage output for water [volts, transducer]	3.36
Voltage output for methanol [volts, transducer]	1.23

Standard	Methanol	Water
Voltage	1.23	3.36
ST(dyn/cm)	22.1	71.9

Calibration Line & Equation

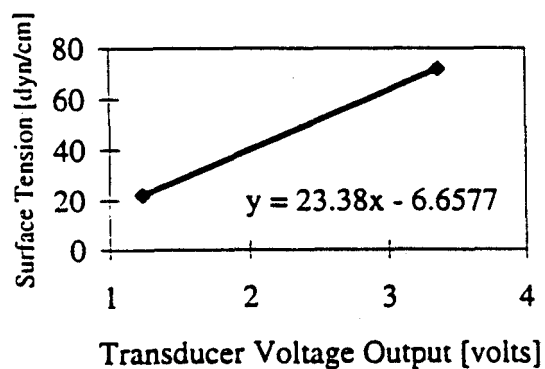


Table A4.4.1
Baseline Lubricants Injected with R-22

Lubricant Sample	<i>Transducer:</i>	<i>Oscilloscope:</i>		<i>Experimental values:</i>	
	Output (V)	divisions	sec/div	Bubble freq (Hz)	ST (dynes/cm)
Witco 3GS	1.56	1.6	0.5	1.3	29.0
	1.58	2.1	0.2	2.4	29.5
	1.58	2.3	0.1	4.3	29.5
	1.60	0.8	0.2	6.3	30.0
	1.61	0.6	0.2	8.3	30.2
	1.64	0.9	0.1	11.1	30.9
	1.65	0.3	0.2	16.7	31.1
	1.65	0.2	0.2	25.0	31.1
	1.66	0.2	0.2	25.0	31.4
Witco 4GS	1.60	1.2	0.5	1.7	30.0
	1.61	1.1	0.5	1.8	30.2
	1.64	1.4	0.2	3.6	30.9
	1.64	1.1	0.2	4.5	30.9
	1.65	0.7	0.2	7.1	31.1
	1.66	0.6	0.2	8.3	31.4
	1.69	0.8	0.1	12.5	32.1
	1.70	0.4	0.2	12.5	32.3
	1.75	0.4	0.1	25.0	33.5

Table A4.4.2
Baseline Lubricants Injected with R-12

Lubricant Sample	<i>Transducer:</i>	<i>Oscilloscope:</i>		<i>Experimental values:</i>	
	Output (V)	divisions	sec/div	Bubble freq (Hz)	ST (dynes/cm)
Witco 3GS	1.62	2.1	0.2	2.4	30.4
	1.63	1.8	0.2	2.8	30.7
	1.63	1.1	0.2	4.5	30.7
	1.64	0.8	0.2	6.3	30.9
	1.57	1.6	0.1	6.3	29.3
	1.62	1.1	0.1	9.1	30.4
	1.61	1.0	0.1	10.0	30.2
	1.66	0.5	0.2	10.0	31.4
	1.64	0.6	0.1	16.7	30.9
	1.67	0.3	0.2	16.7	31.6
Witco 4GS	1.57	2.6	0.5	0.8	29.3
	1.58	1.6	0.5	1.3	29.5
	1.58	1.8	0.2	2.8	29.5
	1.59	1.2	0.2	4.2	29.7
	1.62	1.1	0.2	4.5	30.4
	1.61	0.9	0.2	5.6	30.2
	1.62	0.8	0.2	6.3	30.4
	1.64	0.5	0.2	10.0	30.9
	1.69	0.3	0.2	16.7	32.1

Table A4.5

Dynamic Interfacial Tension: Single-component HFCs
(R-134a Trial 1)

Equations relating temperature of standard liquids to surface tension

Data from CRC Handbook of Chemistry & Physics

Water/Air Interface

$$ST = -0.1544T[^\circ\text{C}] + 75.823$$

Methanol/Air Interface

$$ST = -0.094T[^\circ\text{C}] + 24.490$$

Calibration Data

Temperature [$^\circ\text{F}$]	74
Temperature [$^\circ\text{C}$]	23.33
Surface tension of water [dyn/cm, CRC]	72.22
Surface tension of methanol [dyn/cm, CRC]	22.30
Voltage output for water [volts, transducer]	3.695
Voltage output for methanol [volts, transducer]	1.27

Standard	Methanol	Water
Voltage	1.27	3.695
ST (dyn/cm)	22.30	72.22

Calibration Line & Equation

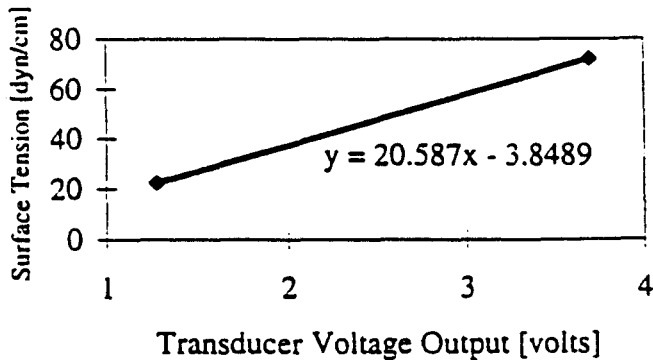


Table A4.5.1
R-134a Trial 1

Lubricant Sample	<i>Transducer:</i>	<i>Oscilloscope:</i>		<i>Experimental values:</i>	
	Output (V)	divisions	sec/div	Bubble freq (Hz)	ST (dynes/cm)
ICI RL68H	1.46	1.3	0.5	1.5	26.2
	1.47	2.4	0.2	2.1	26.4
	1.48	1.95	0.2	2.6	26.6
	1.55	1.6	0.2	3.1	28.1
	1.58	0.5	0.2	10.0	28.7
	1.55	0.5	0.2	10.0	28.1
	1.63	0.4	0.2	12.5	29.7
	1.57	0.7	0.1	14.3	28.5
	1.59	0.3	0.2	16.7	28.9
Witco SL68	1.43	1.85	0.5	1.1	25.6
	1.48	1.2	0.2	4.2	26.6
	1.48	0.95	0.2	5.3	26.6
	1.50	0.8	0.2	6.3	27.0
	1.52	0.6	0.2	8.3	27.4
	1.54	0.4	0.2	12.5	27.9
	1.58	0.35	0.2	14.3	28.7
	1.59	0.3	0.2	16.7	28.9

Table A4.5

Dynamic Interfacial Tension: Single-component HFCs
(R-134a Trial 2)

Equations relating temperature of standard liquids to surface tension

Data from CRC Handbook of Chemistry & Physics

Water/Air Interface

$$ST = -0.1544T[^\circ\text{C}] + 75.823$$

Methanol/Air Interface

$$ST = -0.094T[^\circ\text{C}] + 24.490$$

Calibration Data

Temperature [$^\circ\text{F}$]	75
Temperature [$^\circ\text{C}$]	23.89
Surface tension of water [dyn/cm, CRC]	72.13
Surface tension of methanol [dyn/cm, CRC]	22.24
Voltage output for water [volts, transducer]	2.37
Voltage output for methanol [volts, transducer]	1.22

Standard	Methanol	Water
Voltage	1.22	2.37
ST (dyn/cm)	22.24	72.13

Calibration Line & Equation

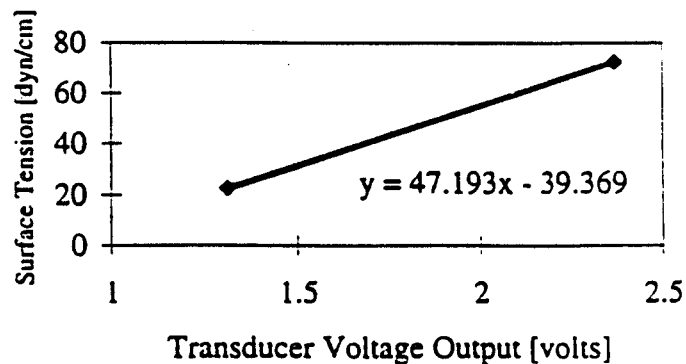


Table A4.5.2
R-134a Trial 2

Lubricant Sample	Transducer:	Oscilloscope:		Experimental values:	
	Output (V)	divisions	sec/div	Bubble freq (Hz)	ST (dynes/cm)
ICI RL68H	1.45	2.2	0.2	2.3	32.2
	1.49	1.1	0.2	4.5	34.0
	1.51	0.9	0.2	5.6	34.8
	1.47	0.9	0.2	5.6	33.1
	1.51	0.5	0.2	10.0	34.8
	1.54	0.4	0.2	12.5	36.1
	1.56	0.4	0.2	12.5	37.0
	1.54	0.4	0.2	12.5	36.1
	1.62	0.35	0.2	14.3	39.6
Witco SL68	1.43	2.2	0.5	0.9	31.4
	1.45	1.45	0.5	1.4	32.0
	1.45	2.1	0.2	2.4	32.2
	1.48	1.9	0.2	2.6	33.5
	1.47	1.05	0.2	4.8	33.1
	1.50	0.75	0.2	6.7	34.4
	1.51	0.6	0.2	8.3	34.8
	1.56	0.4	0.2	12.5	37.0
	1.57	0.35	0.2	14.3	37.4

Table A4.5

Dynamic Interfacial Tension: Single-component HFCs
(R-125 Trials 1 & 2)

Equations relating temperature of standard liquids to surface tension

Data from CRC Handbook of Chemistry & Physics

Water/Air Interface

$$ST = -0.1544T[^\circ\text{C}] + 75.823$$

Methanol/Air Interface

$$ST = -0.094T[^\circ\text{C}] + 24.490$$

Calibration Data

Temperature [$^\circ\text{F}$]	75
Temperature [$^\circ\text{C}$]	23.89
Surface tension of water [dyn/cm, CRC]	72.13
Surface tension of methanol [dyn/cm, CRC]	22.24
Voltage output for water [volts, transducer]	2.34
Voltage output for methanol [volts, transducer]	1.25

Standard	Methanol	Water
Voltage	1.25	2.34
ST (dyn/cm)	22.24	72.13

Calibration Line & Equation

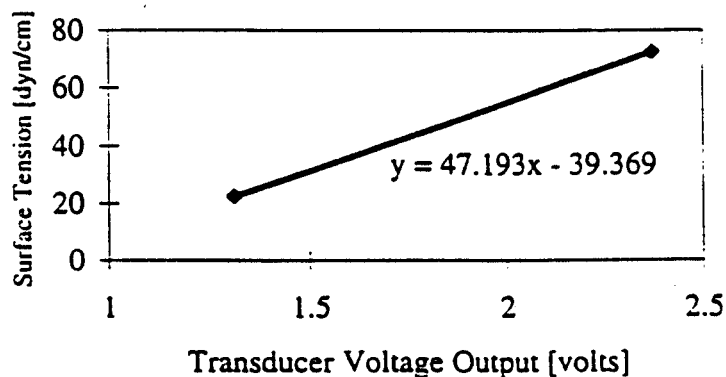


Table A4.5.3
R-125 Trial I

Lubricant Sample	<i>Transducer:</i>	<i>Oscilloscope:</i>		<i>Experimental values:</i>	
	Output (V)	divisions	sec/div	Bubble freq (Hz)	ST (dynes/cm)
ICI RL68H	1.43	3.1	0.5	0.6	30.5
	1.45	1.9	0.5	1.1	31.4
	1.46	0.9	0.5	2.2	31.9
	1.49	1	0.2	5.0	33.2
	1.52	0.5	0.2	10.0	34.6
	1.53	0.4	0.2	12.5	35.1
	1.55	0.35	0.2	14.3	36.0
	1.58	0.25	0.2	20.0	37.3
	1.63	0.2	0.2	25.0	39.6
Witco SL68	1.43	3.8	0.5	0.5	30.5
	1.45	1.05	0.5	1.9	31.4
	1.47	0.5	0.5	4.0	32.3
	1.5	0.6	0.2	8.3	33.7
	1.53	0.4	0.2	12.5	35.1
	1.57	0.3	0.2	16.7	36.9
	1.59	0.3	0.2	16.7	37.8
	1.65	0.2	0.2	25.0	40.6

Table A4.5.4
R-125 Trial 2

Lubricant Sample	<i>Transducer:</i>	<i>Oscilloscope:</i>		<i>Experimental values:</i>	
	Output (V)	divisions	sec/div	Bubble freq (Hz)	ST (dynes/cm)
ICI RL68H	1.48	2.4	0.5	0.8	32.8
	1.51	2	0.2	2.5	34.1
	1.53	1.35	0.2	3.7	35.1
	1.55	0.85	0.2	5.9	36.0
	1.57	0.6	0.2	8.3	36.9
	1.6	0.5	0.2	10.0	38.3
	1.63	0.4	0.2	12.5	39.6
	1.65	0.7	0.1	14.3	40.6
	1.64	0.7	0.1	14.3	40.1
	1.7	0.6	0.1	16.7	42.8
	1.8	0.3	0.1	33.3	47.4
Witco SL68	1.45	4	0.5	0.5	31.4
	1.45	1.7	0.5	1.2	31.4
	1.46	1.3	0.5	1.5	31.9
	1.48	2.6	0.2	1.9	32.8
	1.48	2.1	0.2	2.4	32.8
	1.49	1.4	0.2	3.6	33.2
	1.51	0.8	0.2	6.3	34.1
	1.53	0.6	0.2	8.3	35.1
	1.56	0.4	0.2	12.5	36.4
	1.6	0.25	0.2	20.0	38.3
	1.65	0.2	0.2	25.0	40.6
	1.73	0.35	0.1	28.6	44.2

Table A4.5

Dynamic Interfacial Tension: Single-component HFCs
(R-32)

Equations relating temperature of standard liquids to surface tension

Data from CRC Handbook of Chemistry & Physics

Water/Air Interface

$$ST = -0.1544T[^\circ\text{C}] + 75.823$$

Methanol/Air Interface

$$ST = -0.094T[^\circ\text{C}] + 24.490$$

Calibration Data

Temperature [$^\circ\text{F}$]	72
Temperature [$^\circ\text{C}$]	22.22
Surface tension of water [dyn/cm, CRC]	72.39
Surface tension of methanol [dyn/cm, CRC]	22.40
Voltage output for water [volts, transducer]	3.62
Voltage output for methanol [volts, transducer]	1.2

Standard	Methanol	Water
Voltage	1.2	3.62
ST (dyn/cm)	22.40	72.39

Calibration Line & Equation

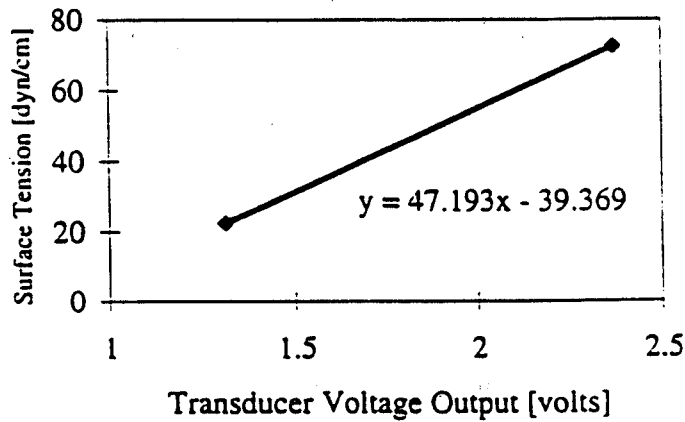


Table A4.5.5
R-32

Lubricant Sample	<i>Transducer:</i>	<i>Oscilloscope:</i>		<i>Experimental values:</i>	
	Output (V)	divisions	sec/div	Bubble freq (Hz)	ST (dynes/cm)
ICI RL68H	1.515	1.05	0.5	1.9	28.9
	1.53	1.1	0.2	4.5	29.2
	1.55	0.8	0.2	6.3	29.6
	1.58	0.55	0.2	9.1	30.3
	1.59	0.35	0.2	14.3	30.5
	1.645	0.3	0.2	16.7	31.6
	1.71	0.2	0.2	25.0	32.9
	1.88	0.3	0.1	33.3	36.4
Witco SL68	1.48	0.95	0.5	2.1	28.2
	1.5	0.4	0.5	5.0	28.6
	1.53	0.75	0.2	6.7	29.2
	1.57	0.43	0.2	11.6	30.0
	1.655	0.2	0.2	25.0	31.8
	1.76	0.17	0.2	29.4	34.0
	1.885	0.3	0.1	33.3	36.6
	1.905	0.3	0.1	33.3	37.0

Table A4.5

Dynamic Interfacial Tension: Single-component HFCs
(R-143a & R-125 Trial 3)

Equations relating temperature of standard liquids to surface tension

Data from CRC Handbook of Chemistry & Physics

Water/Air Interface

$$ST = -0.1544T[^\circ\text{C}] + 75.823$$

Methanol/Air Interface

$$ST = -0.094T[^\circ\text{C}] + 24.490$$

Calibration Data

Temperature [$^\circ\text{F}$]	71
Temperature [$^\circ\text{C}$]	21.67
Surface tension of water [dyn/cm, CRC]	72.48
Surface tension of methanol [dyn/cm, CRC]	22.45
Voltage output for water [volts, transducer]	2.39
Voltage output for methanol [volts, transducer]	1.22

Standard	Methanol	Water
Voltage	1.22	2.39
ST (dyn/cm)	22.45	72.48

Calibration Line & Equation

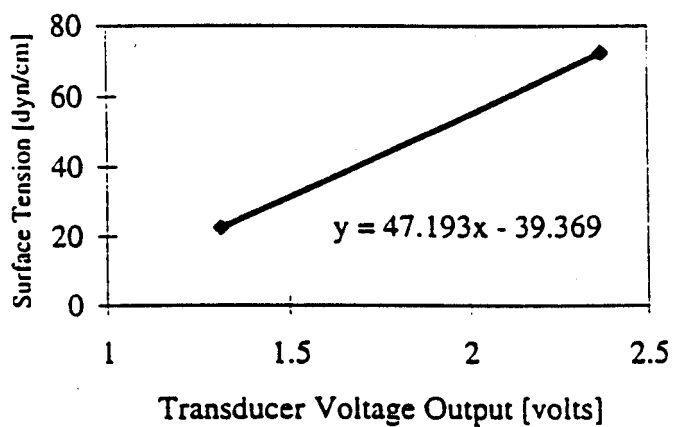


Table A4.5.6

R-143a

Lubricant Sample	<i>Transducer:</i>	<i>Oscilloscope :</i>		<i>Experimental values:</i>	
	Output (V)	divisions	sec/div	Bubble freq (Hz)	ST (dynes/cm)
ICI RL68H	1.44	2.00	0.5	1.0	31.9
	1.46	0.90	0.5	2.2	32.7
	1.48	1.20	0.2	4.2	33.6
	1.51	0.60	0.2	8.3	34.9
	1.545	0.40	0.2	12.5	36.3
	1.58	0.30	0.2	16.7	37.8
	1.54	0.25	0.2	20.0	36.1
	1.64	0.40	0.1	25.0	40.4
Witco SL68	1.505	2.1	0.5	1.0	34.6
	1.51	1.9	0.5	1.1	34.9
	1.55	1.3	0.2	3.8	36.6
	1.565	0.75	0.2	6.7	37.2
	1.61	0.4	0.2	12.5	39.1
	1.62	0.3	0.2	16.7	39.6
	1.66	0.5	0.1	20.0	41.3
	1.73	0.4	0.1	25.0	44.3

Table A4.5.7
R-125 (Trial 3)

Lubricant Sample	<i>Transducer:</i>	<i>Oscilloscope :</i>		<i>Experimental values:</i>	
	Output (V)	divisions	sec/div	Bubble freq (Hz)	ST (dynes/cm)
ICI RL68H	1.46	1.8	0.5	1.1	32.7
	1.48	0.7	0.5	2.9	33.6
	1.5	1.7	0.2	2.9	34.4
	1.515	0.85	0.2	5.9	35.1
	1.535	0.6	0.2	8.3	35.9
	1.56	0.4	0.2	12.5	37.0
	1.55	0.7	0.1	14.3	36.6
	1.65	0.5	0.1	20.0	40.8
Witco SL68	1.45	0.7	0.5	2.9	32.3
	1.485	0.35	0.5	5.7	33.8
	1.5	0.75	0.2	6.7	34.4
	1.525	0.45	0.2	11.1	35.5
	1.565	0.3	0.2	16.7	37.2
	1.62	0.6	0.1	16.7	39.6

Table A4.6

Dynamic Interfacial Tension: HFC Blends
(R-404A, 407C Trial 1)

Equations relating temperature of standard liquids to surface tension

Data from CRC Handbook of Chemistry & Physics

Water/Air Interface

$$ST = -0.1544T[^\circ\text{C}] + 75.823$$

Methanol/Air Interface

$$ST = -0.094T[^\circ\text{C}] + 24.490$$

Calibration Data

Temperature [$^\circ\text{F}$]	71
Temperature [$^\circ\text{C}$]	21.67
Surface tension of water [dyn/cm, CRC]	72.48
Surface tension of methanol [dyn/cm, CRC]	22.45
Voltage output for water [volts, transducer]	2.37
Voltage output for methanol [volts, transducer]	1.31

Standard	Methanol	Water
Voltage	1.31	2.37
ST (dyn/cm)	22.45	72.48

Calibration Line & Equation

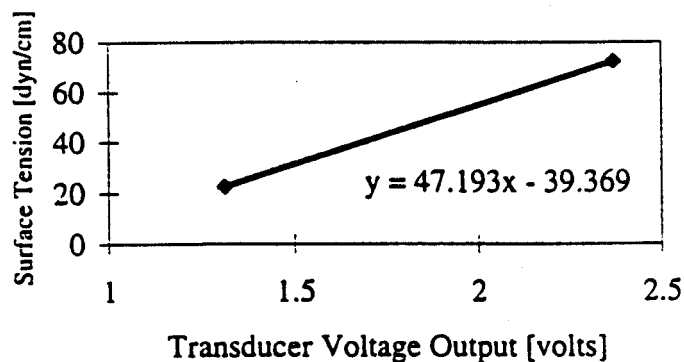


Table A4.6.1
R-404A Trial 1

Lubricant Sample	<i>Transducer:</i>	<i>Oscilloscope:</i>		<i>Experimental values:</i>	
	Output (V)	divisions	sec/div	Bubble freq (Hz)	ST (dynes/cm)
ICI RL68H	1.55	2.1	0.5	1.0	30.8
	1.55	1.0	0.5	2.0	30.8
	1.585	0.4	0.5	5.0	32.4
	1.605	0.25	0.5	8.0	33.4
	1.62	0.6	0.2	8.3	34.1
	1.64	0.4	0.2	12.5	35.0
	1.655	0.35	0.2	14.3	35.7
	1.68	0.25	0.2	20.0	36.9
	1.72	0.35	0.1	28.6	38.8
Witco SL68	1.55	1.7	0.5	1.2	30.8
	1.58	1.15	0.5	1.7	32.2
	1.58	0.6	0.5	3.3	32.2
	1.60	0.9	0.2	5.6	33.1
	1.635	0.45	0.2	11.1	34.8
	1.66	0.4	0.2	12.5	36.0
	1.685	0.5	0.1	20.0	37.2
	1.85	0.4	0.1	25.0	44.9

Table A4.6.2
R-407C Trial 1

Lubricant Sample	<i>Transducer:</i>	<i>Oscilloscope:</i>		<i>Experimental values:</i>	
	Output (V)	divisions	sec/div	Bubble freq (Hz)	ST (dynes/cm)
ICI RL68H	1.63	2.1	0.5	1.0	34.6
	1.64	1.4	0.5	1.4	35.0
	1.68	0.3	0.5	6.7	36.9
	1.70	0.45	0.2	11.1	37.9
	1.735	0.4	0.2	12.5	39.5
	1.785	0.3	0.2	16.7	41.9
	1.8	0.5	0.1	20.0	42.6
	1.87	0.3	0.1	33.3	45.9
Witco SL68	1.54	1.6	0.5	1.3	30.3
	1.54	1.2	0.5	1.7	30.3
	1.54	1.0	0.5	2.0	30.3
	1.565	0.6	0.5	3.3	31.5
	1.61	0.25	0.5	8.0	33.6
	1.63	0.5	0.2	10.0	34.6
	1.67	0.35	0.2	14.3	36.4
	1.70	0.3	0.2	16.7	37.9
	1.82	0.4	0.1	25.0	43.5

Table A4.6

Dynamic Interfacial Tension: HFC Blends
(R-410A Trial 1)

Equations relating temperature of standard liquids to surface tension

Data from CRC Handbook of Chemistry & Physics

Water/Air Interface

$$ST = -0.1544T[^\circ\text{C}] + 75.823$$

Methanol/Air Interface

$$ST = -0.094T[^\circ\text{C}] + 24.490$$

Calibration Data

Temperature [$^\circ\text{F}$]	71
Temperature [$^\circ\text{C}$]	21.67
Surface tension of water [dyn/cm, CRC]	72.48
Surface tension of methanol [dyn/cm, CRC]	22.45
Voltage output for water [volts, transducer]	2.3
Voltage output for methanol [volts, transducer]	1.16

Standard	Methanol	Water
Voltage	1.16	2.3
ST (dyn/cm)	22.45	72.48

Calibration Line & Equation

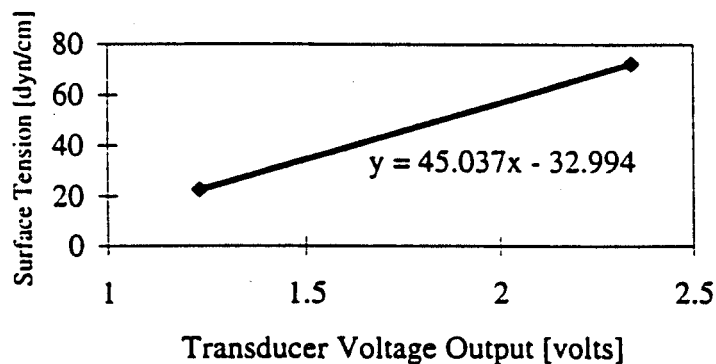


Table A4.6.3
R-410A Trial 1

Lubricant Sample	<i>Transducer:</i>	<i>Oscilloscope:</i>		<i>Experimental values:</i>	
	Output (V)	divisions	sec/div	Bubble freq (Hz)	ST (dynes/cm)
ICI RL68H	1.5	2	0.5	1.0	34.6
	1.51	0.9	0.5	2.2	35.0
	1.54	0.6	0.2	8.3	36.4
	1.55	0.55	0.2	9.1	36.8
	1.61	0.3	0.2	16.7	39.5
	1.65	0.25	0.2	20.0	41.3
	1.71	0.35	0.1	28.6	44.0
	1.83	0.3	0.1	33.3	49.4
Witco SL68	1.45	0.7	0.5	2.9	32.3
	1.485	0.35	0.5	5.7	33.9
	1.5	0.75	0.2	6.7	34.6
	1.525	0.45	0.2	11.1	35.7
	1.565	0.3	0.2	16.7	37.5

Table A4.6

Dynamic Interfacial Tension: HFC Blends
(R-404A, 407C, 410A, all Trial 2)

Equations relating temperature of standard liquids to surface tension

Data from CRC Handbook of Chemistry & Physics

Water/Air Interface

$$ST = -0.1544T[^\circ\text{C}] + 75.823$$

Methanol/Air Interface

$$ST = -0.094T[^\circ\text{C}] + 24.490$$

Calibration Data

Temperature [$^\circ\text{F}$]	72
Temperature [$^\circ\text{C}$]	22.22
Surface tension of water [dyn/cm, CRC]	72.39
Surface tension of methanol [dyn/cm, CRC]	22.40
Voltage output for water [volts, transducer]	2.34
Voltage output for methanol [volts, transducer]	1.23

Standard	Methanol	Water
Voltage	1.23	2.34
ST (dyn/cm)	22.40	72.39

Calibration Line & Equation

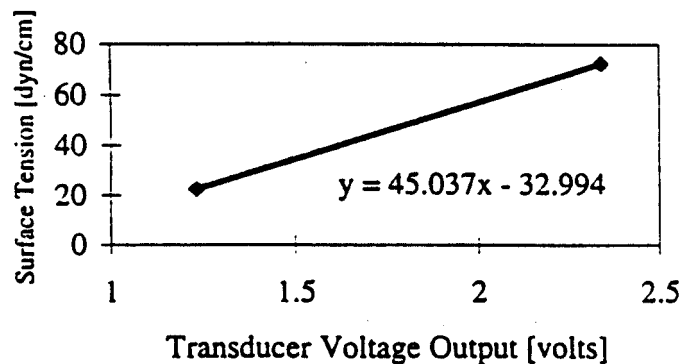


Table A4.6.4
R-404A Trial 2

Lubricant Sample	<i>Transducer:</i>	<i>Oscilloscope:</i>		<i>Experimental values:</i>	
	Output (V)	divisions	sec/div	Bubble freq (Hz)	ST (dynes/cm)
ICI RL68H	1.43	1.1	0.2	4.5	31.4
	1.43	0.9	0.2	5.6	31.4
	1.445	0.8	0.2	6.3	32.1
	1.42	0.3	0.5	6.7	31.0
	1.465	0.5	0.2	10.0	33.0
	1.5	0.4	0.2	12.5	34.6
	1.515	0.3	0.2	16.7	35.2
	1.53	0.25	0.2	20.0	35.9
	1.57	0.4	0.1	25.0	37.7
Witco SL68	1.4	1.5	0.5	1.3	30.1
	1.42	0.9	0.5	2.2	31.0
	1.45	1	0.2	5.0	32.3
	1.445	0.3	0.5	6.7	32.1
	1.48	0.45	0.2	11.1	33.7
	1.51	0.8	0.1	12.5	35.0
	1.51	0.35	0.2	14.3	35.0
	1.53	0.3	0.2	16.7	35.9
	1.64	0.3	0.1	33.3	40.9

Table A4.6.5
R-410A Trial 2

Lubricant Sample	<i>Transducer:</i>	<i>Oscilloscope:</i>		<i>Experimental values:</i>	
	Output (V)	divisions	sec/div	Bubble freq (Hz)	ST (dynes/cm)
ICI RL68H	1.545	3.1	0.5	0.6	36.6
	1.555	1.4	0.5	1.4	37.0
	1.585	0.6	0.2	8.3	38.4
	1.59	0.55	0.2	9.1	38.6
	1.67	0.4	0.2	12.5	42.2
	1.72	0.25	0.2	20.0	44.5
	1.86	0.35	0.1	28.6	50.8
	1.845	0.15	0.2	33.3	50.1
Witco SL68	1.49	1.6	0.5	1.3	34.1
	1.505	0.8	0.5	2.5	34.8
	1.5	1.3	0.2	3.8	34.6
	1.535	0.75	0.2	6.7	36.1
	1.56	0.35	0.2	14.3	37.3
	1.61	0.3	0.2	16.7	39.5
	1.65	0.5	0.1	20.0	41.3
	1.75	0.3	0.1	33.3	45.8

Table A4.6.6
R-407C Trial 2

Lubricant Sample	<i>Transducer:</i>	<i>Oscilloscope:</i>		<i>Experimental values:</i>	
	Output (V)	divisions	sec/div	Bubble freq (Hz)	ST (dynes/cm)
ICI RL68H	1.425	1.3	0.5	1.5	31.2
	1.425	0.7	0.5	2.9	31.2
	1.455	0.9	0.2	5.6	32.5
	1.475	0.55	0.2	9.1	33.4
	1.495	0.3	0.2	16.7	34.3
	1.53	0.5	0.1	20.0	35.9
	1.56	0.4	0.1	25.0	37.3
	1.59	0.35	0.1	28.6	38.6
Witco SL68	1.42	1	0.5	2.0	31.0
	1.445	1.1	0.2	4.5	32.1
	1.45	1	0.2	5.0	32.3
	1.46	1	0.2	5.0	32.8
	1.49	0.55	0.2	9.1	34.1
	1.51	0.5	0.2	10.0	35.0
	1.535	0.3	0.2	16.7	36.1
	1.56	0.25	0.2	20.0	37.3
	1.57	0.5	0.1	20.0	37.7

TABLE A5.1

Baseline Aeration Tests: APPROACH 1

Materials:*Lubricants: Witco 3GS & 4GS mineral oils**Refrigerants: (CFC) R-12, (HCFC) R-22***Conditions:***Temp = 25° C**Pressure = 1 atm***Variables (units):***Refrigerant flow rate (ml/min)**Foam height (cm)**Time (min)***TABLE A5.1.1****30 ml 3GS & R-22**

Time (min)	Refrigerant Flow Rates (ml/min)					Foam Height (cm)
	60	250	350	420	700	
0.0	16	24	32	22	20	↓
0.5	12	17	24	11	9	
1.0	9	10	15	2	5	
1.5	6	8	8	1	1	
2.0	2	2	3	<i>collapsed</i>	<i>collapsed</i>	
2.5	1	1	1			
3.0	<i>collapsed</i>	<i>collapsed</i>	<i>collapsed</i>			

TABLE A5.1.2**30 ml 3GS & R-12**

Time (min)	Refrigerant Flow Rates (ml/min)				Foam Height (cm)
	200	350	700	1000	
0.0	32	29	23	17	↓
0.5	23	20	11	7	
1.0	19	16	5	2	
1.5	15	11	1	1	
2.0	9	7	<i>collapsed</i>	<i>collapsed</i>	
2.5	3	1			
3.0	<i>collapsed</i>	<i>collapsed</i>			

TABLE A5.1

Baseline Aeration Tests

TABLE A5.1.3 30 ml 4GS & R-22

Time (min)	Ref. Flow Rates (ml/min)			Foam Height (cm)
	350	700	1000	
0.0	33	35	15	
0.5	27	29	10	
1.0	20	25	10	
1.5	17	21	9	
2.0	16	19	8	
2.5	15	16	7	
3.0	13	16	5	
3.5	11	14	2	
4.0	8	12	2	
4.5	5	9	1	
5.0	2	5	<i>collapsed</i>	
5.5	1	1		
6.0	<i>collapsed</i>	<i>collapsed</i>		

TABLE A5.1.4 50 ml 4GS & R-22

Time (min)	Ref. Flow Rates (ml/min)			Foam Height (cm)
	350	630	1000	
0.0	29	37	19	
0.5	25	27	16	
1.0	20	22	13	
1.5	16	18	10	
2.0	13	17	8	
2.5	9	14	5	
3.0	6	12	2	
3.5	1	9	1	
4.0	1	7	<i>collapsed</i>	
4.5	<i>collapsed</i>	4		
5.0		2		
5.5		1		
6.0		<i>collapsed</i>		

TABLE A5.1
Baseline Aeration Tests

TABLE A5.1.5 **30 ml 4GS & R-12**


Time (min)	<i>Refrigerant Flow Rates (ml/min)</i>				Foam Height (cm)
	<i>350</i>	<i>470</i>	<i>700</i>	<i>1000</i>	
0.0	20	20	25	22	
0.5	15	14	14	9	
1.0	9	11	9	4	
1.5	4	7	3	2	
2.0	1	2	1	1	
2.5	<i>collapsed</i>	<i>collapsed</i>	<i>collapsed</i>	<i>collapsed</i>	

TABLE A5.2

Baseline Aeration Tests: APPROACH 2

Materials:*Lubricants: Witco 3GS & 4GS mineral oils**Refrigerants: (CFC) R-12, (HCFC) R-22***Conditions:***Temp = 25° C**Pressure = 1 atm***Controlled Variable (units):***Refrigerant flow rate (ml/min)***Observed Variables (units):***Maximum Foam height (cm)**Foam Collapse Time (10^{-1} min)***TABLE A5.2**

Lubricant (vol, type)	Refrigerant (type)	Ref Flow Rate (ml/min)	Max Height (cm)	Collapse Time (10-1 min)	Corresponding Figure
30 ml, 3GS	R-22	60	16	30	FIGURE 5.14
		250	24	30	
		350	32	30	
		420	22	20	
		700	20	20	
30 ml, 3GS	R-12	200	32	30	FIGURE 5.15
		350	29	30	
		700	23	20	
		1000	17	20	
30 ml, 4GS	R-22	350	33	60	FIGURE 5.16
		700	35	60	
		1000	15	60	
50 ml, 4GS	R-22	350	29	45	FIGURE 5.17
		630	37	60	
		1000	19	40	
30 ml, 4GS	R-12	350	20	25	FIGURE 5.18
		470	20	25	
		700	25	25	
		1000	22	25	

TABLE A5.3

HFC Pressure-Release Foaming Tests

Materials:*Lubricants: ICI RL68H polyolester**Refrigerants: R-32, R-125, R-134a, R-143a***Notes***"Mass of tube" = mass of pressure tube + mass of valve A connection + mass of stirring bar**All masses are reported in grams**Amount of refrigerant desorbed reported for trials 9 and higher**"Slow" desorption measured after approximately 15 minutes***TABLE A5.3.1**

	Trial 1	Trial 2	Trial 3	Trial 4
Refrigerant:	R-134a	R-134a	R-134a	R-134a
Lubricant:	ICI POE	ICI POE	ICI POE	ICI POE
Volume of lubricant (ml):	20	20	10	10
Mass of tube:	554.5	554.9	554.7	554.9
Mass of tube + POE:	574.2	574.6	560.9	562.1
Mass of POE:	19.7	19.7	6.2	7.2
Mass of tube + POE + HFC:	592.4	593.4	568.1	570.3
Mass of HFC:	18.2	18.8	7.2	8.2
HFC/POE ratio:	0.92	0.95	1.16	1.14
Pressure drop (psi):	20	20	20	20
Time of pressure drop (sec):	fast (~10)	fast (~10)	fast (~10)	fast (~30)
Initial mixture height (cm):	8	8	4	4
Maximum foam height (cm):	14	13	8	6
Foamability (cm):	6	5	4	2
Foam lifetime (stability, sec):	~10	~10	<10	<10

TABLE A5.3

HFC Pressure-Release Foaming Tests

TABLE A5.3.2

	Trial 5	Trial 6	Trial 7	Trial 8
Refrigerant:	R-134a	R-134a	R-125	R-125
Lubricant:	ICI POE	ICI POE	ICI POE	ICI POE
Volume of lubricant (ml):	10	10	10	10
Mass of tube:	554.5	554.8	554.6	554.5
Mass of tube + POE:	562.4	562.0	564.1	563.6
Mass of POE:	7.9	7.2	9.5	9.1
Mass of tube + POE + HFC:	571	569.7	573.9	572.2
Mass of HFC:	8.6	7.7	9.8	8.6
HFC/POE ratio:	1.09	1.07	1.03	0.95
Pressure drop (psi):	20	20	20	20
Time of pressure drop (sec):	slow (~60)	slow (~180)	fast (~10)	fast (~30)
Initial mixture height (cm):	4	4	4	4
Maximum foam height (cm):	<5	<5	<6	<5
Foamability (cm):	<1	<1	<2	<1
Foam lifetime (stability, sec):	~0	~0	~5	~0

TABLE A5.3

HFC Pressure-Release Foaming Tests

TABLE A5.3.3**Trial 9****Trial 10****Trial 11****Trial 12**

	Trial 9	Trial 10	Trial 11	Trial 12
Refrigerant:	R-134a	R-134a	R-134a	R-134a
Lubricant:	ICI POE	ICI POE	ICI POE	ICI POE
Volume of lubricant (ml):	5	5	5	5
Mass of tube:	555.1	554.5	554.6	555.3
Mass of tube + POE:	560.5	558.8	557.5	558.4
Mass of POE:	5.4	4.3	2.9	3.1
Mass of tube + POE + HFC:	566.4	563.8	565.9	566.7
Mass of HFC:	5.9	5.0	8.4	8.3
HFC/POE ratio:	1.09	1.16	2.90	2.68
Pressure drop (psi):	20	20	20	20
Time of pressure drop (sec):	fast (~10)	fast (~30)	fast (~10)	fast (~30)
Initial mixture height (cm):	4	4	6	6
Maximum foam height (cm):	18	9	22	16
Foamability (cm):	14	5	16	10
Foam lifetime (stability, sec):	~2	~2	~2	~2
Mass of tube + POE + HFC:	561.2	561.7	562.3	562.4
Initial amount desorbed:	5.2	2.1	3.6	4.3
Final mass of tube + POE + HFC:	560.7	560.9	561.6	561.5
Total amount desorbed :	5.7	2.9	4.3	5.2
Initial desorption rate (fast, g/sec):	0.52	0.07	0.36	0.14
Final desorption rate (slow, g/sec):	0.0008	0.0013	0.0012	0.0015

TABLE A5.3

HFC Pressure-Release Foaming Tests

TABLE A5.3.4

	Trial 13	Trial 14	Trial 15	Trial 16
Refrigerant:	R-134a	R-134a	R-134a	R-134a
Lubricant:	ICI POE	ICI POE	ICI POE	ICI POE
Volume of lubricant (ml):	5	5	2	2
Mass of tube:	554.5	554.6	555.4	555.2
Mass of tube + POE:	559.1	559.4	557.5	557.2
Mass of POE:	4.6	4.8	2.1	2.0
Mass of tube + POE + HFC:	565.2	574.3	569.7	568.4
Mass of HFC:	6.1	14.9	12.2	11.2
HFC/POE ratio:	1.33	3.10	5.81	5.60
Pressure drop (psi):	50	50	20	20
Time of pressure drop (sec):	fast (~10)	fast (~30)	fast (~10)	fast (~30)
Initial mixture height (cm):	4	6	6	6
Maximum foam height (cm):	8	15	34+	34+
Foamability (cm):	4	9	28+	28+
Foam lifetime (stability, sec):	~2	~5	~30	~30
Mass of tube + POE + HFC:	562.1	565.2	561.7	561.2
Initial amount desorbed:	3.1	9.1	8.0	7.2
Final mass of tube + POE + HFC:	561.6	564.5	561.1	560.5
Total amount desorbed :	3.6	9.8	8.6	7.9
Initial desorption rate (fast, g/sec):	0.31	0.30	0.80	0.24
Final desorption rate (slow, g/sec):	0.0008	0.0006	0.0010	0.0012

TABLE A5.3

HFC Pressure-Release Foaming Tests

TABLE A5.3.5

	Trial 17	Trial 18	Trial 19	Trial 20
Refrigerant:	R-143a	R-143a	R-143a	R-143a
Lubricant:	ICI POE	ICI POE	ICI POE	ICI POE
Volume of lubricant (ml):	5	5	5	5
Mass of tube:	555.3	555.5	555.7	555.4
Mass of tube + POE:	559.1	559.6	560.0	559.1
Mass of POE:	3.8	4.1	4.3	3.7
Mass of tube + POE + HFC:	563.7	564.1	564.1	570.1
Mass of HFC:	4.6	4.5	4.1	11
HFC/POE ratio:	1.21	1.10	0.95	2.97
Pressure drop (psi):	20	20	50	50
Time of pressure drop (sec):	fast (~10)	fast (~30)	fast (~10)	fast (~10)
Initial mixture height (cm):	4	4	4	4
Maximum foam height (cm):	6	~5	6	9
Foamability (cm):	2	1	2	5
Foam lifetime (stability, sec):	~2	~2	~2	~5
Mass of tube + POE + HFC:	560.7	561.6	562.8	562.4
Initial amount desorbed:	3	2.5	1.3	7.7
Final mass of tube + POE + HFC:	560.1	561.0	562.1	562.1
Total amount desorbed :	3.6	3.1	2.0	8.0
Initial desorption rate (fast, g/sec):	0.30	0.25	0.13	0.77
Final desorption rate (slow, g/sec):	0.0010	0.0010	0.0012	0.0005

TABLE A5.3

HFC Pressure-Release Foaming Tests

TABLE A5.3.6	Trial 21	Trial 22	Trial 23	Trial 24
Refrigerant:	R-143a	R-143a	R-32	R-32
Lubricant:	ICI POE	ICI POE	ICI POE	ICI POE
Volume of lubricant (ml):	2	2	5	5
Mass of tube:	555.1	555.5	555.4	555.1
Mass of tube + POE:	558.0	557.2	559.5	559.4
Mass of POE:	2.9	1.7	4.1	4.3
Mass of tube + POE + HFC:	574.7	566.5	563.0	565.1
Mass of HFC:	16.7	9.3	3.5	5.7
HFC/POE ratio:	5.76	5.47	0.85	1.33
Pressure drop (psi):	20	20	50	70
Time of pressure drop (sec):	fast (~10)	fast (~30)	fast (~10)	fast (~10)
Initial mixture height (cm):	6	6	4	4
Maximum foam height (cm):	34+	34+	<5	<5
Foamability (cm):	28+	28+	<1	<1
Foam lifetime (stability, sec):	~20	~30	0	0
Mass of tube + POE + HFC:	564.2	559.6	560.1	561.0
Initial amount desorbed:	10.5	6.9	2.9	4.1
Final mass of tube + POE + HFC:	563.6	559.1	559.7	560.0
Total amount desorbed :	11.1	7.4	3.3	5.1
Initial desorption rate (fast, g/sec):	1.05	0.23	0.29	0.41
Final desorption rate (slow, g/sec):	0.0010	0.0008	0.0007	0.0017

TABLE A5.3

HFC Pressure-Release Foaming Tests

TABLE A5.3.7**Trial 25****Trial 26**

	Trial 25	Trial 26
Refrigerant:	R-32	R-32
Lubricant:	ICI POE	ICI POE
Volume of lubricant (ml):	5	5
Mass of tube:	555.6	555.5
Mass of tube + POE:	559.2	560.2
Mass of POE:	3.6	4.7
Mass of tube + POE + HFC:	563.0	565.4
Mass of HFC:	3.8	5.2
HFC/POE ratio:	1.06	1.11
Pressure drop (psi):	50	70
Time of pressure drop (sec):	fast (~30)	fast (~30)
Initial mixture height (cm):	4	4
Maximum foam height (cm):	<5	<5
Foamability (cm):	<1	<1
Foam lifetime (stability, sec):	0	0
Mass of tube + POE + HFC:	560.7	561.1
Initial amount desorbed:	2.3	4.3
Final mass of tube + POE + HFC:	560.4	560.4
Total amount desorbed :	2.6	5.0
Initial desorption rate (fast, g/sec):	0.08	0.14
Final desorption rate (slow, g/sec):	0.0005	0.0012

TABLE A5.3.8a

HFC Pressure-Release Foaming Tests

Data Summary

Trial No.	Refrigerant	POE volume	Ref to Lub Ratio	Pressure Drop	Drop time	Foamability
1	134a	20 ml	1 to 1	20 psi	10 sec	6 cm
2	134a	10 ml	1 to 1	20 psi	10 sec	5 cm
3	134a	10 ml	1 to 1	20 psi	10 sec	4 cm
4	134a	10 ml	1 to 1	20 psi	30 sec	2 cm
5	134a	10 ml	1 to 1	20 psi	60 sec	<1 cm
6	134a	10 ml	1 to 1	20 psi	180 sec	<1 cm
7	125	10 ml	1 to 1	20 psi	10 sec	<2 cm
8	125	10 ml	1 to 1	20 psi	30 sec	<1 cm
9	134a	5 ml	1 to 1	20 psi	10 sec	14 cm
10	134a	5 ml	1 to 1	20 psi	30 sec	5 cm
11	134a	5 ml	3 to 1	20 psi	10 sec	16 cm
12	134a	5 ml	3 to 1	20 psi	30 sec	10 cm
13	134a	5 ml	3 to 1	50 psi	10 sec	4 cm
14	134a	5 ml	3 to 1	50 psi	30 sec	9 cm
15	134a	2 ml	6 to 1	20 psi	10 sec	28+ cm
16	134a	2 ml	6 to 1	20 psi	30 sec	28+ cm

TABLE A5.3.8b

HFC Pressure-Release Foaming Tests

Data Summary

Trial No.	Refrigerant	POE volume	Ref to Lub Ratio	Pressure Drop	Drop time	Foamability
17	143a	5 ml	1 to 1	20 psi	10 sec	2 cm
18	143a	5 ml	1 to 1	20 psi	30 sec	1 cm
19	143a	5 ml	1 to 1	50 psi	10 sec	2 cm
20	143a	5 ml	3 to 1	50 psi	10 sec	5 cm
21	143a	2 ml	6 to 1	20 psi	10 sec	28+ cm
22	143a	2 ml	6 to 1	20 psi	30 sec	28+ cm
23	32	5 ml	1 to 1	50 psi	10 sec	<1 cm
24	32	5 ml	1 to 1	70 psi	10 sec	<1 cm
25	32	5 ml	1 to 1	50 psi	30 sec	<1 cm
26	32	5 ml	1 to 1	70 psi	30 sec	<1 cm

TABLE A5.4

HFC Pressure-Release Desorption

Data Summary

Refrigerant	POE volume	Ref to Lub Ratio	Pressure Drop	Drop time	Initial Desorption Rate
134a	5 ml	1 to 1	20 psi	10 sec	0.52 g/sec
134a	5 ml	1 to 1	20 psi	30 sec	0.07 g/sec
134a	5 ml	3 to 1	20 psi	10 sec	0.36 g/sec
134a	5 ml	3 to 1	20 psi	30 sec	0.14 g/sec
134a	5 ml	3 to 1	50 psi	10 sec	0.31 g/sec
134a	5 ml	3 to 1	50 psi	30 sec	0.30 g/sec
134a	2 ml	6 to 1	20 psi	10 sec	0.80 g/sec
134a	2 ml	6 to 1	20 psi	30 sec	0.24 g/sec
143a	5 ml	1 to 1	20 psi	10 sec	0.30 g/sec
143a	5 ml	1 to 1	20 psi	30 sec	0.25 g/sec
143a	5 ml	1 to 1	50 psi	10 sec	0.13 g/sec
143a	5 ml	3 to 1	50 psi	10 sec	0.77 g/sec
143a	2 ml	6 to 1	20 psi	10 sec	1.05 g/sec
143a	2 ml	6 to 1	20 psi	30 sec	0.23 g/sec
32	5 ml	1 to 1	50 psi	10 sec	0.29 g/sec
32	5 ml	1 to 1	70 psi	10 sec	0.41 g/sec
32	5 ml	1 to 1	50 psi	30 sec	0.08 g/sec
32	5 ml	1 to 1	70 psi	30 sec	0.14 g/sec